Norges miljø- og
biovitenskapelige
universitet

Master's Thesis 2017 60 ECTS
Department of Animal and Aquaculture Sciences

Mechanical properties of the vertebral column and ribs of farmed fish with emphasis on Atlantic Salmon

Jingyang Yao
Master of Science in Aquaculture

Acknowledgement

The work here presented was performed at Nofima ÅS, Norway, during 2016-2017.

I am extremely thankful of my supervisor, Turid Mørkøre, for leading me into such an interesting and fulfilled project. The experience of working with her was fantastic and gave me a lot of motivation and fun. Thank you for all the constructive suggestion along the entire procedure of my work and forever encouragement during my stay here.

I am also grateful of my co-supervisor, Thomas Larsson, for his endless patience and kindness to all of my questions. Further, I sincerely thank Målfrid Tofteberg Bjerke and Inger Øien Kristiansen for the help on my practical work in lab.

Last but not least, I would like to thank Norwegian University of Life Sciences for offering me the opportunity to study and Nofima Marine for supporting me to accomplish my experiments and thesis.

Jingyang Yao

Ås, June 2017

Abstract

The main aim of the thesis was to characterize mechanical properties of the vertebral column and ribs of Atlantic salmon and to recommend a method for measurements of mechanical properties of vertebrae and ribs. Every fourth vertebrae and every second rib was analyzed within the same weight class (4 kg) of salmon. Additionally, variation in mechanical properties among 4 kg, 5 kg and 6 kg salmon vertebrae and ribs, between salmon, rainbow trout and common carp, and the effect of frozen storage were analyzed. The instrument used was TA-XT2 Texture Analyzer. Samples collected from three different section in vertebral column of salmon and trout were chemically analysed for fat content, dry matter and ash. The results showed significant variation in mechanical properties along the vertebral column, between weight classes, between the fish species, and between fresh and frozen vertebrae. There was not a consistent relationship between thickness and the mechanical properties. The mechanical strength of the ribs decreased in the posterior direction, with the highest strength closest to the vertebral column. The fat content of the salmon vertebrae (17-22%) was higher compared with trout (11-15%), while the ash content was higher of trout (21-23%) compared with salmon (17-18%). Vertebrae which had been frozen also proved useful for mechanical measurements.

Based on results from this study, the recommended method for analyzing mechanical properties of salmon is to analyse vertebrae 12 to 28 (counting from tail) because of the stable mechanical properties within this range, and hence low risk to conclude wrongly due to mistaken counting. The total work (N*sec) required to compress the vertebrae to 70% of total thickness was the most representative parameter for data analyses. The method was also applicable on Rainbow trout. The rib located nearest the head, measured at a position close to the vertebral column, proved the best option for detecting representative variation of mechanical properties of salmon ribs.

Key words: Atlantic Salmon, mechanical properties, fish skeletons

Contents

Acknowledgement I

Abstract II

Contents III

List of figures VI

List of tables IX

1. Introduction 1

2. Background 4

2.1. Bone structure 4

2.2. Bone research methodology 5

2.2.1. Invasive testing methods 6

2.2.2. Noninvasive testing methods 7

Ⅰ. Ultrasonic imaging 7

Ⅱ. Computerized tomography (CT) 7

Ⅲ. Magnetic resonance imaging (MRI) 8

2.2.3. Mechanical analysis of bone 9

Ⅰ. The challenge of bone mechanical analysis 9

Ⅱ. Previous studies of bone mechanical properties 10

Ⅲ. Bone biomechanics 10

2.3. Fish skeleton structure and function 11

2.4. Fish vertebrae microstructure 15

2.5. Composition and application 17

3. Meterial and Method 19

3.1. Fish samples 19

3.2. Vertebral column dissection and measurement 20

3.3. Rib dissection and measurement 21

3.4. Overview of the fish material used in the study 23

3.5. Composition analysis 23
3.5.1. Fat content 24
3.5.2. Dry matter and ash 25
3.6. Statistical analysis 26
4. Results 27
4.1. Mechanical properties of salmon vertebrae 27
4.2. Vertebrae comparison of different salmon weight classes 32
4.3. Vertebrae comparison of different fish species 36
4.4. Effect of frozen storage on vertebrae texture 42
4.5. Mechanical properties of salmon ribs 45
4.6. Ribs comparison of different salmon weight classes 48
4.7. Ribs comparison of different fish species 51
4.8. Chemical composition of salmon and trout 52
5. Discussion 55
5.1 Mechanical properties of Atlantic Salmon vertebrae and ribs 55
5.2 Mechanical properties of vertebrae and ribs compared with various weight classes in salmon 57
5.3 Mechanical properties of vertebrae and ribs compared with different fish species 58
5.4 Mechanical properties compared in fresh and frozen vertebrae 60
5.5 Chemical composition of salmon and trout 60
6. Conclusion 61
Reference 63
Appendix 71
Appendix 1: Product list 71
Appendix 2: Force-time graphs for the eighth, twelfth, thirty-second and thirty-sixth vertebrae (V8, V12, V32, V36) of different Salmon weight classes 72
Appendix 3: Total average force-time graphs for the eighth, twelfth, thirty-second and thirty-sixth vertebra (V8, V12, V32, V36) of different Salmon weight classes 73

Appendix 4: Force-time graphs for the eighth, twelfth, thirty-second and thirty-sixth vertebrae (V8, V12, V32, V36) of different fish species.....75

Appendix 5: Force-time graph for the eighth, twelfth, thirty-second and thirty-sixth vertebra (V8, V12, V32, V36) of fresh and frozen Salmon.....79

Appendix 6: Force-time graph for the eighth, twelfth, thirty-second and thirty-sixth vertebra (V8, V12, V32, V36) of fresh and frozen Trout.....81

List of figures

Fig 2.1 Salmon vertebra structure diagram……..12

Fig 2.2 Carp vertebra and rib structure diagram (By Ivy Livingstone)…….. .14

Fig 2.3 Cancellous bone of the salmon vertebrae viewed from the front and side…..17

Fig 3.1 Vertebral column dissection and measurement……...21

Fig 3.2 Rib dissection and measurement…….....22

Fig 3.3 Position A, B, C for rib measurement……..22

Fig 4.1 Thickness (mm) of every fourth vertebrae (V4-V48) along the vertebral column of 4kg Atlantic Salmon……...27

Fig 4.2 Force-time graphs for every fourth vertebra (V4-V48) of 4 kg Atlantic Salmon…….28

Fig 4.3 Total average force-time graphs for every fourth vertebra (V4-V48) of 4 kg Atlantic Salmon……. ……29

Fig 4.4 Maximum compression force (Newton) of every fourth vertebrae (V4-V48) along the vertebral column of 4 kg Atlantic Salmon. ……. ……...30

Fig 4.5 The force (N) and area (N*s) at different compression depth: 0.5 mm, 1 mm, 1.5 mm, 2 mm and strain: 0.5 percent, 1 percent, 1.5 percent, 2 percent of every fourth vertebrae (V4-V48) along the vertebral column of 4 kg Atlantic Salmon……..30

Fig 4.6 Thickness (mm) comparison of the eighth, twelfth, thirty-second and thirty-sixth vertebra (V8, V12, V32, V36) along the vertebral column of different weight classes (4 kg, 5 kg, 6 kg) Atlantic Salmon. ……. ……...32

Fig 4.7 Maximum compression force (N) of the eighth, twelfth, thirty-second and thirty-sixth vertebra (V8, V12, V32, V36) along the vertebral column of different weight classes (4 kg, 5 kg, 6 kg) of Atlantic Salmon. …….……33

Fig 4.8 The compression force (N) at different depth (A at 10%, B at 20%, C at 70% compression depth) of the eighth, twelfth, thirty-second and thirty-sixth vertebra (V8, V12, V32, V36) along the vertebral column of different weight classes (4 kg, 5 kg, 6 kg) Atlantic Salmon.…….……..35

Fig 4.9 Thickness (mm) of every fourth vertebrae along the vertebral column of different fish species (A for V4-V52 of Atlantic Salmon, B for V4-V52 of Rainbow Trout, C for V4-V28 of common Carp).…….…..……37

Fig 4.10 Total average force-time graphs for every fourth vertebra of different fish species (A for V4-V52 of Atlantic Salmon, B for V4-V52 of Rainbow Trout, C for V4-V28 of common Carp)……..…….……...….38

Fig 4.11 Maximum compression force (N) of A, B, C, D vertebra position (15 %, 25 %, 60 %, 70 % of the vertebral column) between different fish species (Atlantic Salmon, Rainbow Trout and Carp)…….…..…..…40

Fig 4.12 Compression force (N) at different depth (A at 15%, B at 70% compression depth) of A, B, C, D vertebra position (15 %, 25 %, 60 %, 70 % of the vertebral column) between fish species (Atlantic Salmon, Rainbow Trout and Carp)……..….41

Fig 4.13 Total average force-time graphs for the eighth, twelfth, thirty-second and thirty-sixth vertebra (V8, V12, V32, V36) of fresh and frozen salmon (A for fresh salmon, B for frozen salmon)…….……..…….…..……42

Fig 4.14 Total average force-time graphs for the eighth, twelfth, thirty-second and thirty-sixth vertebrae (V8, V12, V32, V36) of fresh and frozen trout (A for fresh trout, B for frozen trout) …….…….…….43

Fig 4.15. Maximum compression force (N) of the eighth, twelfth, thirty-second and thirty-sixth vertebrae (V8, V12, V32, V36) along the vertebral column of fresh and frozen fish comparison (A for Atlantic Salmon, B for Rainbow Trout)…….44

Fig 4.16 Thickness (mm) at three positions (A, B, C) of every second rib in 4 kg Atlantic
Salmon.…….…….…….……..……45

Fig 4.17 Breaking force (N) at three positions (A, B, C) of every second rib in 4 kg Atlantic
Salmon.…….…….……..……46

Fig 4.18 Thickness (mm) of three positions (A, B, C) of the twelfth and the fourteen ribs (A for No.12 rib, B for No.14 rib) in various weight classes (4 kg, 5 kg, 6 kg) Atlantic
Salmon.…….…….…….……48

Fig 4.19 Breaking force (Newton) at three positions (A, B, C) of the twelfth and fourteenth ribs (A for No.12 rib, B for No.14 rib) of various weight classes (4 kg, 5 kg, 6 kg) of Atlantic Salmon.……...…….……49

Fig 4.20 Average rib thickness (mm) measured at position B comparing fish species (Atlantic Salmon, Rainbow Trout and Carp).…….……51

Fig 4.21 Average rib breaking force (N) measured at position B comparing fish species (Atlantic Salmon, Rainbow Trout and Carp) …….……51

Fig 4.22 Fat content (%) comparison of three representative sections (V8-V12, V20-V24, V32-V36) along the vertebral column for salmon and trout……...53

Fig 4.23 Dry matter (%) comparison of three representative sections (V8-V12, V20-V24, V32-V36) along the vertebral column for salmon and trout……...53

Fig 4.24 Ash (%) comparison of three representative sections (V8-V12, V20-V24, V32-V36) along the vertebral column for salmon and trout. …….…….54

Fig 5.1 Thickness distribution along the vertebral column of 4 kg salmon…….56

Fig. 5.2 Maximum compression force distribution along the vertebral column of 4 kg salmon (The thickness of the vertebra is described as the maximum compression force)…….…….…….……57

List of tables

Table 3.1 Fish sample information for 4kg, 5kg, 6kg Atlantic salmon……19

Table 3.2 Fish sample information for carp…….……19

Table 3.3 Fish sample information for skeletons of Atlantic salmon and Rainbow trout…….…….…….……...20

Table 3.4 Overview of the fish material used in the study……...……23

Table 4.1 Results from statistical analyses of results presented in Fig. 4.5…….31

Table 4.2 Results from statistical analyses of results presented in Fig 4.7……..33

Table 4.3 Results from statistical analyses of results presented in Fig 4.8……..35

Table 4.4 Results from statistical analyses of results presented in Fig 4.16……45

Table 4.5 Results from statistical analyses of results presented in Fig 4.17……46

Table 4.6 Results from statistical analyses of results presented in Fig. 4.17……...47

Table 4.7 Results from statistical analyses of results presented in Fig. 4.19……...50

1. Introduction

Skeletons as a connective tissue are buried in muscle of vertebrates, such as fish, and are typically not affected by external environmental factors (Håstein, 2004). Because the shape and number of bones in fish are stable, they can therefore have the potential to become the standard by which the development and welfare of fish can be measured and understood.

Long-term natural evolution contributes to the development of bone structure, and enables the skeleton to support maximum external force with minimal material costs and to allow for good function (Bell, 1834, Ramakrishna *et al.*, 2001). In histologic terms, the microstructure of fish bones is similar to that of many other vertebrates. These consist of compact and cancellous bones, which are significantly different in density and strength (Currey, 2002, Totland *et al.*, 2011). Morphologically, bones have superior mechanical properties which are equal to the maximum strength optimization at the point of the least weight (Ross and Metzger, 2004).

In order to provide a more convincing theoretical basis for the process of bone optimization, the study of the mechanical properties of bone has practical significance.

Previous research related to skeletons has taken for the most part a macroscopic view, such as the observation of morphology and development state in the entire fish skeletal system, the nutritional value and utilization of fish bone, and so on. Research on micro-bone is limited. In most cases, high-tech means are used to explore the microstructure of fish bones, such as ultrasonic imaging, computerized tomography, magnetic resonance imaging, and even nanoindentation (Laugier *et al.*, 1997, Genant *et al.*, 2008, Zhang *et al.*, 2002, Cohen *et al.*, 2012). The cost of examining skeletons in this manners is prohibitive, and such research is time consuming. Biomechanics is a new area with rapid development in recent years, which is closely

refer to analyze organisms with mechanical principles and methods. However, according to statistics, only very limited studies have focused on the mechanical properties of fish bone (Cohen *et al.*, 2012). Hence, it is necessary to utilize a simple and intuitive mechanical analysis method in order to better understand the material characteristics of fish skeletons.

Under normal conditions, the mechanical properties of bones cannot be revealed completely due to its anisotropy (Currey, 2014). The special characteristics of bones differ from other homogenetic materials; therefore, suitable mechanical methods and representative parameters should be selected to better estimate the mechanical properties of fish bones. Skeletal deformities usually caused by compression force overload occur in fish in both natural and artificial environments. Problems relating to skeletal deformity occur in salmonids with high frequency at the position of the vertebral column (Branson and Turnbull, 2008). A mechanical model of fish bones can help to predict mechanical damage, improving product quality and providing new control methods. Because the chemical composition of bone also contributes to the variation in bone mechanical properties, it is also important to determine the composition of bone as a basis to provide reasonable parameters (Carter and Spengler, 1978).

The aim of this study was: 1) to describe mechanical properties of Atlantic Salmon vertebrae and ribs in detail; 2) to determine variation in mechanical properties of Atlantic Salmon vertebrae and ribs among weight classes; 3) to compare mechanical properties of vertebrae and ribs among Atlantic Salmon, Rainbow Trout and common Carp; 4) to determine variation in mechanical properties of fresh and frozen vertebrae. 5) to determine variation in chemical composition of salmon and trout vertebrae. Based on the results from points 1-5, recommend a method for measurements of mechanical properties of Atlantic Salmon vertebrae and ribs.

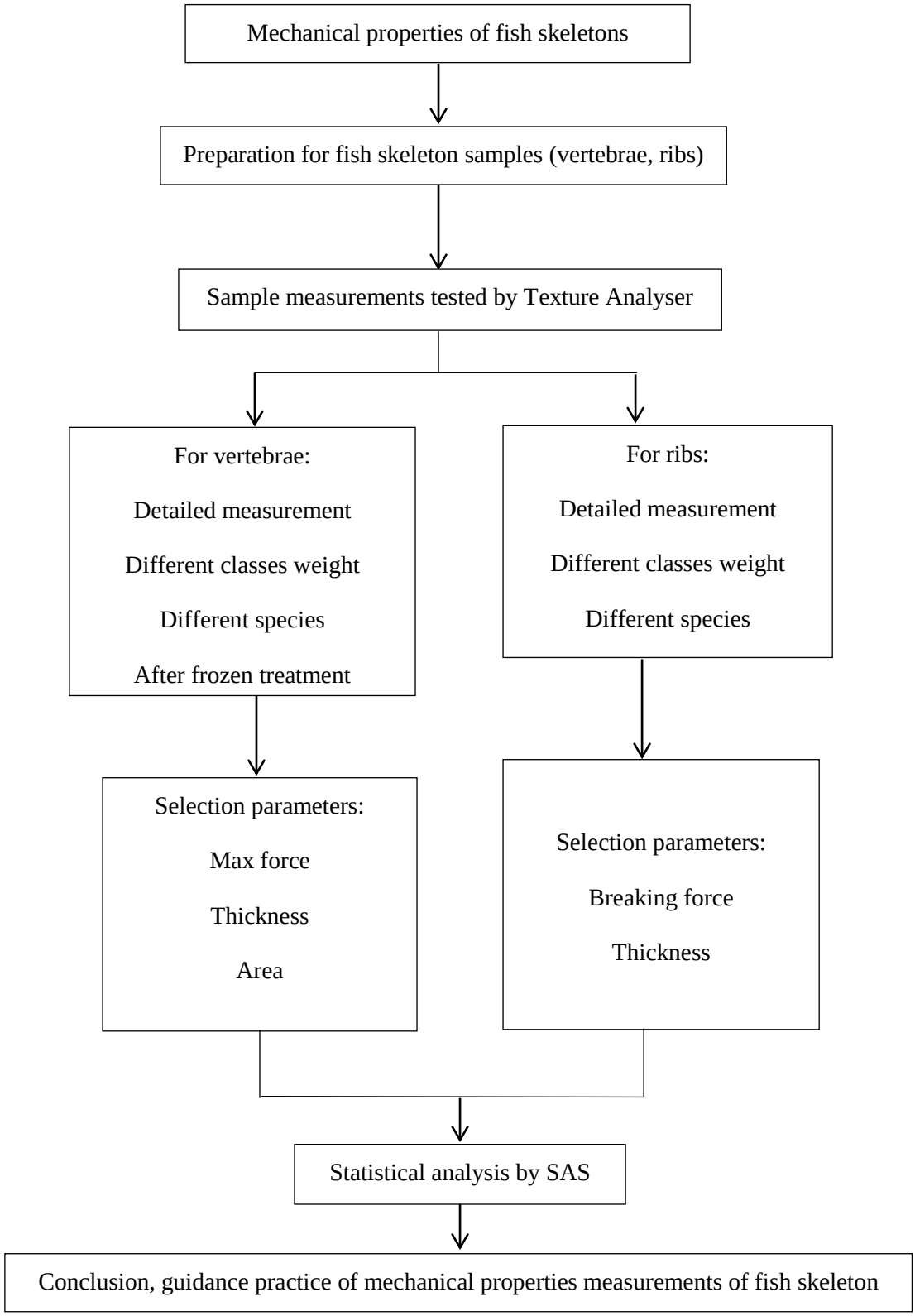
Mechanical properties of fish skeletons
Preparation for fish skeleton samples (vertebrae, ribs)
Sample measurements tested by Texture Analyser
For vertebrae:
Detailed measurement
Different classes weight
Different species
After frozen treatment
For ribs:
Detailed measurement
Different classes weight
Different species
Selection parameters:
Max force
Thickness
Area
Selection parameters:
Breaking force
Thickness
Statistical analysis by SAS
Conclusion, guidance practice of mechanical properties measurements of fish skeleton

2. Background

2.1. Bone structure

Bone is a kind of connective tissues in vertebrates which is composed of bone cells, fiber and matrix (Hall, 2015). The most obvious property of bone is the cell matrix, which has a large amount of calcium salt deposition which in turn results in an adamant texture. The bone structure contains periosteum, bone matrix and bone marrow. The periosteum is a layer full of dense collagen fibers which are tightly attached to the surface of the bones (Markings, 2004). Abundant nerves and blood vessels are distributed in the periosteum and supply nutrients to bones and sensors to nerves (Steele and Bramblett, 1988). In addition, the periosteum includes osteoblasts and osteoclasts, relevant to bone growth and development, proliferation, healing, and rebuilding (Mackie, 2003). Bone matrix is the basis of the bone tissue. Its structure is lamellar-like bone plates. The fibers in the same bone plates are parallel to each other while those of the adjacent bone plates are vertical to each other, which effectively increases the strength of the bones (Currey, 2002). Bone tissue is the main component of the various bones of the skeletal system; its function is to support the body, protect the soft organs, and provide the mechanical infrastructure for movement. Bone marrow fills the medullar cavity and the voids of cancellous bone (Hench and Wilson, 1993, Ratner *et al.*, 2004).

The study of bone is divided into "quantity" (the number and volume of bones) and "quality" (the microstructure, bone collagen, mineralized bone matrix, micro fracture occurance and regeneration ability, etc) (Rubin *et al.*, 2002).

Bone quantity is the sum of bone organic matter and bone minerals. Since there is as of yet no method to measure the bone organic matter in a living body, bone mineral content, also called bone mineral density (BMD), has been determined only in clinical or scientific research, not accurate bone quantity measurement. BMD is a good reference index to indicate bone strength and bone stiffness. In recent years however

researchers have begun to recognize that BMD can only partially show bone strength (Gluer *et al.*, 1994). Bone strength also depends on the quality and the metabolism of the bone. Bone quality will be dictated by bone tissue structure, or in others words, bone microstructure. On this level, bone can also be classified into compact bone and cancellous bone. The texture of the former is formed by tightly entwined bone collagen fibers and is able to withstand great pressure while the latter is a sponge-like structure with many pieces of trabecular bone intertwined (Gibson, 1985, Seeman and Delmas, 2006, Parfitt, 1984)

Seeman has pointed out that BMD can only explain 60 % to 70 % of bone strength (Seeman, 2003). In addition to bone quantity, bone microstructure plays an important role in determining bone strength as well as its biomechanical properties, including the thickness and pore density of the compact bone, and the shape, thickness, connectivity, and anisotropy of cancellous bone. Some studies indicated that bone microstructure is the most significant factor in bone strength, and can be regarded as the key to bone fragility and even function independently from BMD (Dalle Carbonare and Giannini, 2004, Kleerekoper, 2006). Regarding composition, compact bone accounts for 60 % of bone quantity, whereas the effect of cancellous bone is very limited. Therefore, a single measurement of bone quantity is not an accurate measurement of bone gain or loss. Another relevant study has shown that in addition to bone quantity, changes in the architecture of trabecular bone significantly affects the bone strength (Hernandez and Keaveny, 2006).

2.2. Bone research methodology

Bone histomorphometry, a gradually developing area, is a stereology aimed at quantitatively observing and studying bone morphology and structure. This technique has been widely utilized in the diagnosis of metabolical bone diseases and animal experiments. The application of bone histomorphometry not only leads to an understanding of bone characteristics regarding morphology, but provide a quantitative method by which to observe change (Malluche *et al.*, 1982).

The quantitative parameters of cancellous bones mainly include bone mineral density (BMD), bone volume / total volume (BV / TV), connection density (Conn-Dens), structural model index (SMI), trabecular bone number (Tb. N), trabecular bone thickness (Tb. Th), and trabecular bone separation (Tb. Sp). The quantitative parameters of cortical bone include BMD, cortical thickness (Ct.Th), cortical area / total tissue area (Ct. Ar / T. Ar), and bone marrow area / total tissue area (Ma. Ar / T. Ar) (Parfitt *et al.*, 1987).

A large number of studies have shown that quantitative determination of skeletal structure contributes an improved method by which to estimate bone strength. Currently there are numerous methods for detecting the microstructure of trabecular bone, each with its advantages and limitations. These can be generally divided into invasive and noninvasive testing methods. Methods for detecting bone microstructure have developed gradually, from simple to complex, from two-dimensional (2D) to three-dimensional (3D), and from invasive to relatively noninvasive (Cortet *et al.*, 1995).

2.2.1. Invasive testing methods

In traditional bone histomorphometry, the parameters of bone microstructures are gained from the 2D image of mono-layer histological slices. Bone characteristics are then shown to a certain extent via a series of calculations done by software.

Due to the rapid development of science and technology, destructive testing methods are constantly being improved. Beck et al. utilized computer-controlled grinding technology combined with continuous photography through a three-dimensional reconstruction computer program to access the spatial structure image of trabecular bone (Beck *et al.*, 1997). Similarly, Jiang Peng et al. also used conventional trabecular bone staining and cancellous bone embedding technology to see the spatial structure image of trabecular bone (Jiang Peng *et al.*, 2005). However, these type of measurements destroy the integrity of the test object and involve great difficulty in evaluating bone characteristics, especially mechanical properties. It is also necessary

to have experienced experts analyze the two-dimensional and three-dimensional microstructure of trabecular bone. All of these problems limit its use in clinical and scientific research.

2.2.2. Noninvasive testing methods

Ⅰ. Ultrasonic imaging

Quantitative ultrasonometry (QUS) is a new technique that indicates BMD and shows bone structure, elasticity, and brittleness (Hans *et al.*, 1999). This technique has been used to diagnose osteoporosis and predict the risk of fracture (Lin *et al.*, 2001). It uses sound wave reflection and penetration attenuation to evaluate the mechanical properties of bone. The main parameters are ultrasonic sound of speed (SOS) and broadband ultrasound attenuation (BUA). The former is mainly affected by BMD and bone elasticity while the latter depends on BMD and bone microstructure. In addition, it provides information about bone stiffness (Halaba *et al.*, 2005).

Some studies have shown a positive result in the use of QUS to identify osteoporotic fracture (Schott *et al.*, 2005). Osteoporosis is a bone metabolic disease that causes fracture due to a decrease in bone strength and an increase in bone brittleness. Changes in osteoporosis first appear in areas rich in cancellous bone. However, the cortical bone is also involved, and the possibility of fracture is ultimately determined by the cortical bone (Chavassieux *et al.*, 2007). The QUS technique can accurately estimate the porocity and volumetric void of cortical bone, but has the disadvantage that it has a relatively lower accuracy rate when used to measure the changes of bone strength in deep structures.

Ⅱ. Computerized tomography (CT)

CT is a 3D image obtained by a series of X-lines that penetrate the test object. These form an attenuated image, which is then reconstructed by mathematical programming. The resolution of traditional CT cannot distinguish the level of trabecular bones. Thus

far, high resolution computerized tomography (HRCT) and micro-CT (μCT) have been introduced into the study of bone microstructure (Cortet et al., 1998, Link et al., 1998, Cortet *et al.*, 1999)

ⅰ) High resolution computerized tomography (HRCT)

HRCT technique measures the geometric characteristics of bone more accurately than do conventional methods, and can be used to analyze the structure of trabecular bones in a living body (Ito, 2006). Its spatial resolution is however still low. Some parameters can be obtained, but accuracy is sacrificed. Compared to the "gold standard", bone histomorphometry, HRCT overestimates the bone volume fraction (BVF) and underestimates the spatial distance of trabecular bone.

ⅱ) Micro-CT (μCT)

Micro-CT is a relatively noninvasive detection method. It creates a 3D image, which is convenient for observing bone microstructure. The resolution of micro-CT image is high, which make it possible to distinguish cancellous and compact bone. Micro-CT measures the volumetric bone mineral density (vBMD) and tissue mineral density (TMD) that reflects the mineralization of bone tissue. Its morphometric software can provide a large number of trabecular bone space parameters (Mulder *et al.*, 2005). These parameters can be more accurate than the morphometric method, and provide experimental data which cannot be acquired from a 2D method such as the structural model index.

Although micro-CT technique is very advanced and accurate, the cost is high and the technique has its own shortcomings, such as radioactive damage and limitation in observing vision (Ritman, 2002). Moreover, sometimes there is a need to remove the specimen from a living body before analyses.

Ⅲ. Magnetic resonance imaging (MRI)

Magnetic resonance imaging shows the magnetic specificity of material internal nucleus in order to reflect material characteristics. Its imaging capabilities and

methods do not produce ionization of MRI, making it the most attractive imaging tool for the examination of trabecular bones (Majumdar *et al.*, 1996).

High-resolution magnetic resonance (HRMR) and micro magnetic resonance are collectively referred to as MR microscope. MR microscope is a technique for quantitatively measuring the structure of internal bone or isolated trabecular bone specimen. Studies show that the parameters measured by MRI are valuable. When Wehrli used micro-MRI to evaluate the structure of trabecular bone and cortical bone, he pointed out that the obtained results could effectively evaluate the interventional treatment of bone metabolism and prevent of osteoporosis (Wehrli, 2007).

The positive effect of osteoporosis testing via MRI has been recognized, but there are many techniques such as sensitivity, specificity, accuracy, and standardized data processing, and 3D imaging which are still being developed. In addition, the MRI inspection is lengthy, costly, complex, and is currently in the research stage of clinical application (Lester *et al.*, 1995).

2.2.3. Mechanical analysis of bone

Ⅰ. The challenge of bone mechanical analysis

The mechanical properties of bones are defined by their reaction under an applied load or pressure (Fa-Hwa Cheng, 1997). Normally, materials are measured by strength, ductility, hardness, and impact and fracture resistance. The fact that the skeletal structure of an organism is an integrated part of that organism creates a challenge when attempting to measure bone properties. The main factors affecting bone mechanical properties are as follows: ⅰ) Types of organisms vary. Even among the same type of organism there is variation in for example age, sex, lifestyle, growth and developmental conditions. ⅱ) Bone status is to some extent a result of the organism's interaction with its environment. ⅲ) Variation in bone size and shape. Although the lamellar structure of bone makes it possible for it to adapt its function to

its the enviroment, this adds yet another challenge when measuring the mechanical properties of bone.

Ⅱ. Previous studies of bone mechanical properties

The earliest study of the mechanical properties of bone dates back to Galileo's observations in the seventeenth century (Ascenzi, 1993). Galileo proposed that larger vertebrates have disproportionately more robust bones that adapt to mechanical loading, and that this was not only because of the sizes of the vertebrates (Martin, 1999). He also claimed that larger bones are weaker than smaller bones when subjected to the same stress, because the increased weight caused the larger bone to be hollow. These views were however not shared by by most people during the following two hundred years. In the 1830s, Wyman described the architecture of trabecula bones. Bourgery and Ward put forth hypotheses as well, but all of these explanations were proven to be defective (von Meyer, 2011, Wolff, 2012). After studying the human femur, Culmann pointed out that the distribution of trabecular bones followed the direction of major stress. His findings later became the the basis of bone stress trajectories theory (Huiskes, 2000). Wolff 's law was for example also based on these findings, which described bone structure change as a result of mechanical stimulation. This was also regarded as the basis of trabecular architecture (Roesler, 1987, Wolff, 2012). Moreover, Wolff 's hypothesis was able to be expressed as a mathematical model that showed the relationship between bone function and both internal and external structure of bone. However, the code of this "mathematical law" has not yet been cracked (Carter, 1984).

Ⅲ.Bone biomechanics

Bone biomechanics is one of the major branches of biomechanics, and has had contributed significantly to the bio-sciences, medicine, industry, and even our daily lives. For example, achievements in biomechanics have paved the way for advancements in the repair of cartilage injury and in tissue engineering. This alone affirms the importance of this new scientific field (Guilak *et al.*, 2004). Due to these

advancements as well as the the application of engineering technology and the rapid development of high-tech equipment, it is now possible to evaluate the mechanical properties of bone more comprehensively.

Nanoindentation is a new technique in the study of bone biomechanics. It is used to explorer bone composition and the mechanical properties of bone microstructure (Rho and Pharr, 1999, Zysset *et al.*, 1999). The working principle of nanoindentation is to add force to the material being tested by means of a diamond indenter (or other material). It follows the gained stress-strain curve and calculates the mechanical properties of material, such as hardness, elastic modulus, yield strength, etc. (Rho *et al.*, 1999, Ebenstein and Pruitt, 2006). Nanoindentation has many advantages, such as minimal trace of pressing, high spatial resolution, small size of the probe, and no risk of damage to the material being tested, which make it possible to measure small, thin, or anisotropic materials, such as compact bones and trabecular bones (Rho *et al.*, 1999, Zonglai, 2010).

2.3. Fish skeleton structure and function

Fish are vertebrates, which means that they have a vertebral column or "spine". There are two fish categories based on type of skeleton: bony (teleosts) and cartilaginous (elasmobranchs). The skeletons of teleosts consist of bone while the elasmobranchs have cartilaginous skeletons (Mackean, 1969).

According to the growth position, fish skeletons can be divided into axial skeleton and appendicular skeleton. The former refers to the skull, vertebral column, and ribs, while the latter includes the pectoral girdle, pelvic girdle, and actinosts. For all of these, the internal skeleton is buried in muscle. Fish also have an exoskeleton, the external skeleton that supports the body, which includes scales, fin rays and fin spines, etc (Boulenger, 1931). In this study, the focus is on the axiale skeleton, especially the vertebral column and ribs.

As mentioned above, elasmobranchs have a cartilaginous skeletal system and the skeletons of teleosts consist of hard bone matter. This bone can be formed by two differing development paths: ⅰ) Cartilage bones to hard bones: develops throughout the membranous phase, cartilage phase and hardening phase as common bones; ⅱ) Membrane bones to hard bones: membranous phase develops directly into hardness phrase by the ossification of osteoprogenitor cells, but without the cartilage period.

Fish need skeletons for the following reasons: to protect vital organs to support soft tissues - fascia, tendons, ligaments; as anchors for muscles; to manufacture red blood cells; as storage for minerals - calcium, phosphate; and to supply the muscles with an infrastructure for movement (Alexander, 1974).

Morphologically, the vertebral column of fish can be divided into abdominal vertebrae and caudal vertebrae. The two are easily distinguished, because abdominal vertebrae are attached to the ribs while caudal vertebrae are not. The vertebral column's front and back sides are sunken in, known as the amphicoelous vertebra, a characteristic unique to fish. In vertebrates, the basic structure of the vertebral colums originates from fish. The function of the vertebral column is to support the body, protect the spinal cord, haslets, main blood vessels and so on. Each vertebra in both elasmobranchs and teleosts is composed of centrum, neural arch, neural spine, haemal arch, and haemal spine (De Carli and Richardson, 1978, Froese and Pauly, 2012).

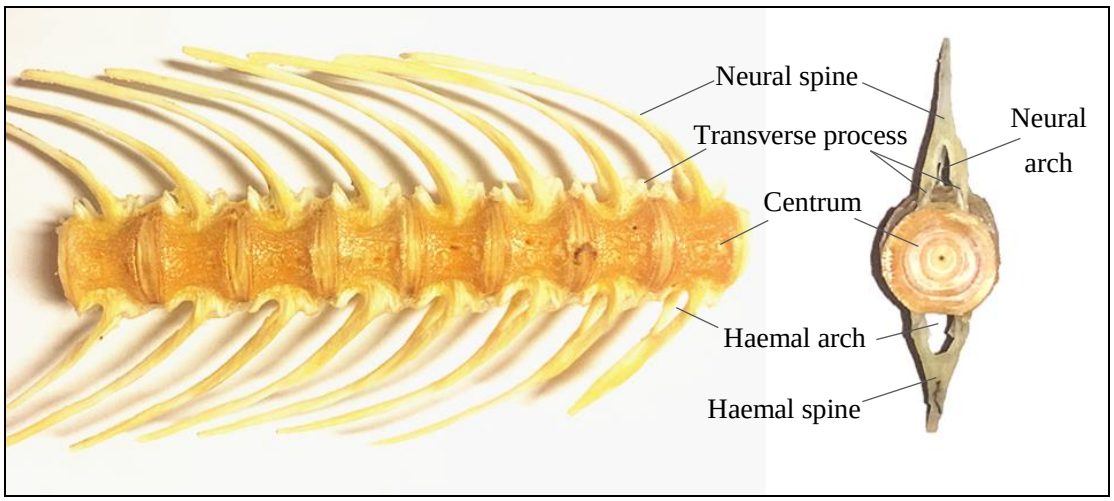

Fig 2.1 Salmon vertebra structure diagram

Fig 2.1 and Fig 2.2 showed the vertebra structure of salmon and carps. Detailed description can be stated as follows:

Centrum: the main part of vertebra load bearing whose interior is full of cancellous bone while the surface of compact bone is thin. The concavity of amphicoelous centrum exists remnant notochord.

Neural arch: a triangular foramen composed of two pedicles that extend from the sides of the vertebral body and pairs of laminae, the broad flat plates that project from the pedicles. The neural arch encloses the spinal cord in order to protect it.

Neural spine: composed of pairs of triangular small bone pieces and connected to each other by ligament.

Transverse process: a small zygopophysis on both sides of the ventral centrum.

Haemal arch and haemal spine: unique to the caudal vertebrae. The hollow archway located below the centrum is contains the tail artery and tail vein. The haemal spine starts from the joint combined with the haemal arch at ventral.

Caudal vertebrae are without transverse processes.

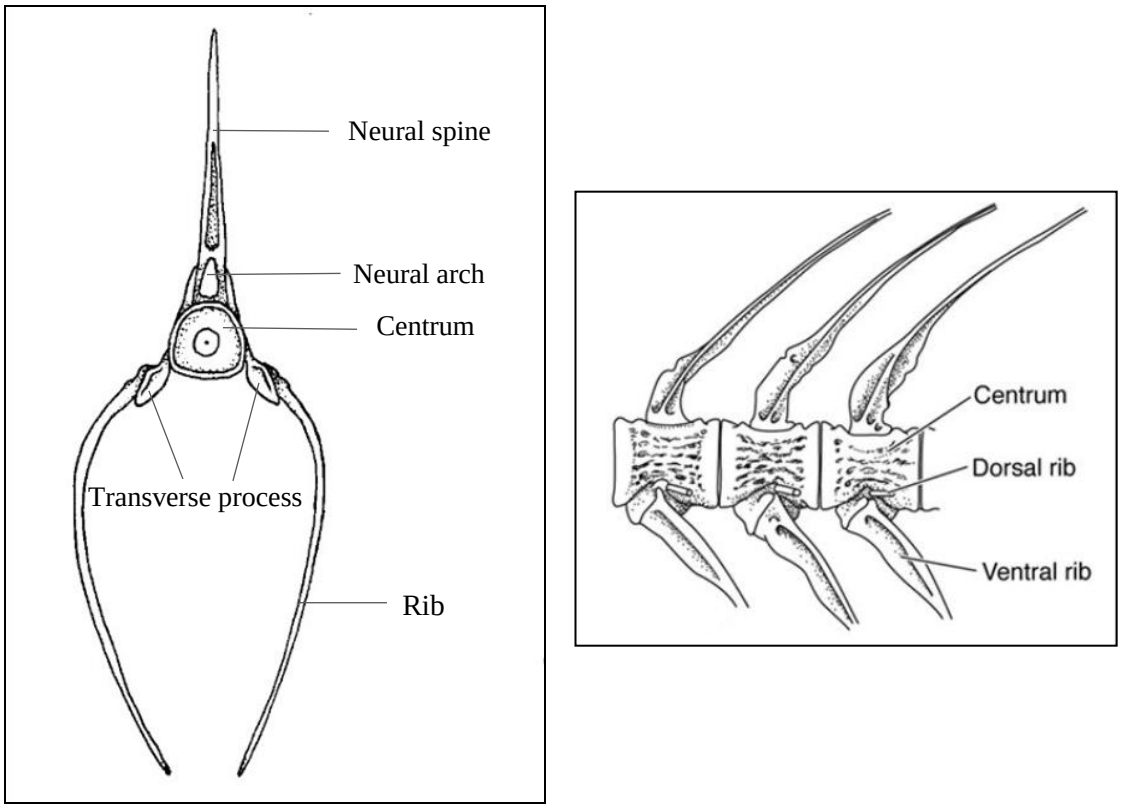

Fig 2.2 Carp vertebra and rib structure diagram (By Ivy Livingstone)

Ribs are components of the axiale skeleton that attach to the transverse process of vertebrae for the purpose of supporting the body and protecting the internal organs. The ribs of teleosts are well developed (Nelson, 1969). They are divided into dorsal ribs and ventral ribs. Regarding material used in the present study, three fish species were analysed: Atlantic Salmon and Rainbow Trout, and common Carp. Atlantic Salmon and Rainbow Trout, that belong to Salmonids, have both dorsal ribs and ventral ribs, while Carp only has ventral ribs.

It should also be noted that carp have intermuscular bone, which is not found in salmonids. Intermuscular bones, or sesame bones in anatomy, are distributed in the myosepta of many fish species, and are partially ossificated by the connective tissue of the myosepta. This type of bone is gradually reduced with the evolution of fish, and has completely disappeared in perciformes (Kyle, 1926, Nelson, 1969).

2.4. Fish vertebrae microstructure

The skeletal system is a hard structure with a series of complex metabolic activities such as constant remodeling and alteration. The entire process involves three types of cells: osteoblasts, osteocytes, and osteoclasts. Histologically, there are two types of bone formation: cellular bone and acellular bone. The latter, without osteocytes and osteoclasts, is easy to distinguish from the former (Moss, 1961, Moss, 1963). Large populations of osteocytes are present in cellular bone, but osteons are absent (Moss, 1965). It is said that osteocytes existed in acellular bone during osteogenesis while dead afterwards. The majority of fish have acellular bone created by osteoblasts, and with the exception of a few phylogenetic primitive teleost species such as salmonids, clopeoids, cydrinidae all are have cellular bone (Horton and Summers, 2009, Krossøy *et al.*, 2009).

The microstructure of fish bone is similar to that of other vertebrates. Acellular bone is regarded as special examples in vertebrates, which consists of unstructured solid matrix. It has been shown that calcium cannot be absorbed into cellular bone, making it impossible for cellular bone to function as a calcium repository (Cohen *et al.*, 2012). In this study, all fish species examined (Atlantic Salmon, Rainbow Trout and Carp) were composed of cellular bone. The report written by Jaquan and Ada (Horton and Summers, 2009) has revealed that although the mechanical properties of acellular bone demonstrated similarities to cellular bone, the mean stiffness of this type of bone is lower than that of fish species that have cellular bone. Despite the mechanical properties of these two type of bones, the mineralization of cellular bone is significantly lower than acellular bone (Cohen *et al.*, 2012).

Since the vertebrae of fish must be stiff enough to provide the necessary support for life activities, an important mechanical characteristic of bone is stiffness (Currey, 2002). This property is affected by both bone composition and its microstructure (Fratzl and Weinkamer, 2007). One of the determining factors is the porosity at the microscale (1-100μm). Normally, bone stiffness will decline if bone porosity

increases. When observed by means of a scanning electron microscope, it is clear that bone is a sandwich-like structure, a combination of compact bone on the surface and cancellous bone with multi-cell at its core. If the volume of solid bone is more than or equal to 70 %, it is known as compact bone. Conversely, if the volume is less than 70 %, it is cancellous bone or trabecular bone (Gibson, 1985).

Cancellous bone is a porous structure connected by a large number of acicular or flaky trabecular bone. These trabecular bones configurate according to the rules of tensile curve, with uneven anisotropy, which will increase the ability of bone to withstand mechanical stress (Yingjian,1996). Studying the anisotropy of cancellous bone is the key to the accurate biomechanical analysis.

Nordvik (Nordvik *et al.*, 2005) divided vertebra into four layers from the scanning images performed in a microcomputed tomography system (SkyScan 1072, SkyScan NV, Aartselaar, Belgium). The first layer, called chordacentrum, formed as a mineralized circular zone. It is said that the first chordacentrum appears in the area below the dorsal fin, then grows gradually toward the head and tail. The second layer is formed by thin collagen fibres surrounding the entire spinal cord. The direction of these continuous fibres are generally longitudinal. From the longitudinal-sectional profile of the second layer, it was observed to be tapered, thinnest closet to the chordacentra and thickest outside the intervertebral ligament. The third layer consists of a bone with collagen fibres circularly distributed externally around the amphicoelous centrum. Osteoblasts deposited osteoid in this layer leaded to the mineralization of layer 2. Layers 2 and 3 developed into the compact bone of the vertebra. Layer 3, which consists of a large number of osteoblasts, makes up the majority of this compact lamellar bone. The fourth layer has a less dense structure compared with the second and the third layers, and is composed of cancellous bone. Cancellous bone are mainly vertical and horizontal beams as stress oriented that form layer 4 into prismatic structure (Fig 2.3).

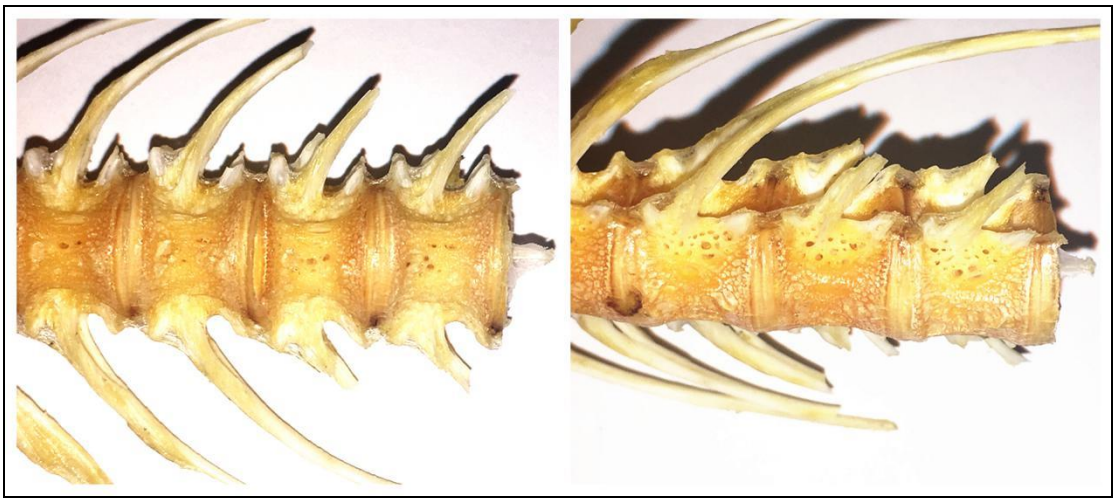

Fig 2.3 Cancellous bone of the salmon vertebrae viewed from the front and side

2.5. Composition and application

During processing of fish products, fish bone is considered a by-product and is always discarded. Relevant statistics show that marine fish waste, such as fish skull and spine, make up 15 % of the raw material, but has a low utilization rate (Richardsen *et al.*, 2015, Slizyte *et al.*, 2016). Other than being processed into fertilizer or feed, efficient utilization of fish bone is still an unsolved problem that needs to be addressed as soon as possible.

Regarding composition, fish bone have high potential for utilization. First, the proportion of protein content is approximately 15 %, which indicates a high biological value (BV) (Martínez-Valverde *et al.*, 2000, Toppe *et al.*, 2007). Second, fish bone is rich in calcium, phosphorus, and other trace elements essential to the human body. Nutritionists have documented that regular intake of fish bone products help preventing osteoporosis. Third, fish bone is not only rich in calcium, but the calcium and phosphorus ratio is also favorable (Chiling *et al.*, 2007). It is generally considered that the body can easily absorb calcium via a supplement that includes fish bone. Moreover, collagen and chondroitin that is beneficial for human skin, can also be

extracted from fish bone. It appears that extracting bone oil might be another way to utilize fish bone.

Compared with mammals, fish bone seems to lack of concern in its physical and chemical properties, which may be a big loss. Szpak reports that fish bone is more prone to experience biotic and abiotic degradation than is mammalian bone (Szpak, 2011). As has been mentioned, the mechanical properties of fish bone exhibit considerable variability, Unfortunately, less attention has been paid to the composition of fish bone than to the bones of mammals. The amino acid composition of fish bone differs considerably from that of mammals, especially in regard to hydroxyproline content. Furthermore, the proportion of ash content and BMD values show that the bone of fish is less mineralized than that of other vertebrates.

Bioapatite, largely distributed in the mineral phase of bone, contributes primarily to two functions in mineralized tissues. One is to improve mechanical performance, such as adding bone stiffness and strength to the structure. The other is physiological support, such as a simple mental reservoir (Lee *et al.*, 1986). The size and the ordering of bioapatite crystals are very similar in fish and mammalian bone, which enables fish bone to be used as an ideal replacement material in some fields.

In order to understand the resources of fish bone and improve the economical value of fish, it is necessary to compare regular composition in fish bones. The main chemical components of fish bone are ash, protein, water, and lipid (Toppe *et al.*, 2007). Calcium and phosphors constitute the major part of the ash. In this study, the concentration was on fat content, dry matter, and ash.

3. Meterial and Method

3.1. Fish samples

On 1 April, 2016, a total of 30 farmed Atlantic salmon (*Salmo salar*, L.) from Sotra Fiskeindustri (SF), Sotra, Bergan, Norway, including three weight classes (4 kg, 5 kg, 6 kg, 10 fish per weight), were collected and stored on ice for 7 days before being filleted. After the samples were filleted, the remaining skeletons were on ice for an additional day before mechanical analyses. Detailed information of whole fish sample group was showed in Table 3.1.

Table 3.1 Fish sample information for 4kg, 5kg, 6kg Atlantic salmon

Fish	Weight class	Number of fish	Average body weight (g)	Maximum weight (g)	Minimum weight (g)	Average length (cm)
Atlantic salmon	4	10	4098.2 ± 63.0	4354	3805	69.5 ± 0.5
Atlantic salmon	5	10	5140.1 ± 55.2	5474	4935	74.5 ± 0.4
Atlantic salmon	6	10	6175.4 ± 70.4	6470	5864	77.0 ± 0.4

Carps (*Cyprinus carpio*, n=9) farmed at the facilities of Czech Republic University were slaughtered on 16th April, 2016 and immediately at -20 °C and transported in frozen state to Norway. The fish were thawed at 4°C after 7 days of frozen storage. Detailed information of carp was showed in Table 3.2.

Table 3.2 Fish sample information for carp

Fish	Number of fish	Average body weight (g)	Maximum weight (g)	Minimum weight (g)
common Carp	9	1209.6 ± 49.3	1358.3	910.6

20 skeletons of Rainbow trout (*Oncorhynchus mykiss*) and 17 skeletons of Atlantic Salmon were collected on 28th and 29th April respectively from Sotra Fiskeindustri (SF). 10 skeletons for each salmon and trout were analysed fresh. The remaining

skeletons were frozen at -20 °C for 7 months before analysing after thawing at 4°C overnight. Detailed information of skeleton sample group was showed in Table 3.3.

Table 3.3 Fish sample information for skeletons of Atlantic salmon and Rainbow trout

Fish Skeleton	Number of fish	Origin	Average vertebrae length (cm)
Atlantic salmon	17	Random fish from SF*	62.4 ± 1.3
Rainbow trout	20	Random fish from SF*	53.2 ± 0.5

*Sotra Fiskeindustri, Sotra, Bergan, Norway

3.2. Vertebral column dissection and measurement

Before dessection, all of the skeletons were labeled. Vertebrae were cut along the vertebral column with shears, as close as possible to the centrum from the tail to the head. Excess connective tissue covering the vertebrae was removed with the blunt side of shears. Vertebrae analyses were performed instrumentally (TA-XT2 Texture Analyser, Stable Micro Systems, Surrey, UK) by compressing a guillotine knife (70 mm width, 3 mm thickness) into the middle position of the vertebra with trigger force 1 Newton at 2 mm/sec until it reached 70 % of the vertebra thickness (Fig 3.1). Each vertebrae column was measured every fourth started from the tail.

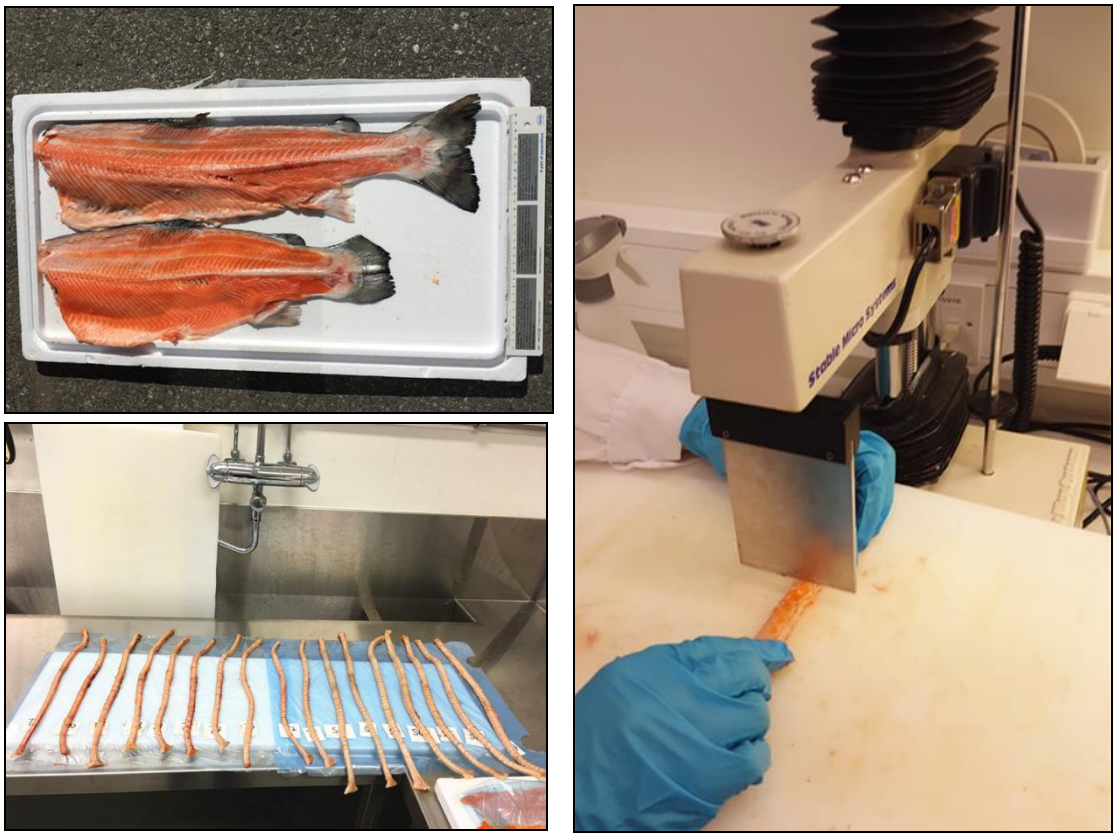

Fig 3.1 Vertebral column dissection and measurement

3.3. Rib dissection and measurement

Ribs were dissected from the right side of fresh samples but left side of frozen samples because of the long-term freezer storage. Every second rib was cut from the skeleton from anterior to posterior with a scalpel. For the 5 kg and the 6 kg Salmon samples, only the twelfth and fourteenth ribs were cut, which is in line with the considerable amount of research that has demonstrated a sizable chance of bone deformity between these two ribs (Mørkøre *et al.*, 2015, Wang, 2016). Excess connective tissue was removed by scalpel. Rib analyses were performed instrumentally (TA-XT2 Texture Analyser, Stable Micro Systems, Surrey, UK) by pressing a guillotine knife (70 mm width, 3 mm thickness) into three position (A, B, C) of each rib with a trigger force of 1 Newton at 2 mm/sec until it broke the rib (Fig 3.2, Fig 3.3). For the 5 kg and 6 kg Salmon samples, only position B was tested. Four Carp samples were measured with three positions and the others were measured at

position B position instead. The force (N) required to puncture the rib surface (termed stiffness) was registered by the resulting time-force graph.

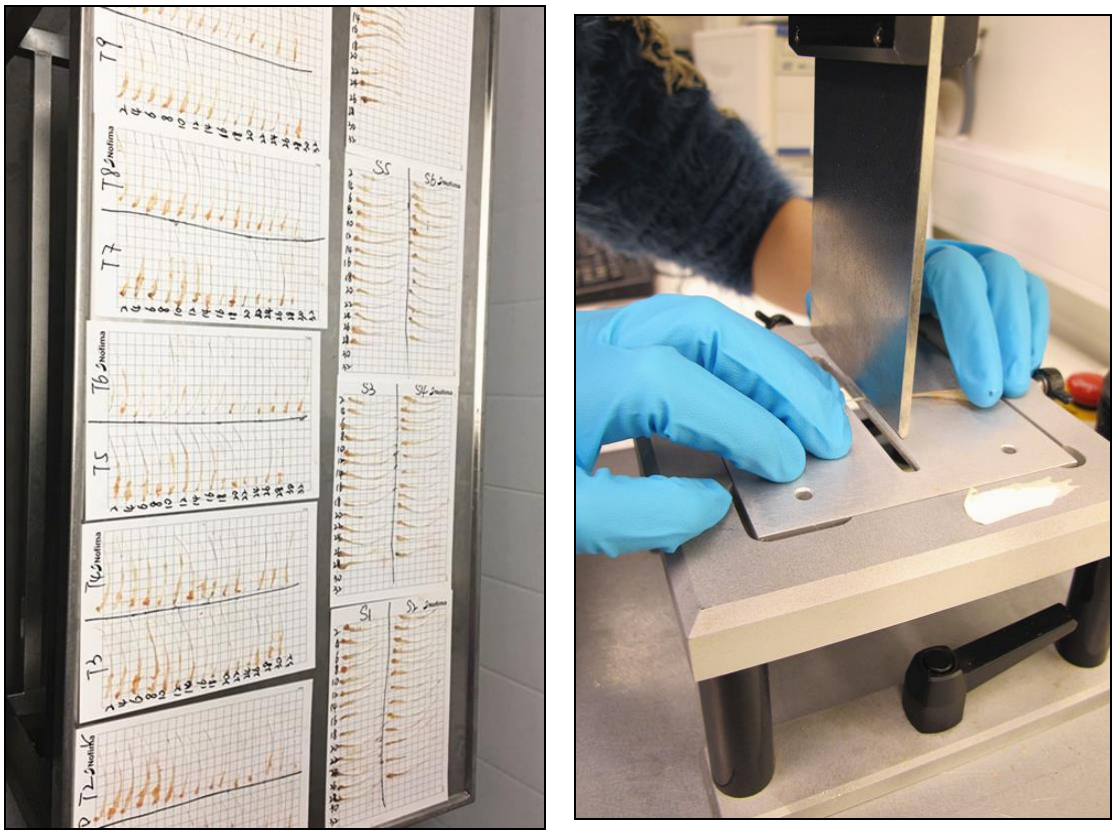

Fig 3.2 Rib dissection and measurement

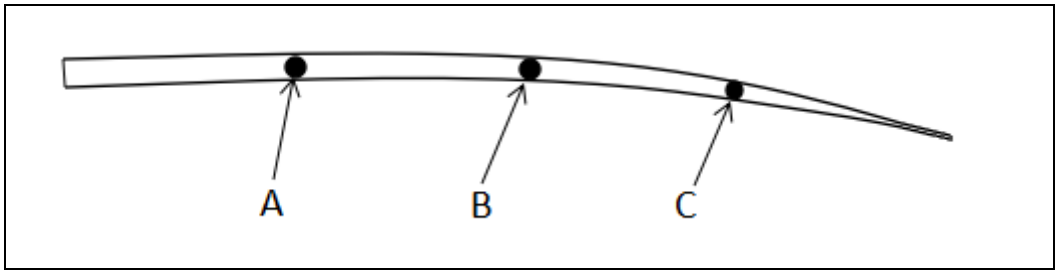

Fig 3.3 Position A, B, C for rib measurement

3.4. Overview of the fish material used in the study

All the fish materials from whole fish group (4 kg, 5 kg and 6 kg Atlantic Salmon and common carp), fish skeleton group (Atlantic Salmon and Rainbow Trout) were measured at various skeleton parts in accordance to Table 3.4.

Table 3.4 Overview of the fish material used in the study

Sample	Vertebrae	Rib	Rib position
Salmon			
4 kg (n=10)	V4-V48	R2-R22	A,B,C
5 kg (n=10)	V8, V12,V32,V36	R12, R14	A,B,C
6 kg (n=10)	V8, V12,V32,V36	R12, R14	A,B,C
Note: Sampled as whole fish from fish processing company			
Fresh sample			
Salmon (n=10)	V4-V52	R2-R22	R12, R14 for A, B, C
Trout (n=10)	V4-V52	R2-R22	R2-R22 for A, B, C
Carp (n=9)	V4-V28	R2-R14	5 fish for B; 4 fish for A, B, C
Note: Salmon and trout sampled as skeletons from fish processing company; Carp sampled from research farming facilities			
Frozen sample			
Salmon (n=7)	V4-V52		
Trout (n=10)	V4-V52		
Note: Sampled as skeletons from fish processing company			

3.5. Composition analysis

Samples of vertebral column were collected by cutting three representative sections (V8-V12 stands for posterior vertebral column, V20-V24 stands for mid vertebral column, V32-V36 stands for anterior vertebral column) from the vertebral column of each frozen Salmon and Trout, and labeled S1, S2, S3 and T1, T2, T3, and V8-V12, V20-V24, V32-V36, respectively. The flesh was removed from the vertebrae manually, and the bone tissue was thoroughly cleaned with a soft and cleaning brush, with 0.9 % NaCl solution. The samples were then dried with paper towel and broken

up with a hammer. The pooled samples for each section (S1-S3 and T1-T3) were mashed in a blender (Waring Commercial blender, Waring Commercial, CT, USA) by adding solid carbon dioxide. They were then immediately frozen and stored at -20° C before analysing.

3.5.1. Fat content

The fat content extraction procedure was done according to Folch extraction principles (Folch *et al.*, 1957). The Folch extraction solution is a mixture of polar (water and methanol) and non-polar solvents (organic chloroform). Due to fat has low solubility in water while can be dissolved in organic solvents, in Folch method, fat was extracted by organic solvent and kept in organic phase referred to this principle of the similar polarity between organic solvent and fat. The fat content was the mass difference after evaporation of this organic phase.

First, a 2 g homogenized sample was placed into a 100 ml Erlenmeyer flask and 6 ml 0.9 % NaCl was added. The content was mixed. A control group was set up in the same way. Then Fifty ml chloroform:methanol (2:1) was added, which contains 0.7 mg/l antioxsidant BHT (2,6-Di-t-butyl-p-cresol). It was homogenized with a homogenizator (T25 digital Ultra Turrax, IKA Werke GmbH & Co. KG, Breisgau, Germany) at the speed of 17×1000 rap for 60 seconds. The procedure (adding 6 ml 0.9% NaCl and homogenize for 5 seconds) was repeated. After being set aside for 2 hours, the homogenate was filltered through a cotton filter inside a funnel into a graded cylinder. The cylinders were covered with lids and kept in laminar flow until the next day. The upper phase was removed with a water-vacuum pump and the lower phase (20ml) was moved with a pipette to a 25 ml empty beaker which had already been weighed. The beakers were all placed on a heating plate (Metoer L5 heating plate, Engmark Meteor AS, Oslo, Norway) in order to allow the chloroform to evaporate, and were left there until dry.

The fat content was calculated according to the formula below:

$$\% \text{ fat} = \text{g fat} \times 100 / \left(\frac{I \times U}{37.5} \right)$$

g fat = evaporated sample in beaker

100 = %

I = weight of the sample in g

U = Pipetted chloroform extract (20ml) in ml beaker

37.5 = Total volume of solvent (33.3 ml × 100/89) = 37.5 ml

(Chloroform in extract solution = 50 × 2/3 = 33.3 ml)

3.5.2. Dry matter and ash

An approximately 2 g homogenized sample was placed into a 25 ml beaker and dried in the heating chambers (Binder FD 23 Drying and heating chambers Classic.Line with forced convection, Binder, Tuttlingen, Germany) at 102° C with a fan speed of 3 for 19 hours. The samples were left in the cabinet for cooling for 20 min before the dry matter was weighed.

Before the ash was measured, the dry matter samples were placed into the cabinet at 102° C with fan speed 3 for 3 hours. They were then cooled in a desiccator and transported to the Muffle ashing furnace (Nabertherm Program Controller S17 Muffle ashing furnace, Nabertherm, Lilienthal, Germany). Furnace program P1 was used as below:

Step 1: 30 min heating until 105° C, held for 3 hours.

Step 2: 30 min heating until 200° C, held for 2 hours.

Step 1: 60 min heating until 550° C, held for 16 hours.

When the procedure was over, the furnace was turned off and and we waited for the temperature to decrease to under 350° C. The ash samples were removed, place into the desiccator and transported to be weighed.

3.6. Statistical analysis

The data for individual vertebrae and ribs were statistically evaluated using the GLM procedure in SAS (version 9.4 TS Level 1M2, SAS Windows Version; SAS Institute, Cary, NC, USA).

For the effect (mainly focus on thickness, maximum compression force and compression force at a specific thickness of vertebra) of fish vertebrae profiles, results were presented as LSmean (Least Squares Means) ± SE (Standard Error Mean). Variation influenced by different vertebra locations, different weight classes, different fish species and frozen storage were analysed and ranked by Least Squares Means. The significance level between treatments was set to $P < 0.05$.

For the effect (mainly focus on thickness, breaking force) of fish ribs profiles, results were presented as LSmean ± SE. Variation influenced by different rib locations, different rib positions, different weight classes and different fish species were analysed and ranked by Least Squares Means. The significance level between treatments was set to $P < 0.05$.

For the chemical compositions of fish vertebrae profiles, results were presented as LSmean ± SE. Variation influenced by different vertebrae sections and different fish species were analysed and ranked by Least Squares Means. The significance level between treatments was set to $P < 0.05$.

4. Results

4.1. Mechanical properties of salmon vertebrae

Vertebrae along the vertebral column were characterized by mechanical analyses of every forth vertebrae of 4 kg Atlantic Salmon (*Salmo salar* L.).

The average vertebrae thickness ranged from 8.9 mm to 10.4 mm (Fig 4.1). Numerically, the vertebrae thickness increased gradually from the tail (V4) to the mid-section of the column (V20-V24). Thereafter the numerical thickness decreased towards the head, reaching a minimum at V40-44. The numerical thickness of the vertebrae closest to head (V48) was similar to that closest to tail (V32). Statistical analyses revealed that the vertebrae thickness of V8-V32 was not significantly different, while V40-V44 was significantly thinnest.

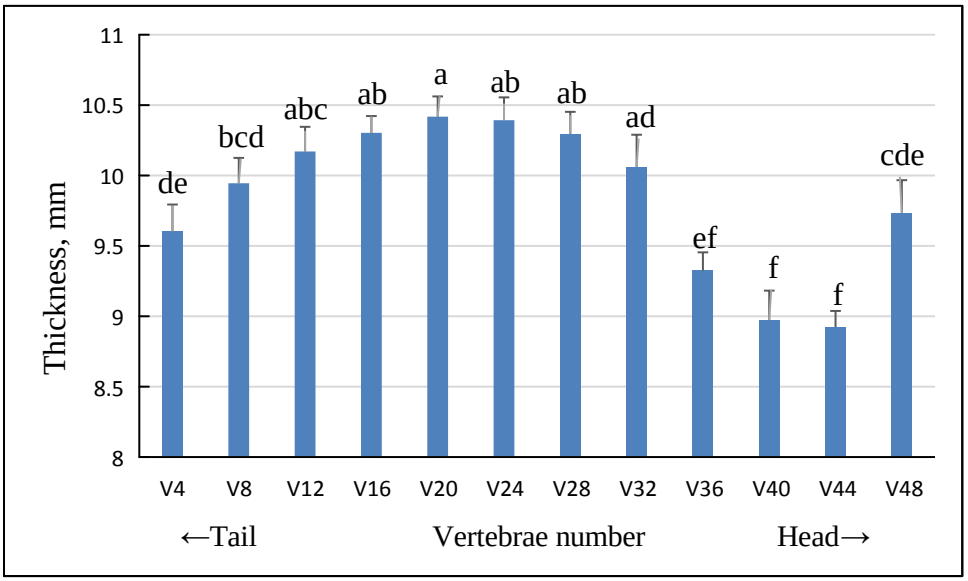

Fig 4.1 Thickness (mm) of every fourth vertebrae (V4-V48) along the vertebral column of 4kg Atlantic Salmon. Results are shown as LSmean ± SE (n = 10). Vertebrae not sharing the same superscripts above the error bars are significantly different ($P < 0.05$).

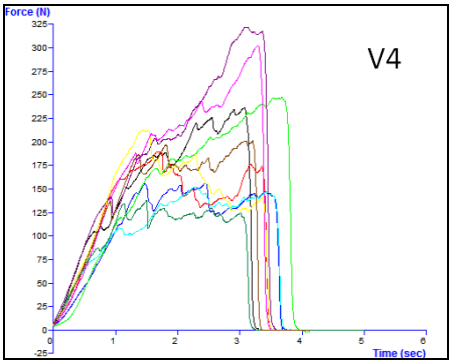

Vertebra 4

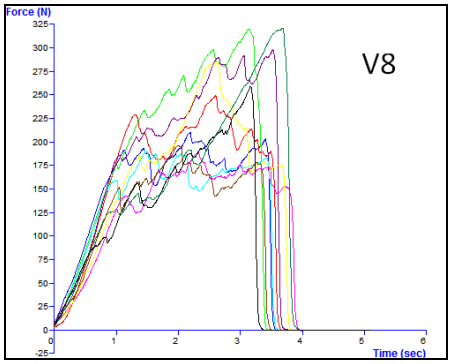

Vertebra 8

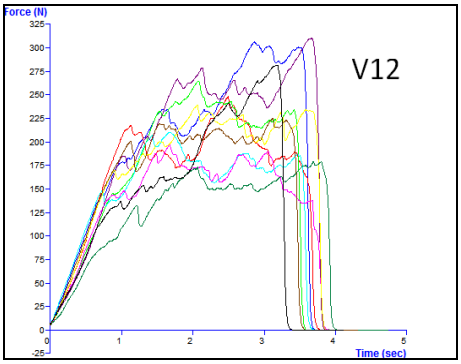

Vertebra 12

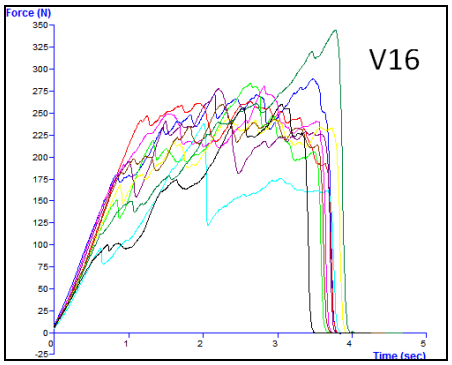

Vertebra 16

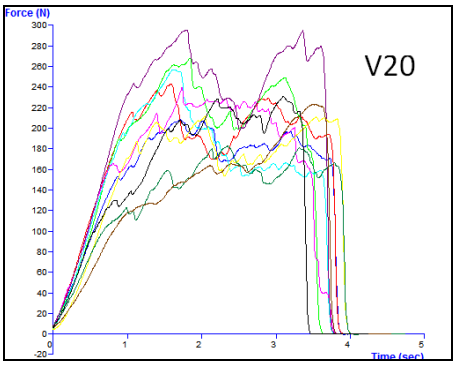

Vertebra 20

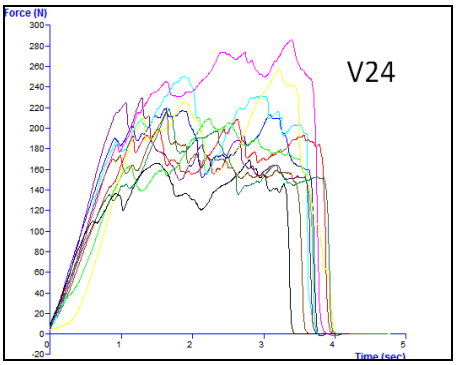

Vertebra 24

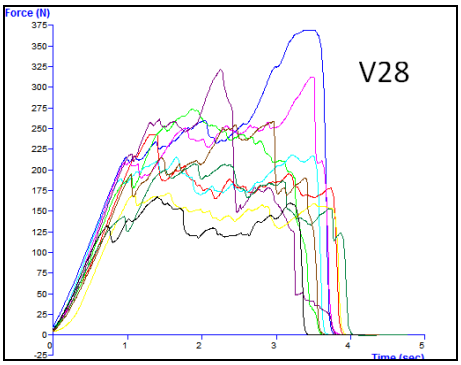

Vertebra 28

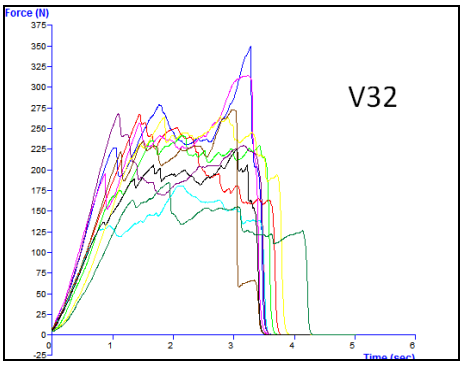

Vertebra 32

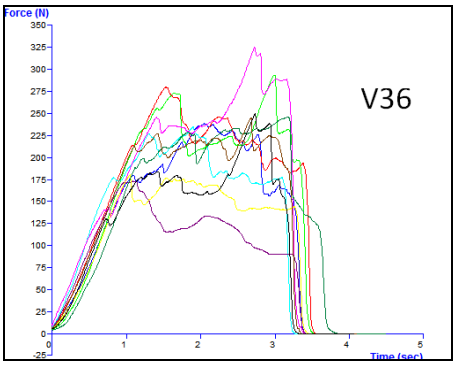

Vertebra 36

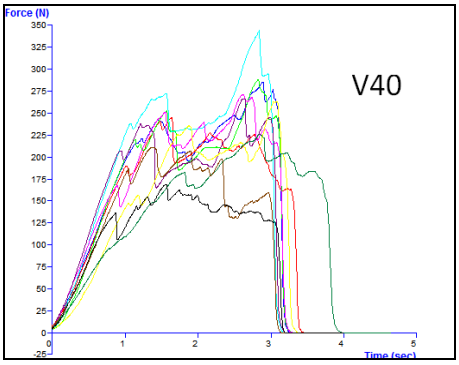

Vertebra 40

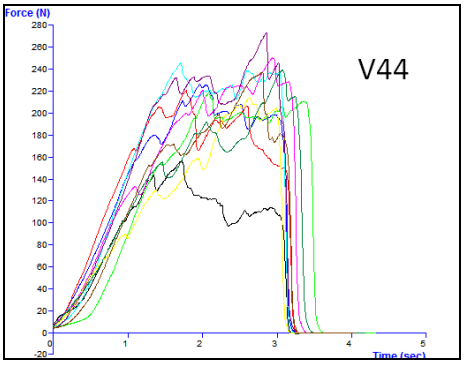

Vertebra 44

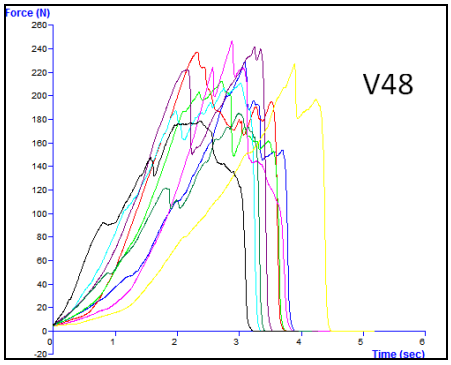

Vertebra 48

Fig 4.2 Force-time graphs for every fourth vertebra (V4-V48) of 4 kg Atlantic Salmon.

The resulting force-time graphs for each vertebra of 4kg salmon are illustrated in Fig 4.2 (all fish, n = 10) and Fig 4.3 (average for the 10 fish). From Fig 4.2 it appears that there was a notable variation between individuals regarding the graph profile (i.e. mechanical properties).

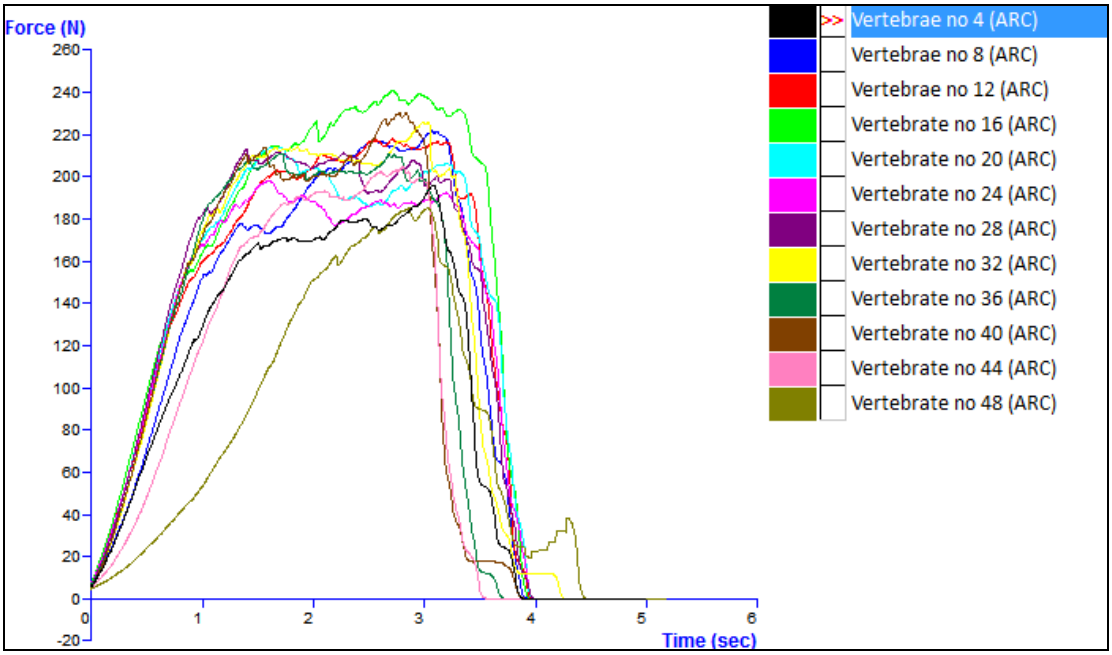

Fig 4.3 Total average force-time graphs for every fourth vertebra (V4-V48) of 4 kg Atlantic Salmon.

The average value of maximum compression force ranged from 216.3 N to 275.3 N (Fig 4.4). Numerically, the maximum force increased gradually from V4 to V16, and achieved the highest value at V16. Then, the numerical force tended to decrease at the mid-section of the column (V20-V24), which was the numerically thickest part of the column (Fig 4.1). Towards the head, the vertebrae thickness decreased, reaching the lowest thickness at V40-44. Statistical analyses showed that the vertebrae maximum compression force between V8 and V40 was not significantly different. With the exception of the V24, the vertebrae close to head (V44-V48) and tail (V4) had lower max compression force.

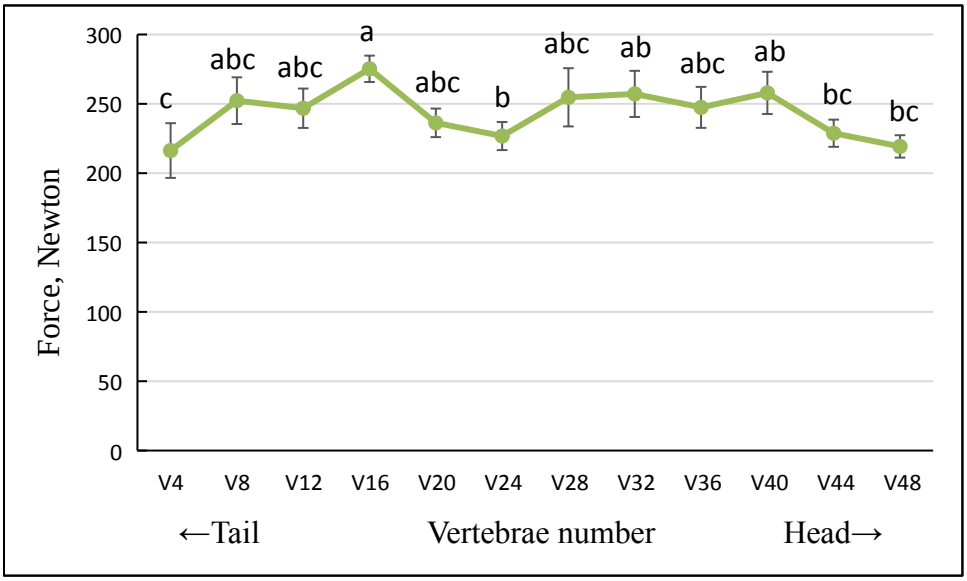

Fig 4.4 Maximum compression force (Newton) of every fourth vertebrae (V4-V48) along the vertebral column of 4 kg Atlantic Salmon. Results are shown as LSmean ± SE (n=10). Vertebrae not sharing the same superscripts above the error bars are significantly different ($P < 0.05$).

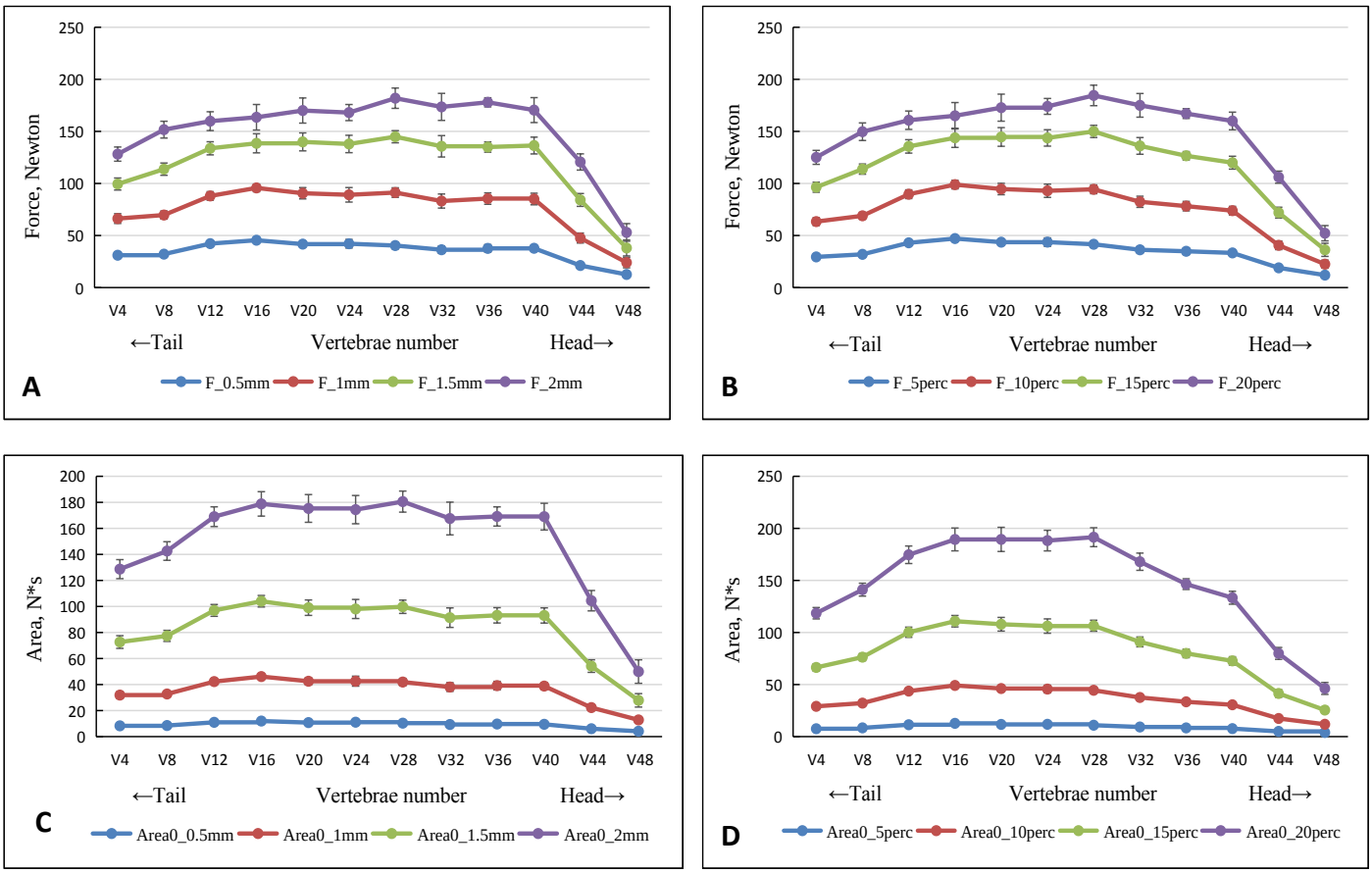

Fig 4.5 The force (N) and the total work (Area, N*s) required to reach at different compression depth: 0.5 mm, 1 mm, 1.5 mm, 2 mm and strain: 0.5 percent, 1 percent, 1.5 percent, 2 percent of every fourth vertebrae (V4-V48) along the vertebral column of 4 kg Atlantic Salmon. (A) Force at 0.5-2 mm compression depth. (B) Force at compression depth of 5-20 percent

of the vertebra thickness. (C) The total work (Area, N*s) required to reach the different points at 0.5-2 mm compression depth. (D) The total work (Area, N*s) required to reach at 5-20 percent compression related to the thickness of the vertebra. Results are shown as LSmean ± SE (n=10).

Table 4.1 Results from statistical analyses of results presented in Fig. 4.5

	V4	V8	V12	V16	V20	V24	V28	V32	V36	V40	V44	V48
Force (N)												
0.5 mm	c	c	ab	a	ab	ab	ab	bc	bc	abc	d	e
1 mm	c	bc	a	a	a	a	a	ab	a	a	d	e
1.5 mm	c	bc	ab	a	a	a	a	a	a	a	cd	e
2 mm	de	cd	abc	abc	abc	abc	a	abc	ab	abc	e	f
5 percent	d	d	ab	a	a	a	abc	bcd	cd	d	e	f
10 percent	d	d	ab	a	ab	ab	ab	b	c	d	e	f
15 percent	e	de	abc	ab	ab	ab	a	abc	bcd	cd	f	g
20 percent	c	bc	ab	ab	ab	ab	a	a	ab	ab	d	e
*Area(N*s)*												
0-0.5 mm	d	cd	ab	a	ab	ab	abc	bcd	bcd	bcd	e	f
0-1 mm	c	c	ab	a	ab	ab	ab	bc	abc	bc	d	e
0-1.5 mm	c	bc	a	a	a	a	a	ab	a	a	d	e
0-2 mm	cd	bc	a	a	a	a	a	ab	a	a	d	e
0-5 percent	c	c	a	a	a	a	ab	bc	c	c	d	d
0-10 percent	d	cd	ab	a	a	a	a	bc	cd	d	e	e
0-15 percent	e	de	ab	a	a	a	a	bc	cd	de	f	g
0-20 percent	e	d	ab	ab	ab	ab	a	bc	cd	de	f	g

Note: Vertebrae not sharing the same letter within the same row are significantly different ($P < 0.05$).

Compare with Fig. 4.5 A and Fig. 4.5 B, whether at 2 mm or 20 percent of the vertebrae, the compression force ranged no more than 200 Newton. As shown in Fig. 4.5 C and Fig. 4.5 D, the total work (represented by the "area" under the graph) required to reach 2 mm and 20% compression depth was both less than 200 N*s. The variation in force at various compression depth showed a similar pattern when measured as force (N) at 0-2 mm compression depth (Fig. 4.5 A) or 5-20 percent compression depth (Fig. 4.5 B). The force was increasing from V4-V12 (Table. 4.1), being stable from V12-V28. From V28-V40 the force was either stable or decreasing, but from V40-V48 the force was consistently decreasing. The total area (Fig. 4.5 C and Fig. 4.5 D) showed similar, but more significant variation in pattern. The most significant variation was observed at 0-20 percent compression depth. In addition,

V12-V28 was the common section of vertebral column that did not show significantly difference.

4.2. Vertebrae comparison of different salmon weight classes

Vertebrae along the vertebral column were characterized by mechanical analyses of the eighth, twelfth, thirty-second and thirty-sixth vertebra (V8, V12, V32, V36) of different sizes (4 kg, 5 kg, 6 kg) of Atlantic Salmon.

The average vertebrae thickness of the three weight classes of salmon ranged from 9.3 mm to 12.0 mm (Fig 4.6). A significant increased vertebrae thickness was observed with increasing body weight, from 4 kg to 6 kg. Statistical analyses revealed that the thirty-sixth vertebra was significantly thinner than the eighth, twelfth, and thirty-second vertebrae in all weight classes of salmon, whereas no significant difference was found in the thickness of the eighth, twelfth, or thirty-second vertebra within the same size of salmon, with the exception of 6 kg salmon at V32.

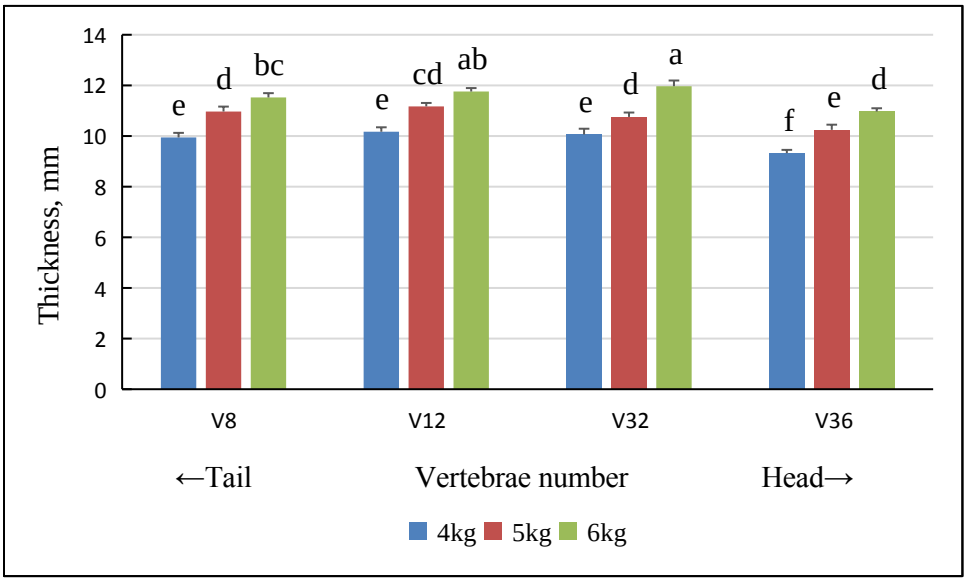

Fig 4.6 Thickness (mm) comparison of the eighth, twelfth, thirty-second and thirty-sixth vertebra (V8, V12, V32, V36) along the vertebral column of different weight classes (4 kg, 5 kg, 6 kg) Atlantic Salmon. Results are shown as LSmean ± SE (n=10, with the exception of V8 of 6 kg where n=9, V12 of 6 kg salmon where n=8). Vertebrae not sharing the same superscripts above the error bars are significantly different ($P < 0.05$).

Average maximum compression force of three sizes of salmon ranged from 246.8 N to 325.7 N (Fig 4.7). The patterns of 4 kg and 5 kg salmon showed a clear similarity, while that of the 6 kg salmon showed a dissimilarity. Numerically, the maximum force increased from V12 to V32 of 4 kg and 5 kg salmon, but decreased in the same section of 6 kg salmon. Table 4.2 showed that significant difference of maximum force appeared among measured vertebrae in 4 kg salmon as well as 6 kg salmon, whereas for the 5 kg salmon, the maximum compression force of all measured vertebrae did not demonstrate a significant difference. Vertebra 8 and Vertebra 12 of 4 kg salmon showed a significant difference in maximum compression force compare with other two weight classes. 5 kg salmon also presented a significant variation in maximum compression force at V32.

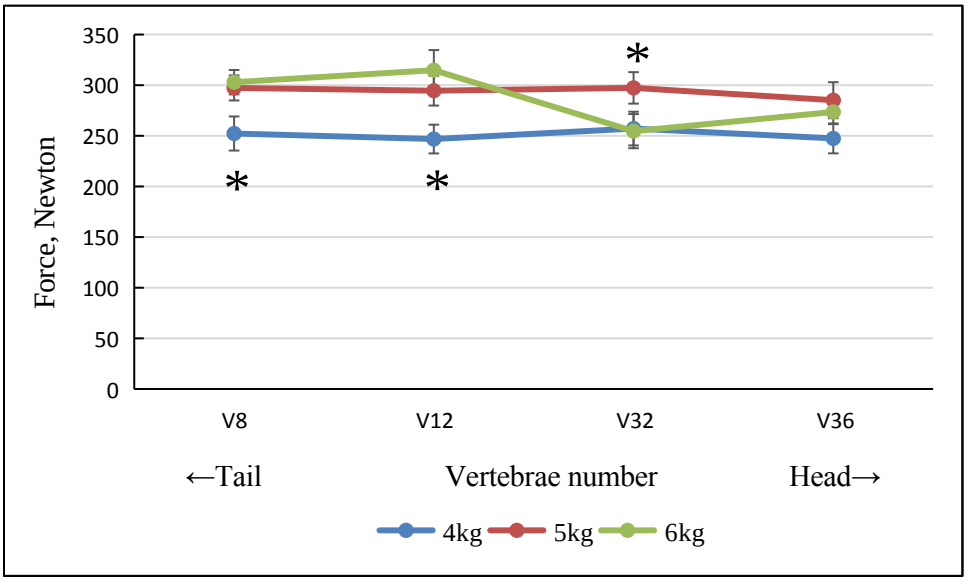

Fig 4.7 Maximum compression force (N) of the eighth, twelfth, thirty-second and thirty-sixth vertebra (V8, V12, V32, V36) along the vertebral column of different weight classes (4 kg, 5 kg, 6 kg) of Atlantic Salmon. Results are shown as LSmean ± SE (n=10, with the exception of V8 of 6 kg where n=9, V12 of 6 kg where n=8). Vertebrae with "*" in the figure not sharing the same letter with other weight classes are significantly different ($P < 0.05$).

Table 4.2 Results from statistical analyses of results presented in Fig 4.7

	V8	V12	V32	V36
4kg	e	e	cd	e
5kg	abc	ad	abc	ae
6kg	ab	a	de	be

Note: Vertebrae not sharing the same letter within the same row are significantly different ($P < 0.05$).

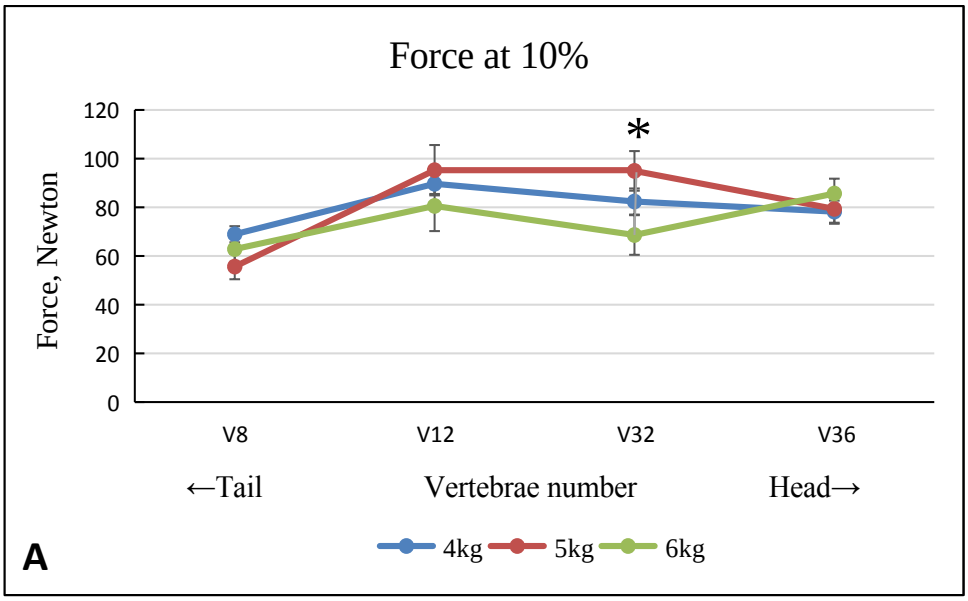
Force at 10%
120
100
80
60
40
20
0
Force, Newton
*
V8
V12
V32
V36
←Tail
Vertebrae number
Head→
4kg
5kg
6kg
A

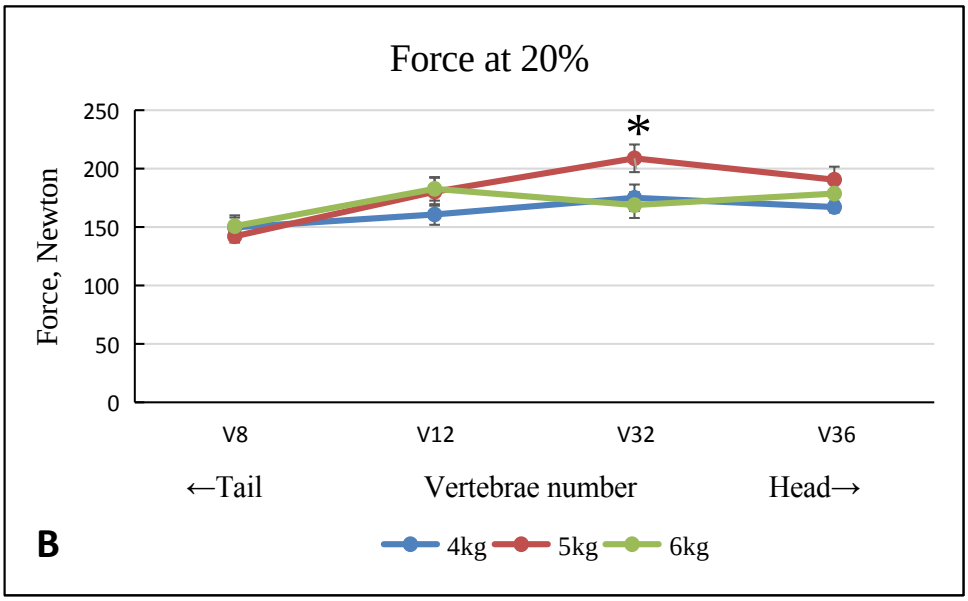
Force at 20%
250
200
150
100
50
0
Force, Newton
*
V8
V12
V32
V36
←Tail
Vertebrae number
Head→
4kg
5kg
6kg
B

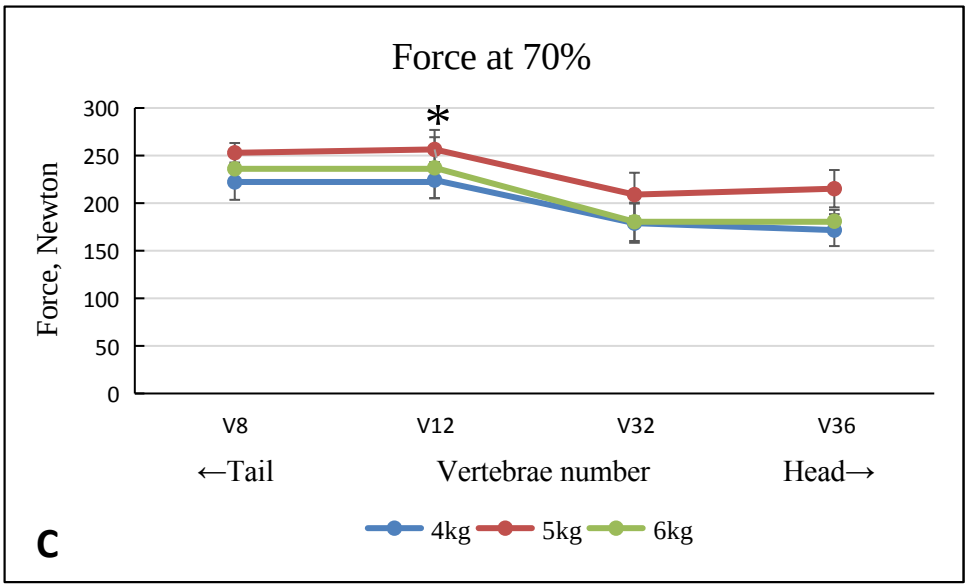

Fig 4.8 The compression force (N) at different depth (A at 10%, B at 20%, C at 70% compression depth) of the eighth, twelfth, thirty-second and thirty-sixth vertebra (V8, V12, V32, V36) along the vertebral column of different weight classes (4 kg, 5 kg, 6 kg) Atlantic Salmon. Results are shown as LSmean ± SE (n=10, with the exception of V8 of 6 kg where n=9, V12 of 6 kg where n=8). Vertebrae with "*" in the figure not sharing the same letter with other weight classes are significantly different ($P < 0.05$).

Table 4.3 Results from statistical analyses of results presented in Fig 4.8

	V8	V12	V32	V36
Force at 10 % (N)				
4kg	cde	ab	abc	bcd
5kg	e	a	a	bcd
6kg	de	abc	cde	ab
Force at 20 % (N)				
4kg	ef	cf	be	bf
5kg	f	bc	a	ab
6kg	def	ab	bf	bcd
Force at 70 % (N)				
4kg	ab	ab	b	b
5kg	a	a	ab	ab
6kg	ab	b	b	b

Note: Vertebrae not sharing the same letter within the same row are significantly different ($P < 0.05$).

The force at 10 percent of the vertebra thickness, ranged from 55.7 N to 95.2 N. At 20 percent and 70 percent thickness, the compression force ranged from 142.1 N to 208.8

N and from 171.7 N to 256.5 N, respectively. Numerically, the compression force increased from V8 to V12 for all sizes of fish. For V32 to V36 the compression force showed a slight decrease in 4 kg and 5 kg fish at 10 percent and 20 percent compression depth, while for the 6 kg salmon the compression force increased in that section. According to the statistical analyses (Table 4.3), no variation in force was observed within the same weight of salmon at the 70 percent of vertebra thickness. The compression force between different weight classes of salmon did not vary significantly, with the exception of 5 kg salmon (both thirty-second vertebrae at 10 % and 20 % compression depth and twelfth vertebrae at 70 % compression depth).

4.3. Vertebrae comparison of different fish species

The variation in vertebrae thickness varied significantly among the fish species. The vertebrae thickness of salmon ranged from 9.5 mm to 12.2 mm, trout from 8.4 mm to 9.6 mm, and Carp from 6.0 mm to 10.8 mm (Fig 4.9). Numerically, for both salmon and trout, the vertebrae thickness increased gradually from the tail (V4) up to the maximum value at the mid-section of the column (salmon at V20, trout at V28). Thereafter, the numerical thickness decreased towards the head, reaching a minimum at V40-44. Statistical analyses showed that for Salmon, vertebrae thickness at V12-V28 was not significantly different; the same was true of the thinnest section (V44-V52) closest to the head. Trout did not differ significantly at V16-V40. With Carp, the vertebrae thickness increased from the tail (V4) to the head (V28) with a comparatively significant difference, with the exception of a short section between V4 and V8, V12 and V16.

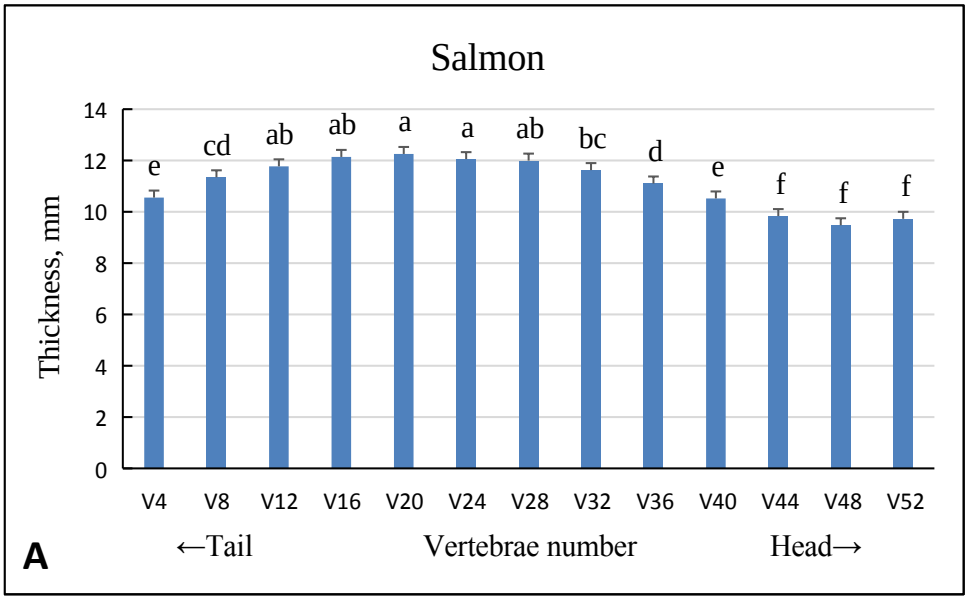
Salmon
Thickness, mm
14
12
10
8
6
4
2
0
e
cd
ab
ab
a
a
ab
bc
d
e
f
f
f
V4
V8
V12
V16
V20
V24
V28
V32
V36
V40
V44
V48
V52
←Tail
Vertebrae number
Head→
A

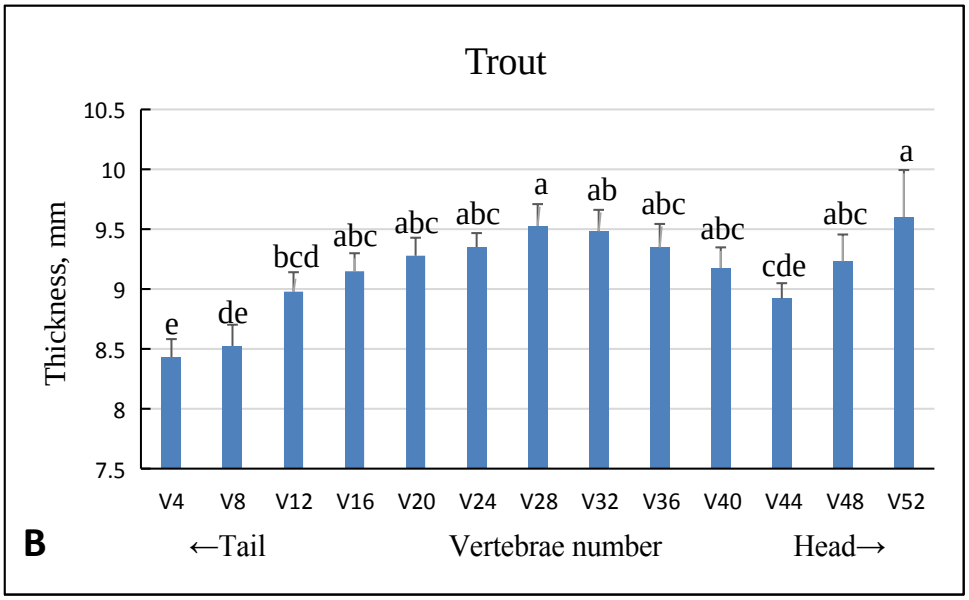
Trout
Thickness, mm
10.5
10
9.5
9
8.5
8
7.5
e
de
bcd
abc
abc
abc
a
ab
abc
abc
cde
abc
a
V4
V8
V12
V16
V20
V24
V28
V32
V36
V40
V44
V48
V52
←Tail
Vertebrae number
Head→
B

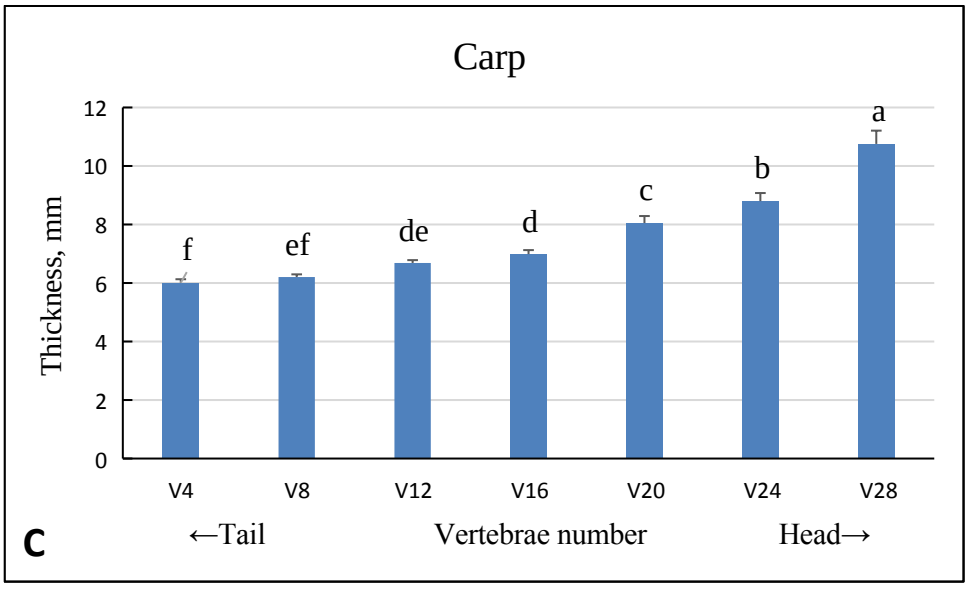
Carp
Thickness, mm
12
10
8
6
4
2
0
f
ef
de
d
c
b
a
V4
V8
V12
V16
V20
V24
V28
←Tail
Vertebrae number
Head→
C

Fig 4.9 Thickness (mm) of every fourth vertebrae along the vertebral column of different fish species (A for V4-V52 of Atlantic Salmon, B for V4-V52 of Rainbow Trout, C for V4-V28 of common Carp). Results are shown as LSmean ± SE (For Salmon and Trout: n=10, with the exception of V12, V20 of Salmon where n=8, V28 of Salmon where n=9,V12 and V52 of Trout where n=9; For Carp: n=9). Vertebrae not sharing the same superscripts above the error bars are significantly different ($P < 0.05$).

Total average resulting force-time graphs for each vertebra of salmon, trout and carp are illustrated in Fig 4.10. From this figure, it is clear that that there is a notable variation within and among the different species of fish regarding the graph profile (i.e. mechanical properties).

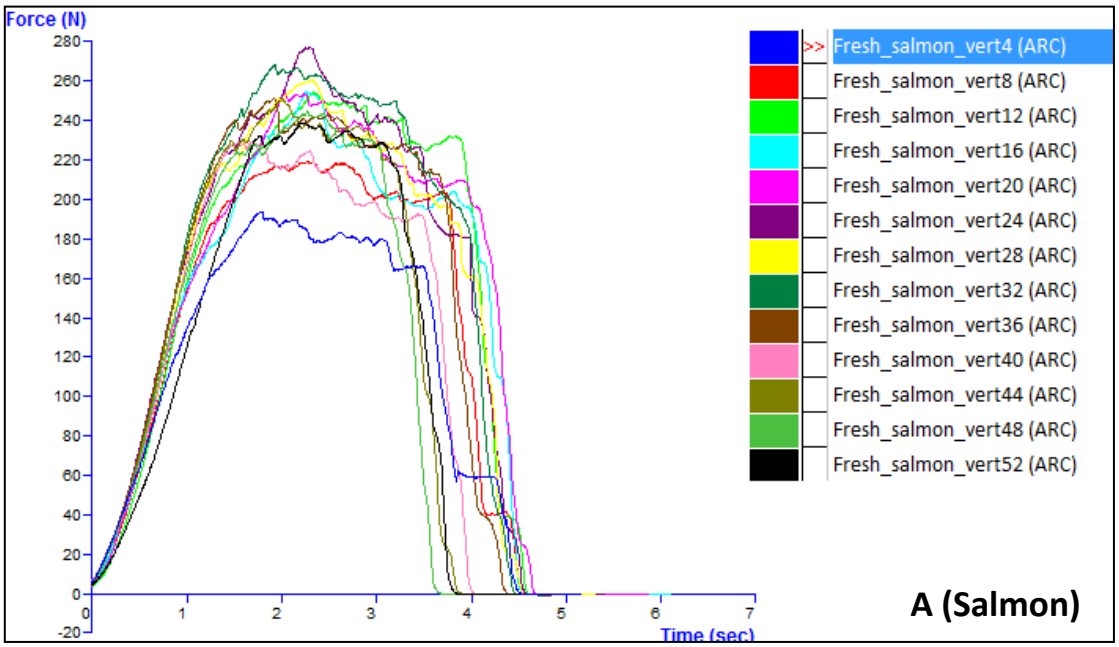

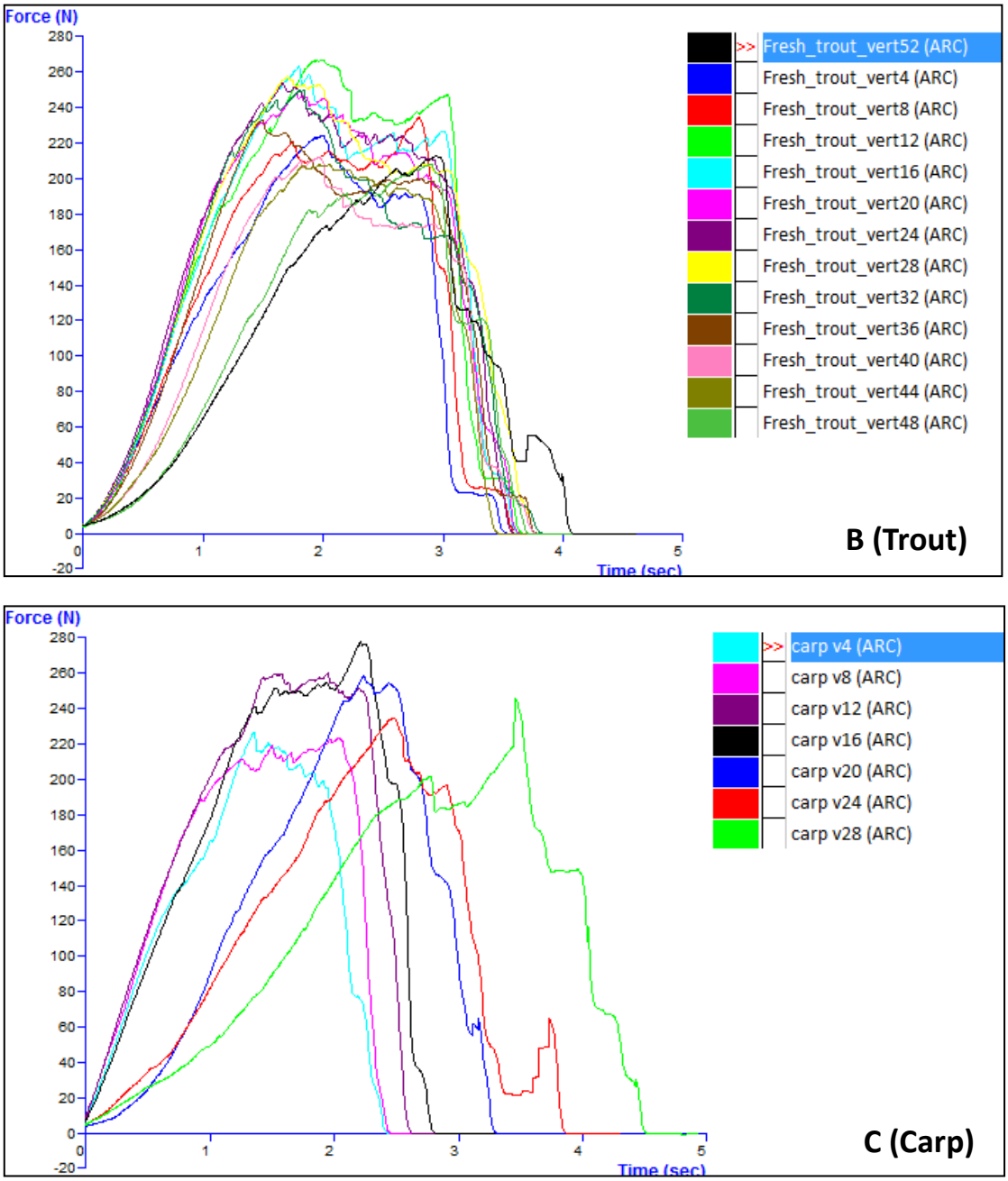

Fig 4.10 Total average force-time graphs for every fourth vertebra of different fish species (A for V4-V52 of Atlantic Salmon, B for V4-V52 of Rainbow Trout, C for V4-V28 of common Carp).

While the body length of salmon and trout is similar, carp is somewhat shorter. Because of this, it is necessary to unify the positions used for measurement in the three species. Vertebrae 8, 12, 32, and 36 in salmon and trout were aligned with vertebrae 4, 8, 16, and 20 in carp. In general, the treatment for comparison among species were set at A (15 %), B (25 %), C (60 %), D (70 %) at the vertebral column from tail to head of the various fish species (Fig 4.11).

The average maximum compression force for Salmon ranged from 250.9 N to 305.1 N, for trout from 251.0 N to 291.3 N, and for carp from 247.5 N to 306.3 N. The numerical maximum compression force at B (25 %) and C (60 %) was higher than that of A (15 %) and D (70 %) for salmon and trout. For carp, the maximum compression force increased from tail to head. Statistical analyses showed that the maximum compression force at A (15 %) and C (60 %) of the vertebral column was not significantly different between different fish species. At B (25 %), there was no significant difference between salmon and trout. Moreover, at D (70 %), the maximum compression force of trout and carp was significantly different.

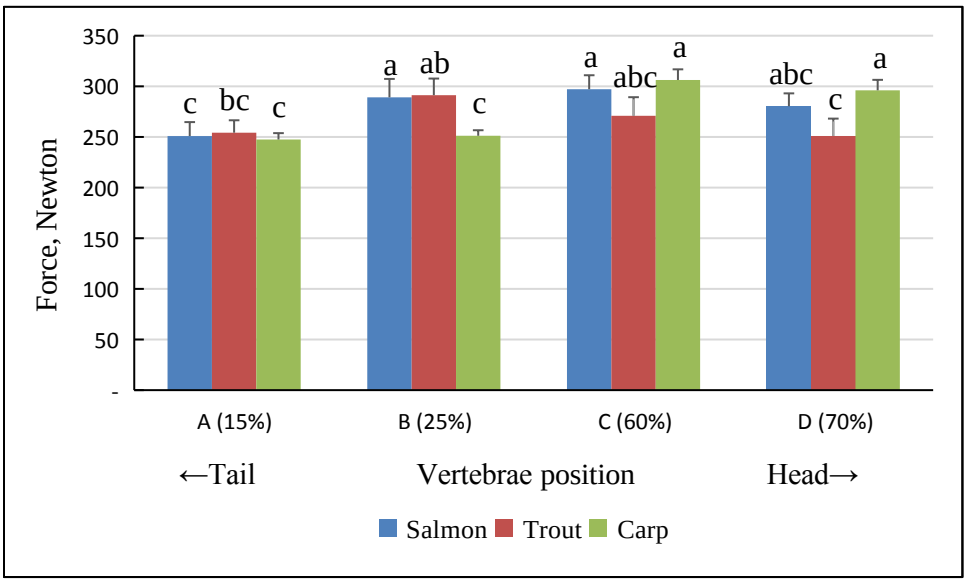

Fig 4.11 Maximum compression force (N) of A, B, C, D vertebra position (15 %, 25 %, 60 %, 70 % of the vertebral column) between different fish species (Atlantic Salmon, Rainbow Trout and Carp). Results are shown as LSmean ± SE (For Salmon and Trout: n=10, with the exception of V12 of Salmon where n=8, V12 of Trout where n=9; For carp: n=9). Vertebra not sharing the same superscripts above the error bars are significantly different ($P < 0.05$).

As Fig 4.12 illustrated, the compression force of salmon at 15% of the vertebra thickness ranged from 124.5 N to 148.4 N, trout varied from 80.7 N to 104.9 N, carp ranged from 31.8 N to 104.8 N. At 70 % vertebra thickness, the compression force of salmon ranged from 184.8 N to 212.4 N. For trout, the variation was 167.2 N to 250.3 N and for carp from 185.7 N to 293.7 N. In Fig 4.12 A, the numerical compression force at all positions (A, B, C, D) of salmon was significantly higher than the other

two species. With the exception of D (70 %), statistical analyses demonstrated that there was no significant difference in the compression force between trout and carp. Comparison of the compression force at 70 % of the vertebra (Fig 4.12 B) showed that salmon and trout were not significantly different at any position (A, B, C, D). For carp, with the exception of B (25 %), statistical analyses revealed that the compression force between carp and the other two species were varied significantly, and its compression force value was distinctly higher than the other species at C (60 %). At D (70 %), although the numerical compression force of carp was the highest, it was not significantly different from trout.

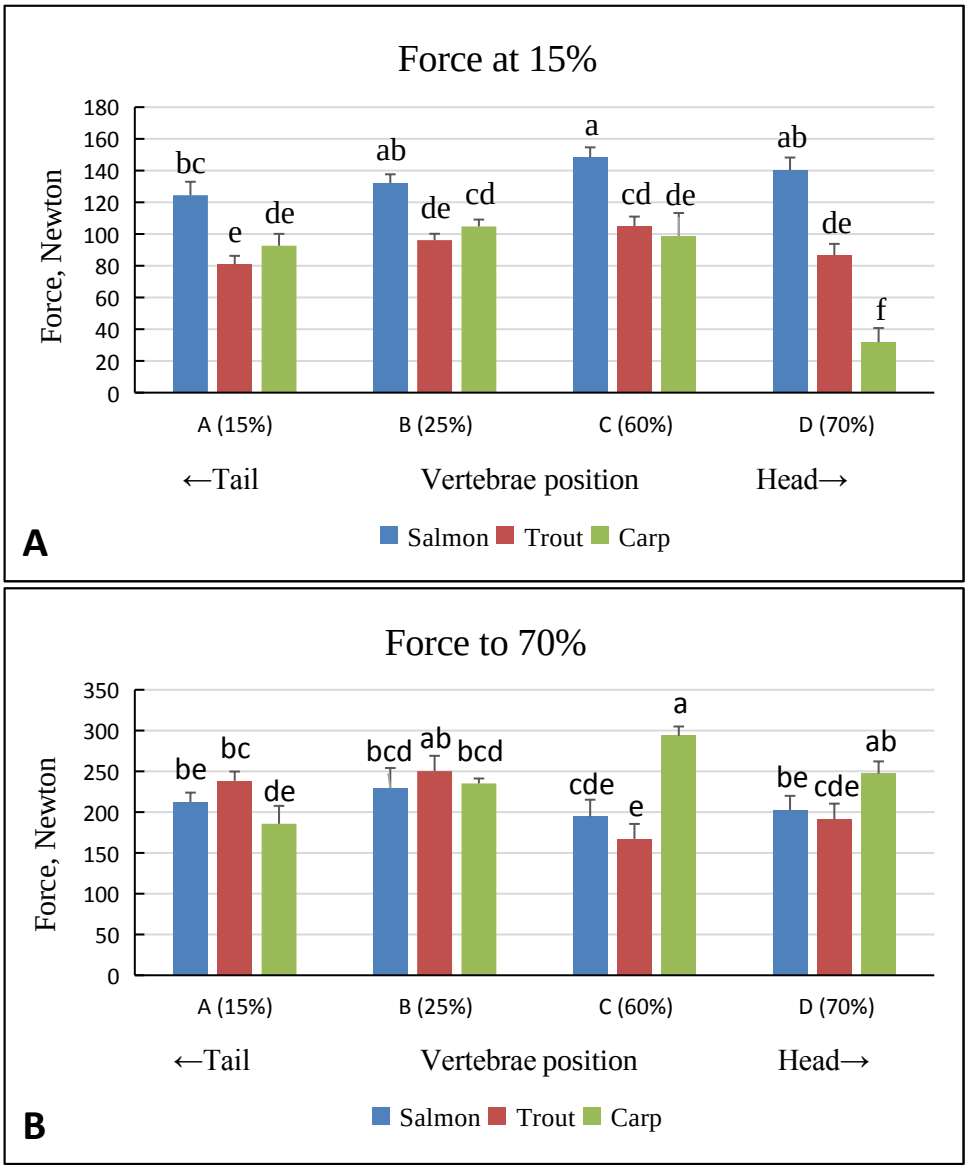

Fig 4.12 Compression force (N) at different depth (A at 15%, B at 70% compression depth) of A, B, C, D vertebra position (15 %, 25 %, 60 %, 70 % of the vertebral column) between fish species

(Atlantic Salmon, Rainbow Trout and Carp). Results are shown as LSmean ± SE (For Salmon and Trout: n=10, with the exception of V12 of salmon where n=8, V12 of trout where n=9; For carp: n=9). Vertebra not sharing the same superscripts above the error bars are significantly different ($P < 0.05$).

4.4. Effect of frozen storage on vertebrae texture

Total average resulting force-time graphs of the eighth, twelfth, thirty-second and thirty-sixth vertebra (V8, V12, V32, V36) for fresh and frozen Salmon are illustrated in Fig 4.13. Fig 4.14 shows the same type of graph, but compares fresh and frozen trout. These two figures revealed that there appears to be a variation after fresh samples are frozen (i.e. mechanical properties).

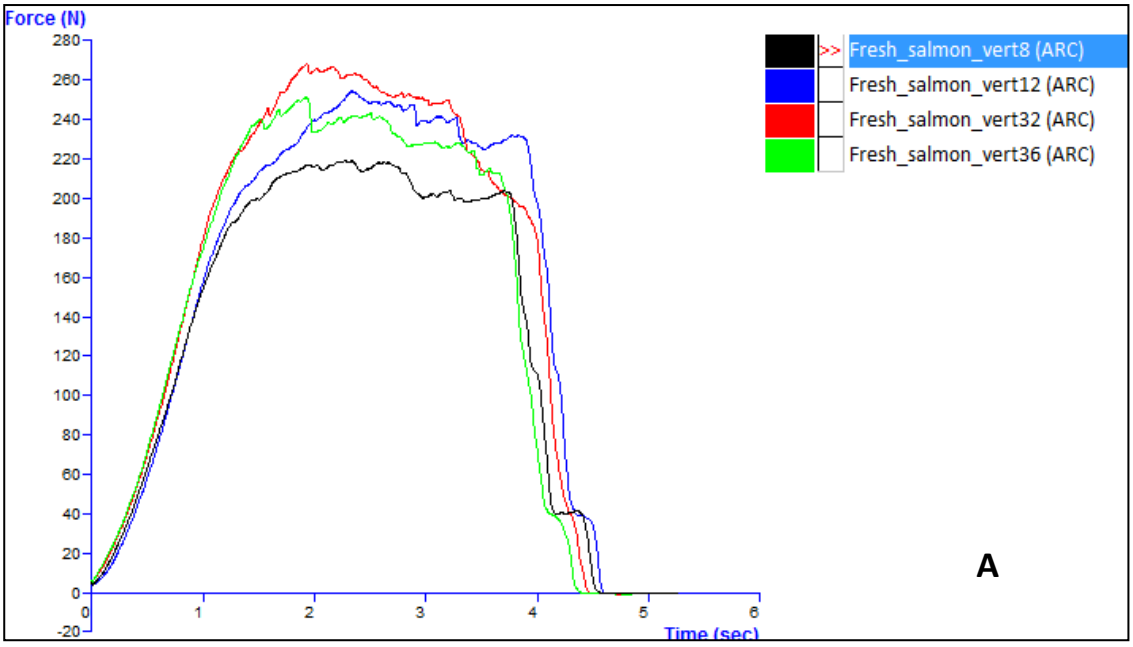

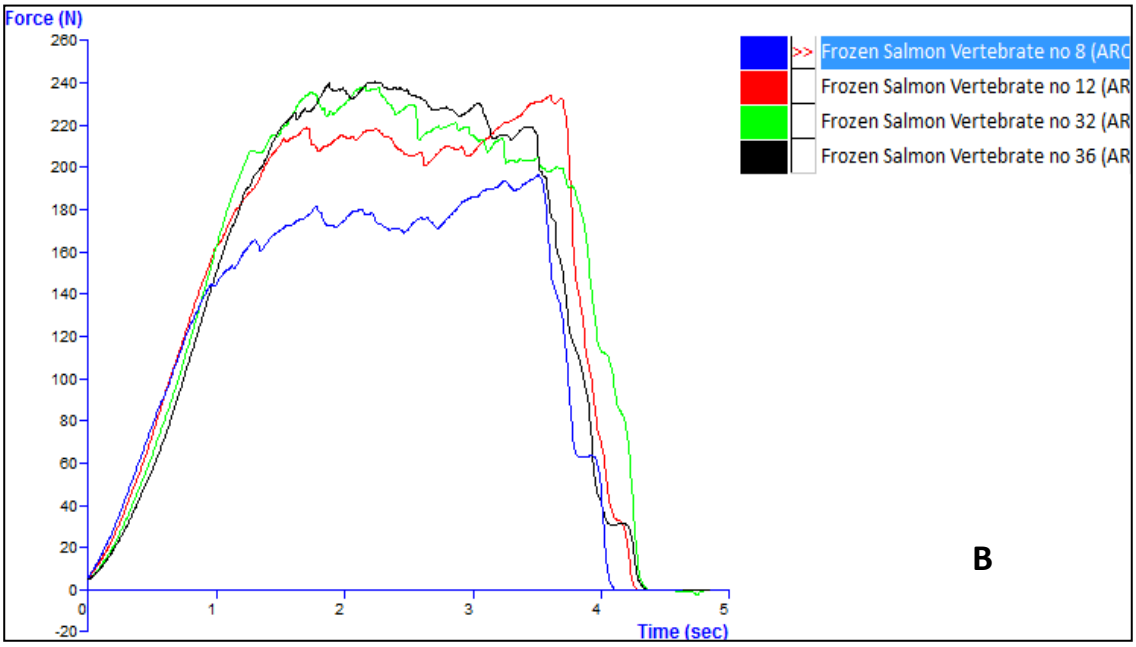

Fig 4.13 Total average force-time graphs for the eighth, twelfth, thirty-second and thirty-sixth vertebra (V8, V12, V32, V36) of fresh and frozen salmon (A for fresh salmon, B for frozen salmon).

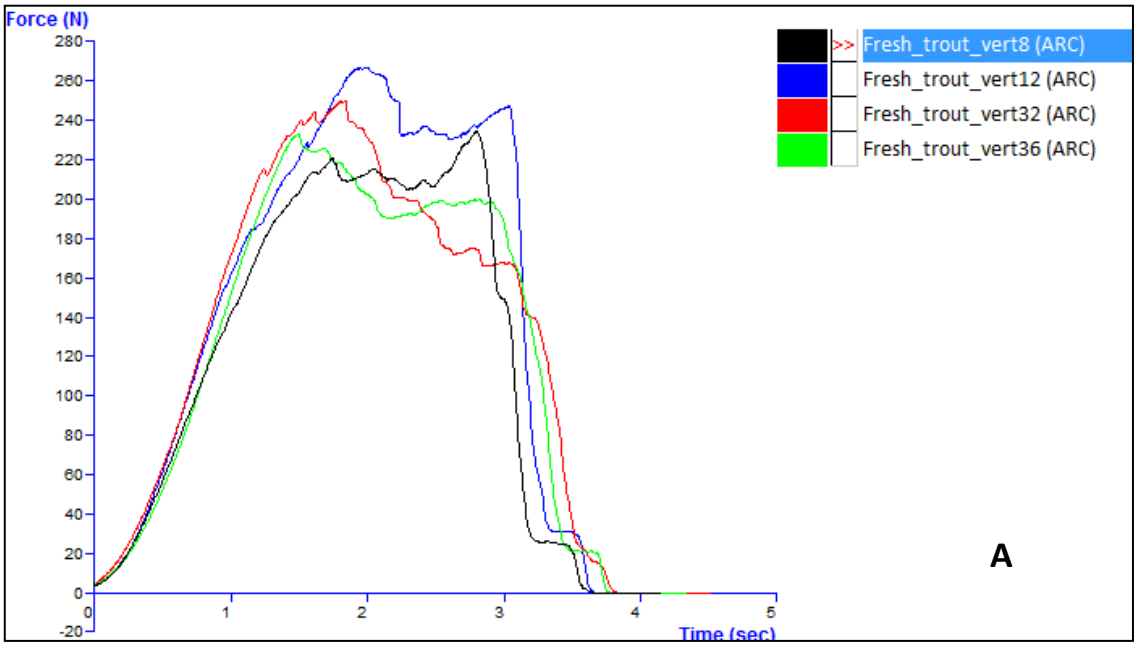

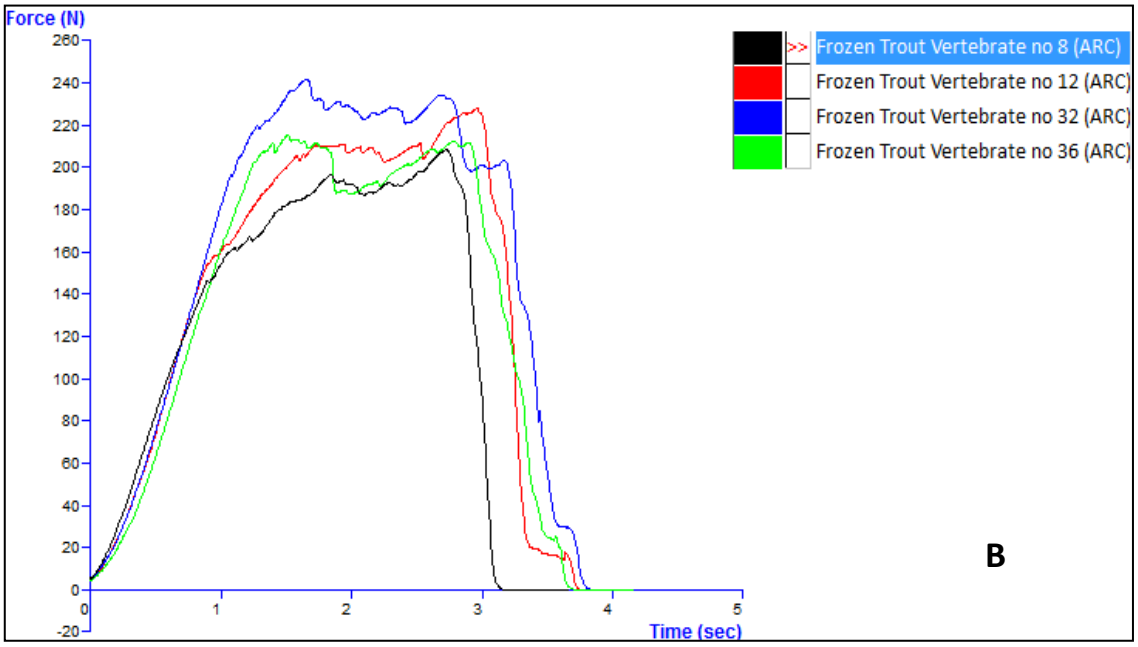

Fig 4.14 Total average force-time graphs for the eighth, twelfth, thirty-second and thirty-sixth vertebrae (V8, V12, V32, V36) of fresh and frozen trout (A for fresh trout, B for frozen trout).

The average maximum compression force of fresh salmon ranged from 250.9 N to 305.1 N and varied from 213.7 N to 283.7 N for frozen salmon (Fig 4.15 A). Numerically, the maximum compression force of the eighth, twelfth, thirty-second and thirty-sixth vertebrae of fresh salmon were all higher than those of frozen salmon. However, statistical analyses showed no significant difference between fresh and frozen salmon for V8, V32 and V36, and a significant difference at V12.

The average maximum compression force of fresh trout ranged from 251.0 N to 291.3 N and varied from 255.0 N to 279.7 N for frozen trout (Fig 4.15 B). Numerically, the maximum compression force of the eighth and twelfth vertebrae of fresh trout were higher than those of frozen trout, and the thirty-second and thirty-sixth vertebrae of frozen trout were higher than those of fresh trout. Statistical analyses showed there was no significant difference between fresh and frozen trout for the selected vertebrae.

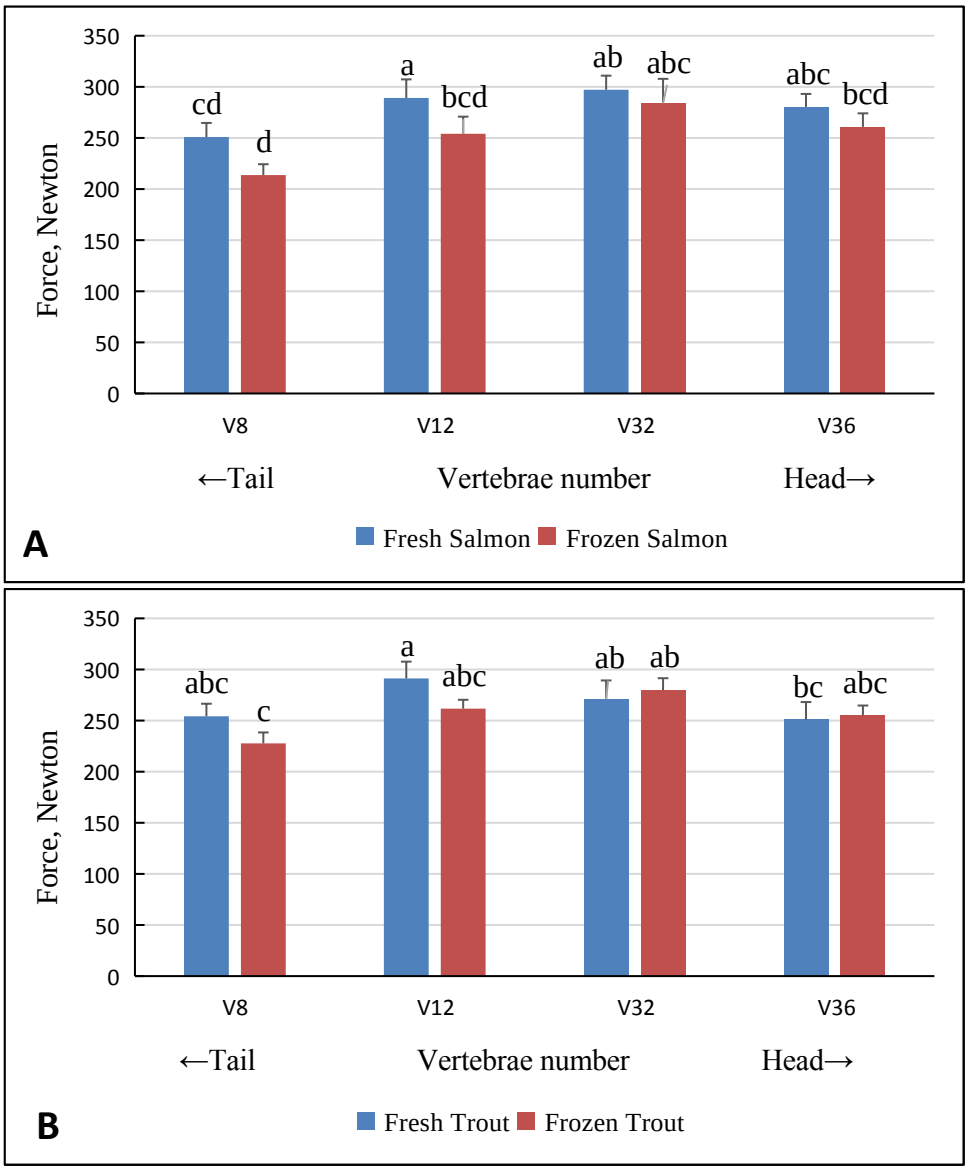

Fig 4.15. Maximum compression force (N) of the eighth, twelfth, thirty-second and thirty-sixth vertebrae (V8, V12, V32, V36) along the vertebral column of fresh and frozen fish comparison (A for Atlantic Salmon, B for Rainbow Trout). Results are shown as LSmean ± SE (For fresh salmon and trout: n=10, with the exception of V12 of salmon where n=8, V12 of trout where n=9; For frozen salmon: n=7; For frozen trout: n=10). Vertebrae not sharing the same superscripts above the error bars are significantly different ($P < 0.05$).

4.5. Mechanical properties of salmon ribs

Ribs were examined by mechanical analyses of every second rib of 4 kg Atlantic Salmon.

The average rib thickness at position A ranged from 0.3 mm to 0.6 mm. At position B

the variation was 0.4 mm to 0.5 mm, and at position C the variation was 0.4 mm to 0.7 mm (Fig 4.16). Statistical analyses revealed that rib thickness was not significantly affected by measuring position A ($P \geq 0.15$), B ($P \geq 0.48$) or C ($P \geq 0.17$), or by rib location, with the exception of the second rib nearest the head (Table 4.21).

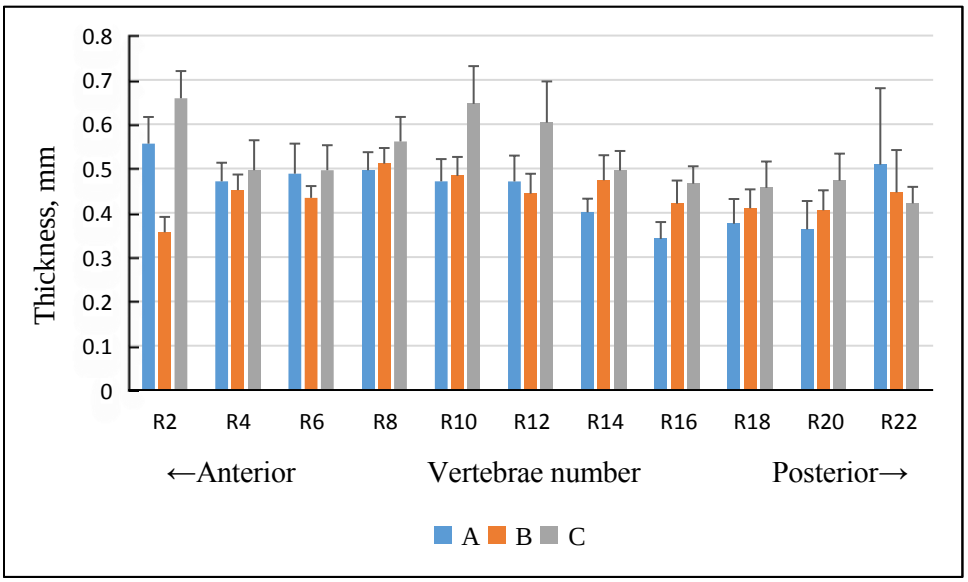

Fig 4.16 Thickness (mm) at three positions (A, B, C) of every second rib in 4 kg Atlantic Salmon. Results are shown as LSmean ± SE (n=10).

Table 4.4 Results from statistical analyses of results presented in Fig 4.16

	R2	R4	R6	R8	R10	R12	R14	R16	R18	R20	R22
P	0.002	0.82	0.67	0.56	0.10	0.22	0.31	0.14	0.57	0.40	0.86

4.5.2 Breaking force variation of salmon ribs

The average breaking force at position A ranged from 9.13 N to 21.53 N. At position B the variation was 8.58 N to 15.06 N, and at position C position the variation was 6.84 N to 12.79 N. Numerically, the breaking force of ribs at various measuring positions (A, B, C) decreased gradually from the anterior (R2) to the posterior (R22) of Salmon (Fig 4.17). Statistical analyses demonstrated that the breaking force was significantly affected by rib location. Moreover, the significant difference level was position A > position B > position C (Table 4.5). The statistical analyses in Table 4.6 demonstrated that when comparing positions A, B, and C for every second rib, the breaking force measured at positions A and B were significantly different, with the exception of the twenty-second rib (posterior area of Salmon), which was not affected

by the measuring position at all. The fourteenth, eighteenth, and twentieth ribs were also significantly different when compared with positions B and C, while the others were not (Table 4.6).

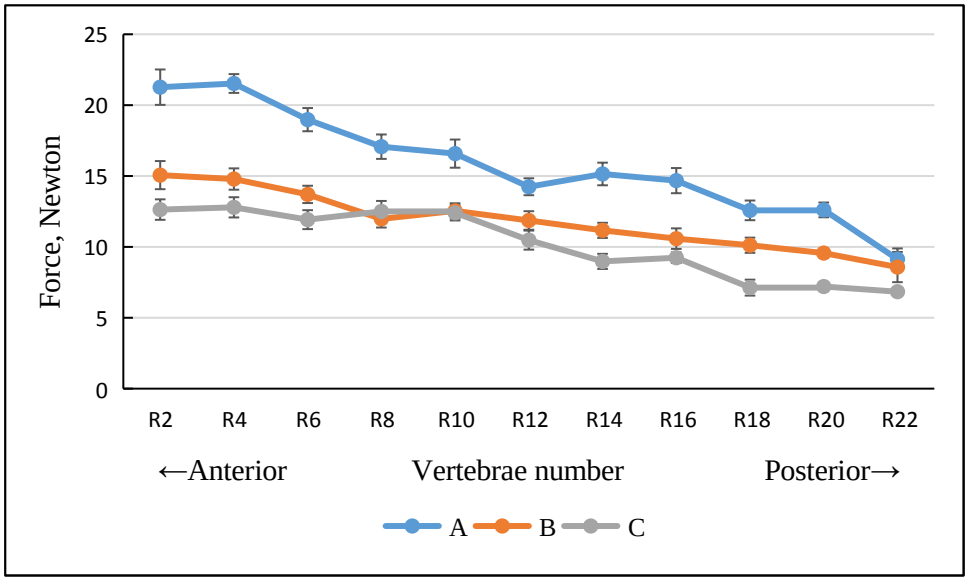

Fig 4.17 Breaking force (N) at three positions (A, B, C) of every second rib in 4 kg Atlantic Salmon. Results are shown as LSmean ± SE (n=10).

Table 4.5 Results from statistical analyses of results presented in Fig 4.17

Position	R2	R4	R6	R8	R10	R12	R14	R16	R18	R20	R22
A	a	a	b	bc	cd	ef	cde	def	f	f	g
B	a	a	ab	bcd	bc	cde	cf	dg	efg	fg	g
C	a	a	ab	a	a	bc	c	c	d	d	d

Note: Ribs not sharing the same letter within the same row are significantly different ($P < 0.05$).

Table 4.6 Results from statistical analyses of results presented in Fig. 4.17

Rib number	*A*	*B*	*C*
R2	a	b	b
R4	a	b	b
R6	a	b	b
R8	a	b	b
R10	a	b	b
R12	a	b	b
R14	a	b	c
R16	a	b	b
R18	a	b	c
R20	a	b	c
R22	a	a	a

Note: Rib positions not sharing the same letter within the same row are significantly different ($P < 0.05$).

4.6. Ribs comparison of different salmon weight classes

The average thickness of rib no. 12 in 4 kg salmon ranged from 0.4 mm to 0.6 mm. In 5 kg Salmon the variation was 0.4 mm to 0.5 mm, and in 6 kg from 0.5 mm to 0.9 mm (Fig 4.18 A). Numerically, at position A the average thickness in 6 kg Salmon was much higher than in 4 kg and 5 kg Salmon. From statistical analyses, it was clear that the average thickness of rib no.12 was not significantly different among sizes when measured at positions B and C. For position A, only 6 kg Salmon showed a significant difference.

The average thickness of rib no.14 in 4 kg Salmon ranged from 0.4 mm to 0.5 mm, in 5 kg Salmon from 0.3 mm to 0.5 mm, and in 6 kg Salmon from 0.4 mm to 0.6 mm (Fig 4.18 B). Statistical analyses showed that there was no significant difference in rib no. 14 among fish sizes at positions A and C. At position B, however, the average thickness in 5 kg and 6 kg Salmon was significantly different.

A comparison of (A) and (B) in Fig 4.18 shows that the average rib thickness was not significantly affected by size class, with the few exceptions mentioned above.

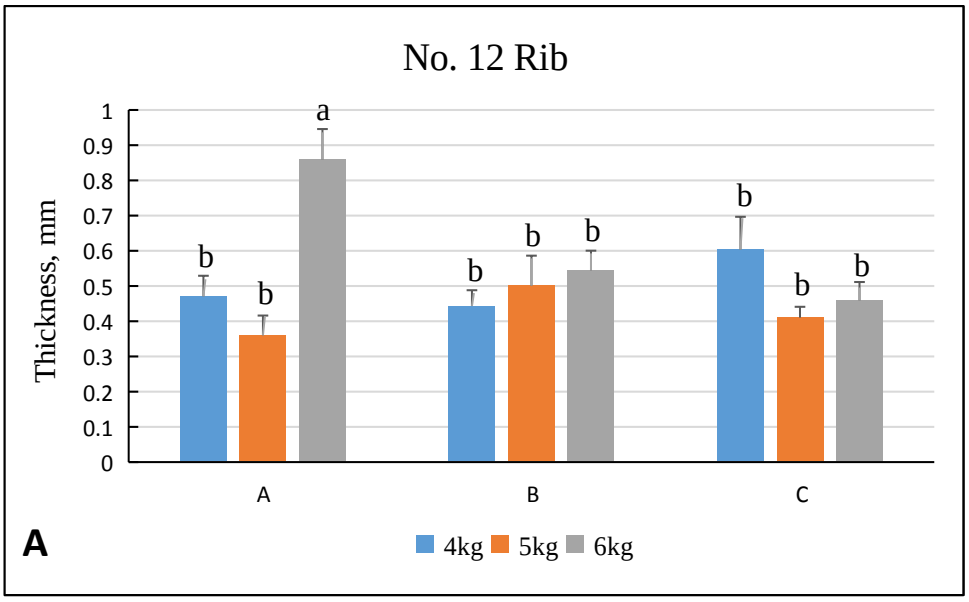

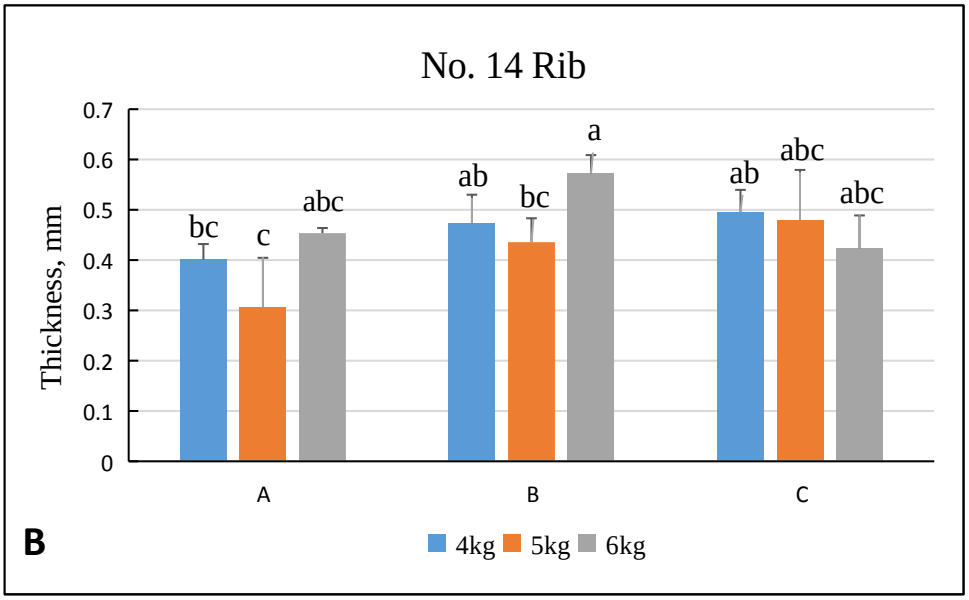

Fig 4.18 Thickness (mm) of three positions (A, B, C) of the twelfth and the fourteen ribs (A for No.12 rib, B for No.14 rib) in various weight classes (4 kg, 5 kg, 6 kg) Atlantic Salmon. Results are shown as LSmean ± SE (n=10). Ribs not sharing the same superscripts above the error bars are significantly different ($P < 0.05$).

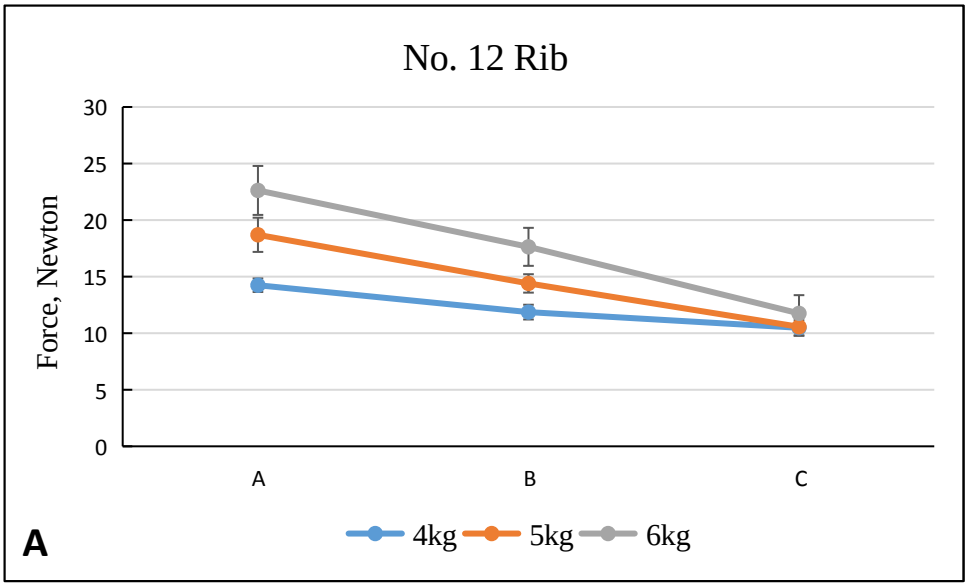

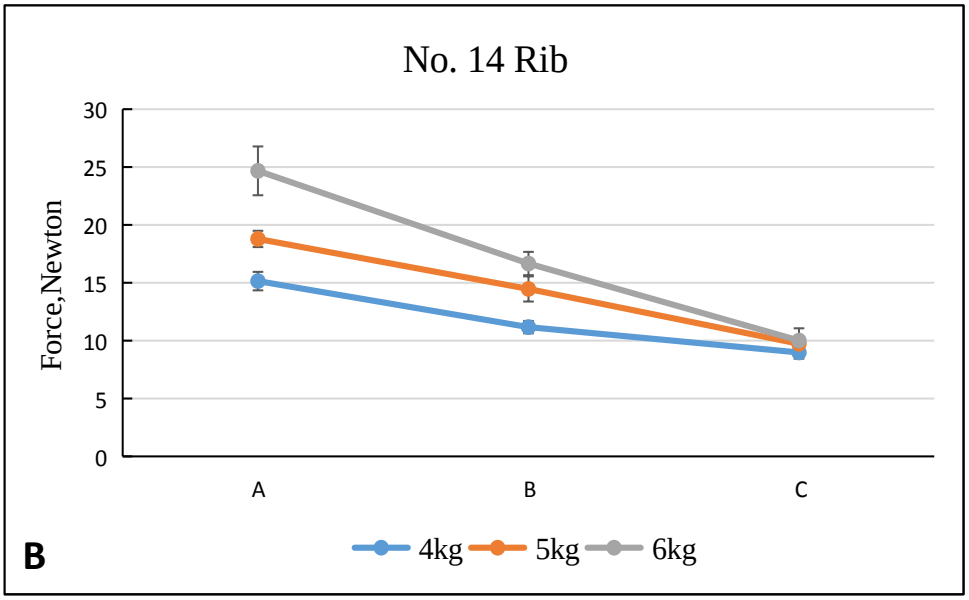

Fig 4.19 Breaking force (Newton) at three positions (A, B, C) of the twelfth and fourteenth ribs (A for No.12 rib, B for No.14 rib) of various weight classes (4 kg, 5 kg, 6 kg) of Atlantic Salmon. Results are shown as LSmean ± SE (n=10).

The average breaking force of rib no. 12 in 4 kg salmon ranged from 10.5 N to 14.2 N, in 5 kg salmon from 10.6 N to 18.7 N, and in 6 kg salmon from 11.8 N to 22.6 N (Fig 4.19 A). Similarly, the average breaking force of rib no. 14 in 4 kg salmon ranged from 9.0 N to 15.1 N, in 5 kg salmon from 9.7 N to 18.8 N, and in 6 kg salmon from 10.0 N to 24.7 N (Fig 4.19 B).

A comparison of (A) and (B) in Fig 4.19 shows that the numerical average breaking force decreased from positions A to C along the rib for all size classes of salmon. At all measuring positions, the breaking force value increased with increased body weight.

Statistical analyses showed that there was a significant difference at position A for different fish size in ribs no.12 and 14. Conversely, there was no significant difference at position C in fish size. At position B, the significant difference level fell between the other two positions mentioned above.

Table 4.7 Results from statistical analyses of results presented in Fig. 4.19

	A	B	C
No.12 Rib			
4kg	c	cd	d
5kg	b	c	d
6kg	a	b	cd
No.14 Rib			
4kg	c	d	d
5kg	b	c	d
6kg	a	bc	d

Note: Ribs not sharing the same letter within the same row or column are significantly different ($P < 0.05$).

4.7. Ribs comparison of different fish species

Statistical analyses revealed that the average rib thickness or breaking force measured at position B of fish species (Atlantic Salmon, Rainbow Trout and Carp) was significantly different (Fig 4.20 and Fig 4.21). Numerically, although the rib thickness value of salmon was greater than that of trout, the breaking force of salmon was less than that of trout.

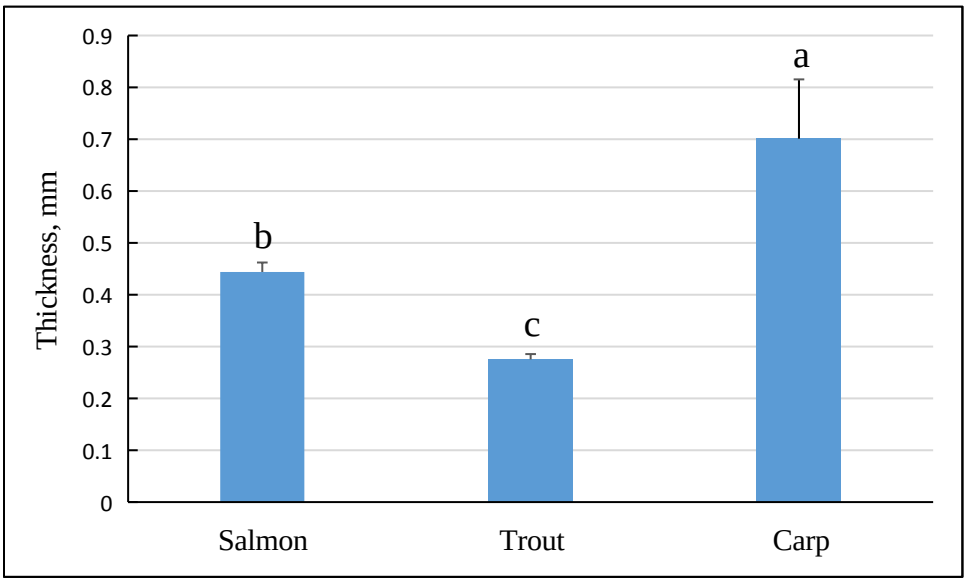

Fig 4.20 Average rib thickness (mm) measured at position B comparing fish species (Atlantic Salmon, Rainbow Trout and Carp). Results are shown as LSmean ± SE (For Salmon and Trout:

n=10; For Carp: n=9). Superscripts not sharing the same letters above the error bars are significantly different (P < 0.05).

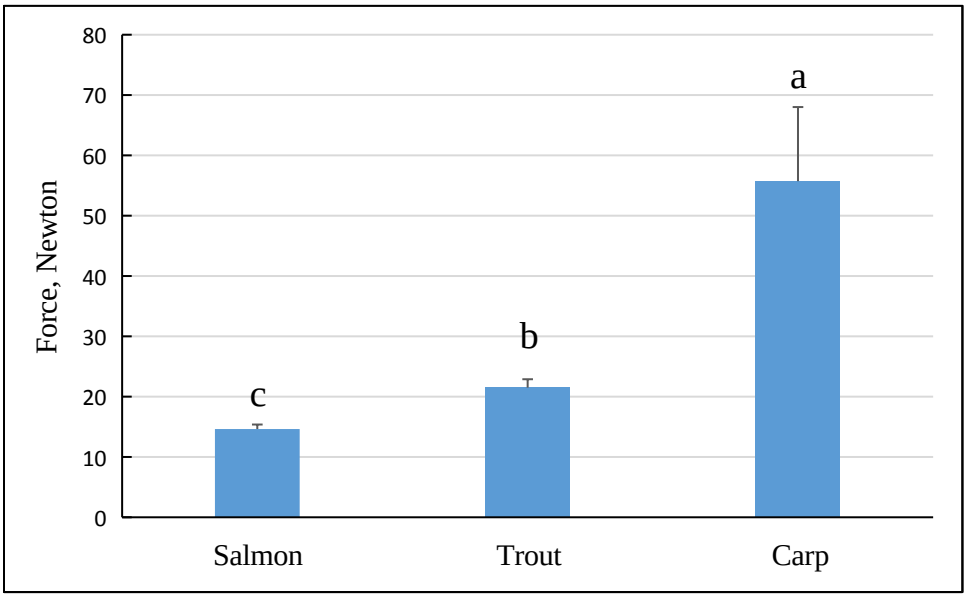

Fig 4.21 Average rib breaking force (N) measured at position B comparing fish species (Atlantic Salmon, Rainbow Trout and Carp). Results are shown as LSmean ± SE (For Salmon and Trout: n=10; For Carp: n=9). Superscripts not sharing the same letters above the error bars are significantly different (P < 0.05).

4.8. Chemical composition of salmon and trout

Three representative sections were used: V8-V12, V20-V24, V32-V36. These stand for the posterior, mid, and anterior sections of the vertebral column, respectively.

Fig 4.22 illustrated the fat content of the salmon vertebrae was higher (17-22%) compared with trout (11-15%). According to statistical analyses, fat content was not significantly different at different locations on the fish vertebral column (V8-V12, V20-V24, V32-V36) (P = 0.0084). There was however a significant difference between fish spices (salmon and trout) (P < 0.0001).

Fig 4.23 and Fig 4.24 showed that both the dry matter value and ash value of trout (dry matter as 51-57%, ash as 21-23%) was higher than those of salmon (dry matter as 51-55%, ash as 17-18%) at all three sections along the vertebral column. Statistical analyses of dry matter indicated a significant difference compared with different

locations along the vertebral column (V8-V12, V20-V24, V32-V36) ($P < 0.0001$). There was however no significant difference between fish species (salmon and trout) ($P = 0.0093$). On the contrary, ash was not significantly different at different locations along the vertebral column (V8-V12, V20-V24, V32-V36) ($P = 0.0694$), but showed a significant difference between fish spices (Salmon and Trout) ($P < 0.0001$).

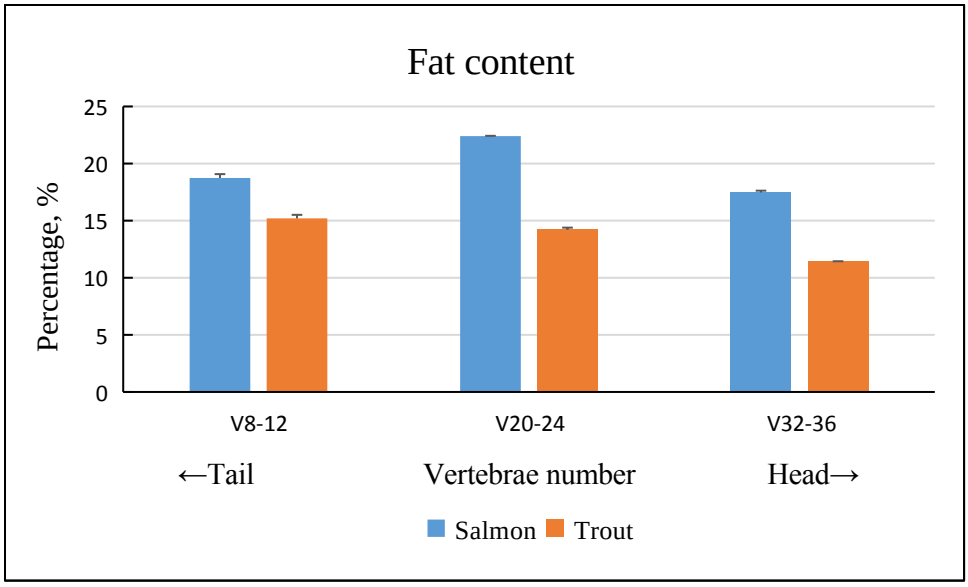

Fig 4.22 Fat content (%) comparison of three representative sections (V8-V12, V20-V24, V32-V36) along the vertebral column for Salmon and Trout. Results are shown as LSmean ± SE (For Salmon: n=7; For Trout: n=10).

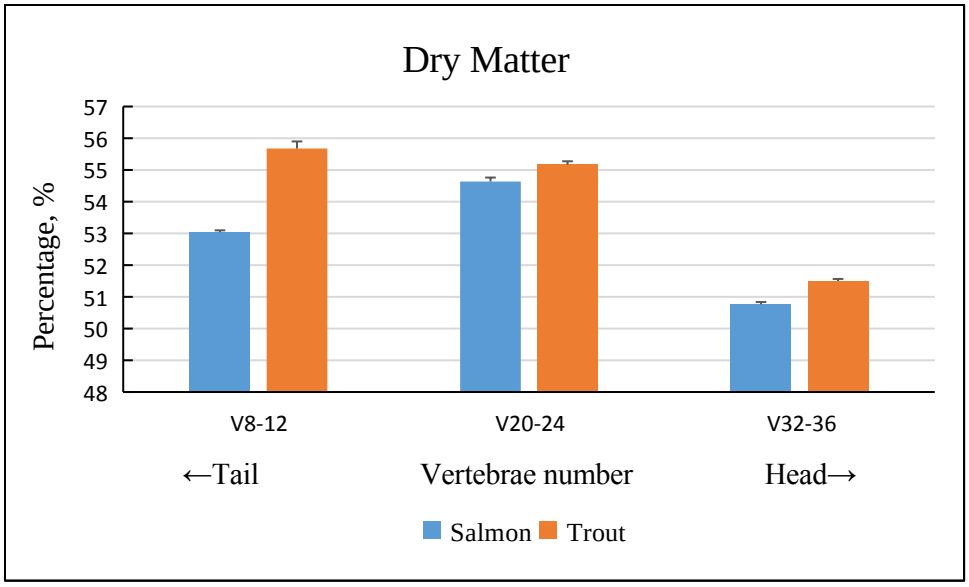

Fig 4.23 Dry matter (%) comparison of three representative sections (V8-V12, V20-V24, V32-V36) along the vertebral column for Salmon and Trout. Results are shown as LSmean ± SE

(For Salmon: n=7; For Trout: n=10).

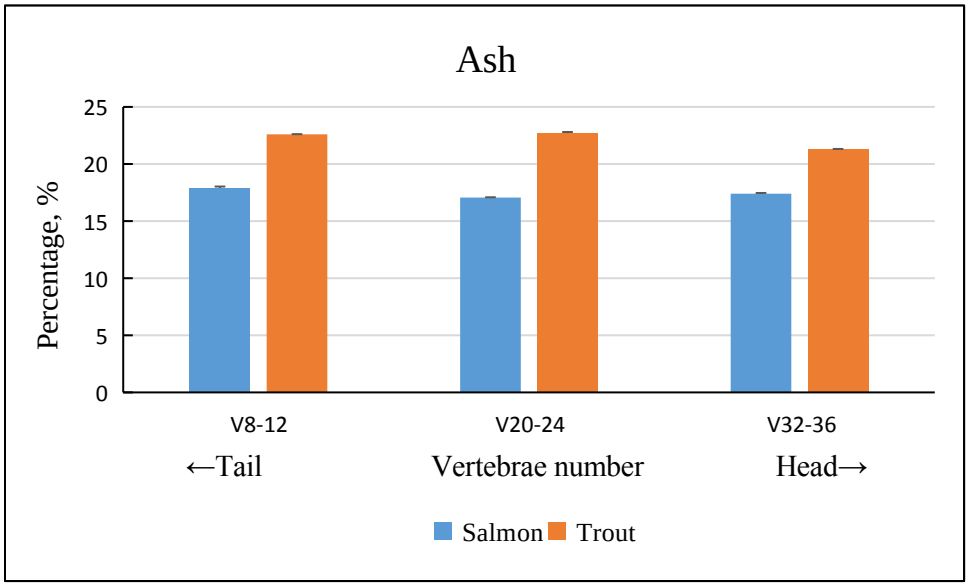

Fig 4.24 Ash (%) comparison of three representative sections (V8-V12, V20-V24, V32-V36) along the vertebral column for Salmon and Trout. Results are shown as LSmean ± SE (For Salmon: n=7; For Trout: n=10).

5. Discussion

Currently, techniques such as 3-D imaging, X-ray, nanoindentation, are utilized to explore the mechanical properties of bones. The greatest challenge when studying the mechanical properties of bone is the fact that bones are different from common engineering materials due to its characteristics, such as anisotropy and heterogeneity (Parnell and Grimal, 2009). In this chapter, I will summarize available methods and selected efficient parameters for mechanical analysis of fish bones, with focus on Salmonis. From the present study, the parameters will be selected based on comparing the influence of various weight classes, fish species, and frozen preservation.

5.1 Mechanical properties of Atlantic Salmon vertebrae and ribs

Detailed measurement of 4 kg salmon showed variation in thickness along the vertebral column as shown in Fig 5.1. The vertebrae thickness increased gradually from the salmon tail to the mid-section of the column, thereafter the thickness decreased to a minimum at the anterior position. Vertebrae closet to the head, however were thicker and similar with those closest to the tail.

A comparison of the maximum compression force of every fourth salmon vertebra and its corresponding thickness showed that the vertebra with maximum thickness value did not show maximum compression force. In other words, the thickness of the vertebra did not correspond to its strength.

The maximum compression force can occur at different compression depth within the same vertebra as compression force continued until 70 percent thickness of the vertebra. Hence, this parameters is not considered as an ideal selection of parameter for describing the mechanical properties of salmon vertebrae. The stable parts illustrated in patterns of the compression force whether at 0.5-2 mm depth or 5-20 percent of vertebra thickness along the entire salmon vertebral column is similar (Fig

4.5). This helps to describe the strength distribution of the entire vertebral column from the head of a salmon to its tail.

The similar patterns was also shown in Fjelldal ’s reports, which presented the relatively thicker vertebrae length, greater stiffness and higher Yield-load in the tail region at V31-V49 along the vertebral column from head to tail (Fjelldal *et al.*, 2004, 2005, 2006). Although the method of division of the the vertebrae region outlined by Kacem et al. (1998) was not used in this study, the section selected to describe the mechanical properties of the Salmon vertebrae was the same (from tail to mid-section, V12-V28).

Through the comparison illustrated in Fig 4.5, although compression force was able to reflect the mechanical properties of salmon vertebrae, the total work (represented by the area under the graph, N*s) required to reach 2 mm and 20 % showed a more detailed variation of mechanical properties, from the observation that the most significant variation was observed at a 0-15 as well as 0-20 percent compression depth. Thus, the total work (area, N*s) required to compress depth was a more accurate parameter by which to describe the mechanical properties of fish vertebrae.

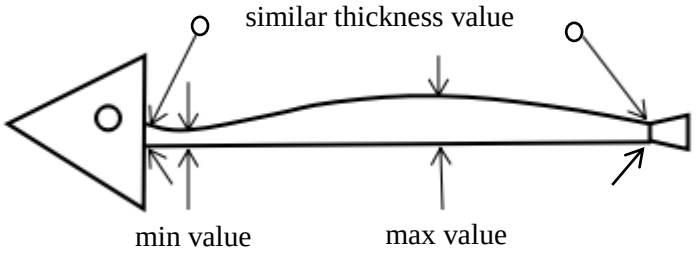

Fig 5.1 Thickness distribution along the vertebral column of 4 kg salmon.

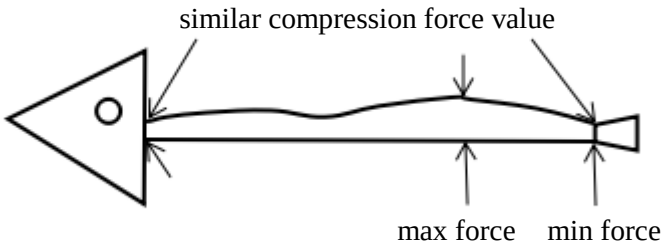

Fig. 5.2 Maximum compression force distribution along the vertebral column of 4 kg salmon (The thickness of the vertebra is described as the maximum compression force).

According to the results in section 4.5, with the exception of the anterior, the thickness of Salmon ribs was not significantly different.This applies both at different sections of the fish body and at different locations in the same rib.

The breaking force of Salmon ribs was significantly reduced from the anterior to posterior sections. In other words, the rib strength of Salmon was much stronger at the position nearest the head than it was toward the tail. Moreover, the measuring position A closer to the vertebral column within the same rib had a greater value of breaking force. From what has been described above, the breaking force of the rib located nearest the head measured at position A reflects the mechanical properties of Atlantic Salmon ribs for the most part, whereas the breaking force of the rib closet to the tail measuring at position C will be the last choice for mechanical analyses.

5.2 Mechanical properties of vertebrae and ribs compared with various weight classes in salmon

A comparison of 4 kg, 5 kg, and 6 kg Salmon shows that the magnitude relationship of average vertebra thickness is significantly expressed as 6 kg > 5 kg > 4 kg.

According to the results in section 4.2, it cannot be proven that the maximum compression force and the compression force of each point measured at various vertebra thicknesses increased as the weight class of Salmon increased. The similar patterns of the maximum compression force of 4 kg and 5 kg Salmon also indicated a

stable difference in the maximum compression force between these two weight classes, whereas 6 kg Salmon showed a different pattern. In other words, the maximum compression force of the measured vertebrae for 4 kg and 5 kg Salmon was more stable than for 6 kg salmon. Since the maximum compression force for V8 and V12 of 4 kg Salmon was significantly lower than that of the other two weight classes, 4 kg Salmon are not the best choice to determine the mechanical properties of Salmon vertebrae.

As shown in Fig 4.8, when compared with 4 kg and 6 kg Salmon, the compression force of measured vertebrae for 5 kg salmon was significantly higher at V32 when the compression depth was at 10 % and 20 %, as well as at V12 when the compression depth was at 70 %. Moreover, the compression force value of measured vertebrae for 5 kg Salmon was greater than that of the other two weight classes at most times. A few studies in addition to Wolff ’s law have reported that size was not significantly related to bone strength (van der Meulen *et al.*). In other words, a limiting value of compression force in vertebrae may occur and was irrelevant to salmon weight class when reached the mechanical loading. Hence, the measured compression force value of 5 kg salmon is much closer to that limiting value in salmon vertebrae strength.

From what has been described above, the vertebrae strength of 5 kg Salmon was more likely to reflect variation in the mechanical properties of Salmon vertebrae than were the other two sizes of Salmon.

Rib thickness was not affected by the weight of Salmon. The breaking force of ribs was however significantly affected by the weight. The position closer to the vertebral column, the more the breaking force was influenced by the weight of the salmon at this position within the same rib. Since the breaking force of both measured ribs demonstrated similar patterns, it makes no difference which rib is chosen to reflect the variation in mechanical properties among different weight classes of Salmon. A measurement made at position A will however be the most accurate to describd the mechanical properties within each weight classe of Salmon.

5.3 Mechanical properties of vertebrae and ribs compared with different fish species

The thickness of the vertebra along the entire vertebral column in salmon and trout fit the model described in Fig. 5.1 to a certain extent, since both are Salmonids. However, carp, – another fish species – showed significant differences compared to Salmonids. The thickness value of the vertebral column in carp gradually decreased from the head to the tail. A comparison of salmon, trout, and carp shows the the magnitude relationship of average vertebrae thickness is significantly expressed as carp > salmon > trout.

In accordance to Fig 4.10, the patterns displayed during compression force during the entire cutting procedure in salmon and trout were relatively concentrated, and were decentralized in carp. The maximum compression force, a mean value obtained from individuals of the same fish species at various compression depths, was observed to be significantly different between Salmonids and carp as well. The maximum compression force at the measured vertebrae from tail to head appeared to increase significantly in carp, whereas compared within Salmonids (salmon and trout), the trend of the maximum compression force at the measuring points along the vertebral column showed similarity, which to some extent fits the model described in Fig 5.2. Consequently, the method used for mechanical analyses of Atlantic Salmon vertebrae can also be utilized in measurements of another a similar Salmonid species, such as Rainbow Trout. Carps however are not suggested for using the same method.

The compression force at 15 % of vertebra thickness in salmon was significantly greater than that in trout (carp as well, although this information can be regarded as irrelevant here). There was however only a slight difference in compression force at 70 % of the vertebra thickness between salmon and trout. Thus, force at 70 % compression depth would be a better choice than force at 15 % compression depth through measuring another fish species of Salmonids, such as Rainbow Trout.

The thickness and breaking force of ribs varied significantly among salmon, trout, and carp. So it was not possible to utilize the same mechanical analyses method of ribs to different fish species.

5.4 Mechanical properties compared in fresh and frozen vertebrae

The compression force of vertebrae in salmon and trout did not change significantly after frozen preservation. For salmon, the maximum compression force was slightly reduced after frozen storage. Frozen storage appeared to both enhance and reduce effects in trout. Consequently, frozen treatments will not greatly affect the mechanical properties of fish vertebrae. Frozen vertebrae can therefore also be used for mechanical measurements.

5.5 Chemical composition of salmon and trout

The dry matter of salmon and trout vertebrae showed no significant difference, whereas vertebrae fat content and ash appeared significantly different between the two species. Therefore, vertebrae fat content and ash measurements can be used to determine fish species. Since dry matter consists of ash and organic matter, it is easy to calculate that the organic matter of salmon and trout vertebrae would show a significant difference as well.

The dry matter at different section in the vertebral column showed a significant difference. This can be hypothesised as being related to the variance of thickness and compression force along the vertebral column. There was no great difference in the fat content and ash of vertebrae at different sections along the vertebral column. Thus, dry matter can be a parameter for determining variation of the various vertebra sections along fish vertebral columns.

6. Conclusion

Mechanical properties of fish vertebrae and ribs observed in this study can be summarized as follows:

1) Mechanical properties of Atlantic Salmon vertebrae and ribs in detail: vertebrae strength in Atlantic Salmon increased from V4-V12 and was stable from V12-V28. From V28-V40 the bone strength was either stable or decreased, whereas from V40-V48 it decreased consistently. Rib strength in salmon showed a significant decrease from the anterior to posterior sections.The measuring point within the same rib closest to the vertebral column showed greater strength.

2) Variation in mechanical properties of Atlantic Salmon vertebrae and ribs among weight classes: the patterns presented vertebrae strength for 4 kg and 5 kg salmon was more stable than that of 6 kg salmon, and 5 kg salmon has significantly greater vertebrae strength than the other two weight classes which presented that 5 kg salmon is much closer to a limiting value of vertebrae strength in salmon. The ribs strength was significantly affected by the weight, and the mechanical loading of the position which closest to the vertebral column within the same rib was more likely to be determined by the weight of salmon.

3) Variation in mechanical properties of vertebrae and ribs among Atlantic Salmon, Rainbow Trout and common Carp: the mechanical loading of carp vertebrae was significantly different from that of Salmonids and a slight difference of vertebrae strength can be measured with a specific method in Salmonid species such as Atlantic Salmon and Rainbow Trout..

4) Variation in mechanical properties of fresh and frozen vertebrae: vertebrae strength of salmon and trout is not significantly affected after frozen preservation.

5) Variation in chemical composition of salmon and trout vertebrae: fat content and ash of vertebrae appear to be significantly different between the two fish species, while dry matter only showed significant difference only at different section in vertebral column.

This study provides a methods for the measurement of mechanical properties of Atlantic Salmon vertebrae and ribs, based on the conclusions stated above and replicate comparison of various methods and parameters used in this study. The method can be generalized as follows:

When conducting mechanical analyses of Atlantic Salmon vertebrae, the section from tail to mid-section along the vertebral column should be used (V12-V28), and the total work (area, N*s) required to compress depth was a more accurate parameter to describe the mechanical properties of fish vertebrae. Five kg Atlantic Salmon was the best choice for standard mechanical analyses compared to 4 kg and 6 kg Atlantic Salmon. A similar Salmonids fish species, such as Rainbow Trout, was also applicable to use this method for mechanical measurements. In order to avoid significantly difference in mechanical analyses within Salmonids, measuring at 70 % of the vertebra thickness would be a better choice to obtain more accurate results than measuring at 15 % compression depth. Frozen vertebrae can also be used for mechanical measurements, since frozen preservation did not affect the mechanical properties of fish vertebrae.

When conducting mechanical analyses of Atlantic Salmon ribs, the rib located nearest the head at position A (closest position to the vertebral column) is a better choice and results in more accurate results, whereas the rib closest to the tail at position C (farthest position to the vertebral column) is the least advantageous point.

Reference

Alexander, R. M. (1974). *Functional design of fishes*, GB.

Ascenzi, A. (1993). "Biomechanics and Galileo Galilei." *Journal of Biomechanics* ***26***(2), 95-100.

Beck, J., B. Canfield, S. Haddock, T. Chen, M. Kothari and T. Keaveny (1997). "Three-dimensional imaging of trabecular bone using the computer numerically controlled milling technique." *Bone* ***21***(3), 281-287.

Bell, J. (1834). *The anatomy and physiology of the human body*, Collins.

Boulenger, E. G. (1931). *Fishes*, Chapman & Hall Limited.

Carter, D., D. P. Fyhrie and R. Whalen (1987). "Trabecular bone density and loading history: regulation of connective tissue biology by mechanical energy." *Journal of Biomechanics* ***20***(8), 785789-787794.

Carter, D. R. (1984). "Mechanical loading histories and cortical bone remodeling." *Calcified tissue international* ***36***(1), S19-S24.

Carter, D. R. and D. M. Spengler (1978). "Mechanical properties and composition of cortical bone." *Clinical orthopaedics and related research* ***135***, 192-217.

Chavassieux, P., E. Seeman and P. Delmas (2007). "Insights into material and structural basis of bone fragility from diseases associated with fractures: how determinants of the biomechanical properties of bone are compromised by disease." *Endocrine reviews* ***28***(2), 151-164.

Chiling, L., Zhonghua, L., Jian Y. (2007). "Development of bone powder expanded food." *Food Research and Development* **28**(4), 108-110.

Cohen, L., M. Dean, A. Shipov, A. Atkins, E. Monsonego-Ornan and R. Shahar (2012). "Comparison of structural, architectural and mechanical aspects of cellular and acellular bone in two teleost fish." *Journal of Experimental Biology* ***215***(11), 1983-1993.

Cortet, B., D. Colin, P. Dubois, B. Delcambre and X. Marchandise (1995). "Methods for quantitative analysis of trabecular bone structure." *Revue du rhumatisme (English ed.)* ***62***(11), 781-793.

Cortet, B., P. Dubois, N. Boutry, P. Bourel, A. Cotten and X. Marchandise (1999). "Image analysis of the distal radius trabecular network using computed tomography." *Osteoporosis international* ***9***(5), 410-419.

Currey, J. D. (2002). *Bones: structure and mechanics*, Princeton university press.

Currey, J. D. (2014). *The mechanical adaptations of bones*, Princeton University Press.

Dalle Carbonare, L. and S. Giannini (2004). "Bone microarchitecture as an important determinant of bone strength." *J Endocrinol Invest* ***27***(1), 99-105.

De Carli, F. and J. Richardson (1978). *The world of fish*, Gallery books.

Ebenstein, D. M. and L. A. Pruitt (2006). "Nanoindentation of biological materials." *Nano Today* ***1***(3), 26-33.

Fa-Hwa Cheng, I. (1997). "Strength of material." *Ohio: McGraw-Hill*.

Fjelldal, P. G., S. Grotmol, H. Kryvi, N. R. Gjerdet, G. L. Taranger, T. Hansen, . . . G. K. Totland (2004). "Pinealectomy induces malformation of the spine and reduces the mechanical strength of the vertebrae in Atlantic salmon, Salmo salar." *Journal of pineal research* ***36***(2), 132-139.

Fjelldal, P. G., E.-J. Lock, S. Grotmol, G. K. Totland, U. Nordgarden, G. Flik and T. Hansen (2006). "Impact of smolt production strategy on vertebral growth and mineralisation during smoltification and the early seawater phase in Atlantic salmon (Salmo salar, L.)." *Aquaculture* ***261***(2), 715-728.

Fjelldal, P. G., U. Nordgarden, A. Berg, S. Grotmol, G. K. Totland, A. Wargelius and T. Hansen (2005). "Vertebrae of the trunk and tail display different growth rates in response to photoperiod in Atlantic salmon, Salmo salar L., post-smolts." *Aquaculture* ***250***(1), 516-524.

Folch, J., M. Lees and G. Sloane-Stanley (1957). "Extraction of fatty acid." *J Biol Chem* ***226***, 497-509.

Fratzl, P. and R. Weinkamer (2007). "Nature's hierarchical materials." *Progress in Materials Science* ***52***(8), 1263-1334.

Froese, R. and D. Pauly (2012). FishBase.

Genant, H., K. Engelke and S. Prevrhal (2008). "Advanced CT bone imaging in osteoporosis." *Rheumatology* ***47***(suppl 4), iv9-iv16.

Gibson, L. J. (1985). "The mechanical behaviour of cancellous bone." *Journal of Biomechanics* ***18***(5), 317-328.

Gluer, C., C. Wu, M. Jergas, S. Goldstein and H. Genant (1994). "Three quantitative ultrasound parameters reflect bone structure." *Calcified tissue international* ***55***(1), 46-52.

Guilak, F., B. Fermor, F. J. Keefe, V. B. Kraus, S. A. Olson, D. S. Pisetsky, . . . J. B. Weinberg (2004). "The role of biomechanics and inflammation in cartilage injury and repair." *Clinical orthopaedics and related research* ***423***, 17-26.

Håstein, T. (2004). Animal welfare issues relating to aquaculture. Global conference on animal welfare: an OIE initiative. European Communities, Paris, France, Citeseer.

Halaba, Z. P., J. Konstantynowicz, W. Pluskiewicz, M. Kaczmarski and J. Piotrowska-Jastrzebska (2005). "Comparison of phalangeal ultrasound and dual energy X-ray absorptiometry in healthy male and female adolescents." *Ultrasound in medicine & biology* ***31***(12), 1617-1622.

Hall, J. E. (2015). *Guyton and Hall textbook of medical physiology*, Elsevier Health Sciences.

Hans, D., C. Wu, C. Njeh, S. Zhao, P. Augat, D. Newitt, . . . H. Genant (1999). "Ultrasound velocity of trabecular cubes reflects mainly bone density and elasticity." *Calcified tissue international* ***64***(1), 18-23.

Hench, L. L. and J. Wilson (1993). *An introduction to bioceramics*, World scientific.

Hernandez, C. and T. Keaveny (2006). "A biomechanical perspective on bone quality." *Bone* ***39***(6), 1173-1181.

Horton, J. M. and A. P. Summers (2009). "The material properties of acellular bone in a teleost fish." *Journal of Experimental Biology* ***212***(9), 1413-1420.

Huiskes, R. (2000). "If bone is the answer, then what is the question?" *J Anat* ***197***(2), 145-156.

Ito, M. (2006). "Assessment of effect of anti-osteoporotic agents using high-resolution CT." *Clinical calcium* ***16***(12), 2034-2042.

Kacem, A., F. Meunier and J. Bagliniere (1998). "A quantitative study of morphological and histological changes in the skeleton of Salmo salar during its anadromous migration." *Journal of Fish Biology* ***53***(5), 1096-1109.

Kleerekoper, M. (2006). "Osteoporosis prevention and therapy: preserving and building strength through bone quality." *Osteoporosis international* ***17***(12), 1707-1715.

Krossøy, C., R. Ørnsrud and A. Wargelius (2009). "Differential gene expression of bgp and mgp in trabecular and compact bone of Atlantic salmon (Salmo salar L.) vertebrae." *J Anat* ***215***(6), 663-672.

Kyle, H. M. (1926). *The biology of fishes*, London.

Laugier, P., P. Droin, A. Laval-Jeantet and G. Berger (1997). "In vitro assessment of the relationship between acoustic properties and bone mass density of the calcaneus by comparison of ultrasound parametric imaging and quantitative computed tomography." *Bone* ***20***(2), 157-165.

Lee, D. D., W. J. Landis and M. J. Glimcher (1986). "The solid, calcium- phosphate mineral phases in embryonic chick bone characterized by high- voltage electron diffraction." *Journal of bone and mineral research* ***1***(5), 425-432.

Lester, B., J. Halbrecht, I. M. Levy and R. Gaudinez (1995). "" Press test" for office diagnosis of triangular fibrocartilage complex tears of the wrist." *Annals of plastic surgery* ***35***(1), 41-45.

Lin, J.-D., J.-F. Chen, H.-Y. Chang and C. Ho (2001). "Evaluation of bone mineral density by quantitative ultrasound of bone in 16 862 subjects during routine health examination." *The British journal of radiology* ***74***(883), 602-606.

Mørkøre, T., T. Larsson, A. S. Kvellestad, E. O. Koppang, M. Åsli, A. Krasnov, . . . K. H. Gannestad (2015). "Mørke flekker i laksefilet. Kunnskapsstatus og tiltak for å begrense omfanget."

Mackean, D. G. (1969). "Introduction to biology."

Mackie, E. (2003). "Osteoblasts: novel roles in orchestration of skeletal architecture." *The international journal of biochemistry & cell biology* ***35***(9), 1301-1305.

Majumdar, S., D. Newitt, A. Mathur, D. Osman, A. Gies, E. Chiu, . . . H. Genant (1996). "Magnetic resonance imaging of trabecular bone structure in the distal radius: relationship with X-ray tomographic microscopy and biomechanics." *Osteoporosis international* ***6***(5), 376-385.

Malluche, H. H., D. Sherman, W. Meyer and S. G. Massry (1982). "A new semiautomatic method for quantitative static and dynamic bone histology." *Calcified tissue international* ***34***(1), 439-448.

Markings, B. (2004). "The skeletal system."

Martin, R. B. (1999). A genealogy of biomechanics. 23rd Annual Conference of the American Society of Biomechanics.

Martínez-Valverde, I., M. J. Periago, M. Santaella and G. Ros (2000). "The content and nutritional significance of minerals on fish flesh in the presence and absence of bone." *Food Chemistry* ***71***(4), 503-509.

Moss, M. L. (1961). "Osteogenesis of acellular teleost fish bone." *American Journal of Anatomy* ***108***(1), 99-109.

Moss, M. L. (1963). "The biology of acellular teleost bone." *Annals of the New York Academy of Sciences* ***109***(1), 337-350.

Moss, M. L. (1965). "Studies of the acellular bone of teleost fish. V." *Cells Tissues Organs* ***60***(2), 262-276.

Mulder, L., J. H. Koolstra, W. A. Weijs and T. M. van Eijden (2005). "Architecture and mineralization of developing trabecular bone in the pig mandibular condyle." *The Anatomical Record Part A: Discoveries in Molecular, Cellular, and Evolutionary Biology* ***285***(1), 659-666.

Nelson, G. J. (1969). "Origin and diversification of teleostean fishes." *Annals of the New York Academy of Sciences* ***167***(1), 18-30.

Nordvik, K., H. Kryvi, G. K. Totland and S. Grotmol (2005). "The salmon vertebral body develops through mineralization of two preformed tissues that are encompassed by two layers of bone." *J Anat* ***206***(2), 103-114.

Parfitt, A. (1984). "Age-related structural changes in trabecular and cortical bone: cellular mechanisms and biomechanical consequences." *Calcified tissue international* ***36***, S123-S128.

Parfitt, A. M., M. K. Drezner, F. H. Glorieux, J. A. Kanis, H. Malluche, P. J. Meunier, . . . R. R. Recker (1987). "Bone histomorphometry: standardization of nomenclature, symbols, and units: report of the ASBMR Histomorphometry Nomenclature Committee." *Journal of bone and mineral research* ***2***(6), 595-610.

Parnell, W. J. and Q. Grimal (2009). "The influence of mesoscale porosity on cortical bone anisotropy. Investigations via asymptotic homogenization." *Journal of the Royal Society Interface* ***6***(30), 97-109.

Peng, J., Aiyuan, W., Mingxue, S. (2005). "Three-dimensional analysis of spatial structure in femur cancellous bone samples." *Chinese journal of orthopedic surgery* ***20***(6), 924-926.

Ramakrishna, S., J. Mayer, E. Wintermantel and K. W. Leong (2001). "Biomedical applications of polymer-composite materials: a review." *Composites science and technology* ***61***(9), 1189-1224.

Ratner, B. D., A. S. Hoffman, F. J. Schoen and J. E. Lemons (2004). *Biomaterials science: an introduction to materials in medicine*, Academic press.

Rho, J.-Y. and G. M. Pharr (1999). "Effects of drying on the mechanical properties of bovine femur measured by nanoindentation." *Journal of Materials Science: Materials in Medicine* ***10***(8), 485-488.

Rho, J. Y., M. E. Roy, T. Y. Tsui and G. M. Pharr (1999). "Elastic properties of microstructural components of human bone tissue as measured by nanoindentation." *Journal of biomedical materials research* ***45***(1), 48-54.

Richardsen, R., R. Nystøyl, G. Strandheim and A. Viken (2015). "Analyse marint restråstoff, 2014: Analyse af tilgang og anvendelse for marint restråstoff i Norge."

Ritman, E. L. (2002). "Molecular imaging in small animals—roles for micro- CT." *Journal of Cellular Biochemistry* ***87***(S39), 116-124.

Roesler, H. (1987). "The history of some fundamental concepts in bone biomechanics." *Journal of Biomechanics* ***20***(11-12), 1025-1034.

Ross, C. F. and K. A. Metzger (2004). "Bone strain gradients and optimization in vertebrate skulls." *Annals of Anatomy-Anatomischer Anzeiger* ***186***(5-6), 387-396.

Rubin, C., A. S. Turner, R. Müller, E. Mittra, K. McLeod, W. Lin and Y. X. Qin (2002). "Quantity and quality of trabecular bone in the femur are enhanced by

a strongly anabolic, noninvasive mechanical intervention." *Journal of bone and mineral research* ***17***(2), 349-357.

Schott, A., D. Hans, F. Duboeuf, P. Dargent-Molina, T. Hajri, G. Breart and P. Meunier (2005). "Quantitative ultrasound parameters as well as bone mineral density are better predictors of trochanteric than cervical hip fractures in elderly women. Results from the EPIDOS study." *Bone* ***37***(6), 858-863.

Seeman, E. (2003). "The structural and biomechanical basis of the gain and loss of bone strength in women and men." *Endocrinology and metabolism clinics of North America* ***32***(1), 25-38.

Seeman, E. and P. D. Delmas (2006). "Bone quality—the material and structural basis of bone strength and fragility." *New England Journal of Medicine* ***354***(21), 2250-2261.

Slizyte, R., K. Rommi, R. Mozuraityte, P. Eck, K. Five and T. Rustad (2016). "Bioactivities of fish protein hydrolysates from defatted salmon backbones." *Biotechnology Reports* ***11***, 99-109.

Steele, D. G. and C. A. Bramblett (1988). *The anatomy and biology of the human skeleton*, Texas A&M University Press.

Szpak, P. (2011). "Fish bone chemistry and ultrastructure: implications for taphonomy and stable isotope analysis." *Journal of Archaeological Science* ***38***(12), 3358-3372.

Toppe, J., S. Albrektsen, B. Hope and A. Aksnes (2007). "Chemical composition, mineral content and amino acid and lipid profiles in bones from various fish species." *Comparative Biochemistry and Physiology Part B: Biochemistry and Molecular Biology* ***146***(3), 395-401.

Totland, G. K., P. G. Fjelldal, H. Kryvi, G. Løkka, A. Wargelius, A. Sagstad, . . . S. Grotmol (2011). "Sustained swimming increases the mineral content and osteocyte density of salmon vertebral bone." *J Anat* ***219***(4), 490-501.

van der Meulen, M. C. H., K. J. Jepsen and B. Mikić "Understanding bone strength: size isn’t everything." *Bone* ***29***(2), 101-104.

von Meyer, G. H. (2011). "The classic: the architecture of the trabecular bone (Tenth Contribution on the Mechanics of the Human Skeletal Framework)." *Clinical Orthopaedics and Related Research®* ***469***(11), 3079.

Wang, W. (2016). The effect of dietary antioxidants on hyperpigmented fillet spots of Atlantic salmon (Salmo salar L.), Norwegian University of Life Sciences, Ås.

Wehrli, F. W. (2007). "Structural and functional assessment of trabecular and cortical bone by micro magnetic resonance imaging." *Journal of Magnetic Resonance Imaging* ***25***(2), 390-409.

Whalen, R., D. Carter and C. Steele (1988). "Influence of physical activity on the regulation of bone density." *Journal of Biomechanics* ***21***(10), 825-837.

Wolff, J. (2012). *The law of bone remodelling*, Springer Science & Business Media.

Yingjian, W. (1996). "A review on the micromechanical study of cancellous bone." *Advances in Mechanics* ***26***(3), 924-926.

Zhang, Y., F. Cui, X. Wang, Q. Feng and X. Zhu (2002). "Mechanical properties of skeletal bone in gene-mutated stöpsel dtl28d and wild-type zebrafish (Danio rerio) measured by atomic force microscopy-based nanoindentation." *Bone* ***30***(4), 541-546.

Zonglai, J., Yubo, F. (2010). *Biomechanics-from basic to frontiers*, Beijing: Science press.

Zysset, P. K., X. E. Guo, C. E. Hoffler, K. E. Moore and S. A. Goldstein (1999). "Elastic modulus and hardness of cortical and trabecular bone lamellae measured by nanoindentation in the human femur." *Journal of Biomechanics* ***32***(10), 1005-1012.

Appendix

Appendix 1: Product list

Table 1. Product list

Product Name	Company	Country
Chloroform	VWR international, LLC	MA, USA
Methanol	VWR international, LLC	MA, USA
Sodium chloride	VWR international	PA, USA
BHT (2,6-Di-t-butyl-p-cresol)	Sigma Chemical Co. St. Louis	MO, USA
The TA-XT2 Texture Analyser	Stable Micro Systems	Surrey, UK
Ika® T25 digital Ultra Turrax	IKA Werke GmbH & Co. KG	Breisgau, Germany
Waring Commercial® blender	Waring Commercial	CT, USA
DeltaRange® XS603S Precision Balance	Mettler-Toledo	OH, USA
Metoer® L5 heating plate	Engmark Meteor AS	Oslo, Norway
Binder® FD 23 drying and heating chambers Classic.Line with forced convection	Binder	Tuttlingen, Germany
Nabertherm® Program Controller S17 Muffle ashing furnace	Nabertherm	Lilienthal, Germany

Appendix 2: Force-time graphs for the eighth, twelfth, thirty-second and thirty-sixth vertebrae (V8, V12, V32, V36) of different Salmon weight classes

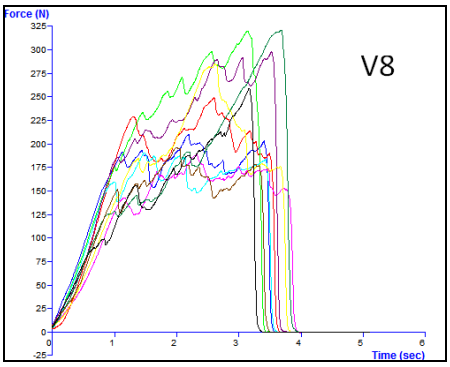

4kg Salmon Vertebrate 8 (n=10)

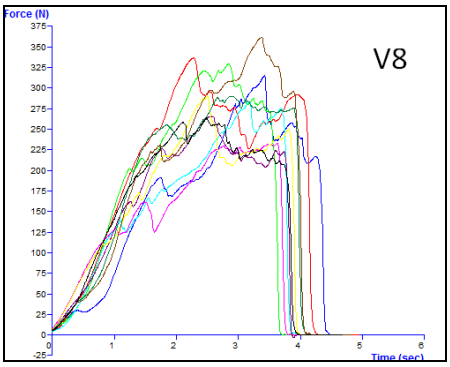

5kg Salmon Vertebrate 8 (n=10)

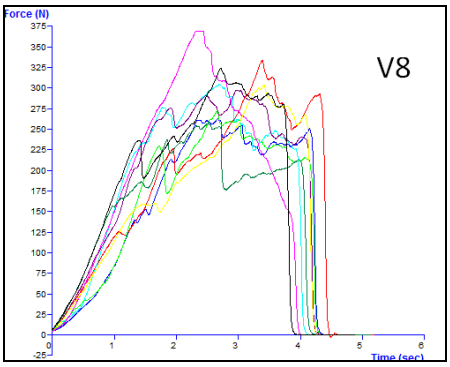

6kg Salmon Vertebrate 8 (n=9)

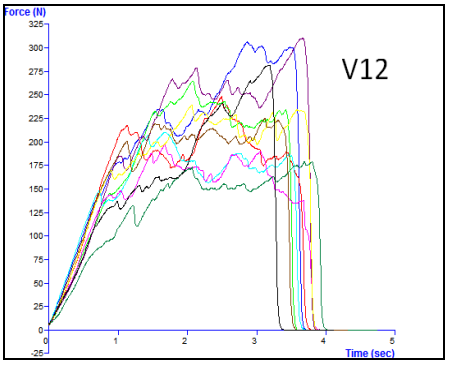

4kg Salmon Vertebrate 12 (n=10)

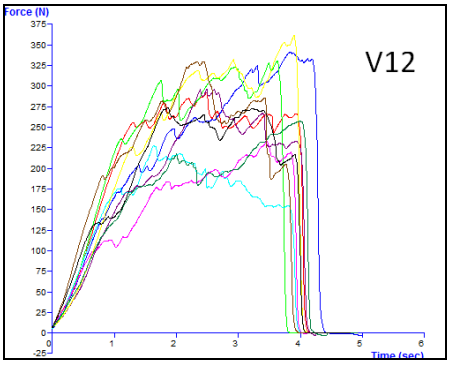

5kg Salmon Vertebrate 12 (n=10)

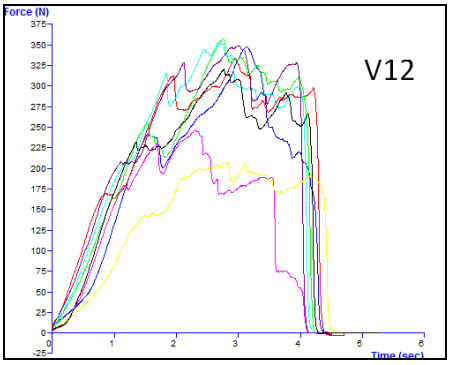

6kg Salmon Vertebrate 8 (n=8)

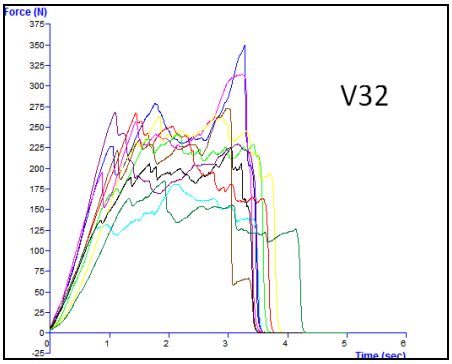

4kg Salmon Vertebrate 32 (n=10)

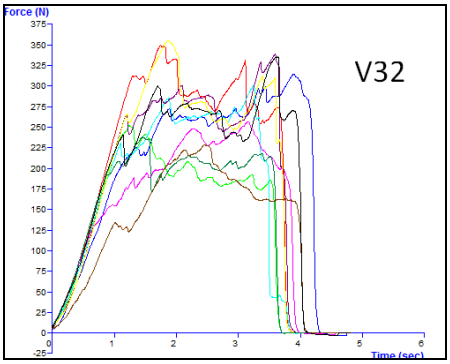

5kg Salmon Vertebrate 32 (n=10)

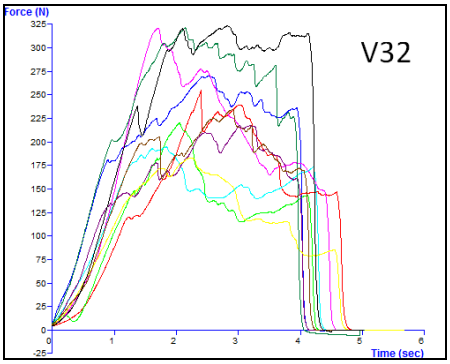

6kg Salmon Vertebrate 32 (n=10)

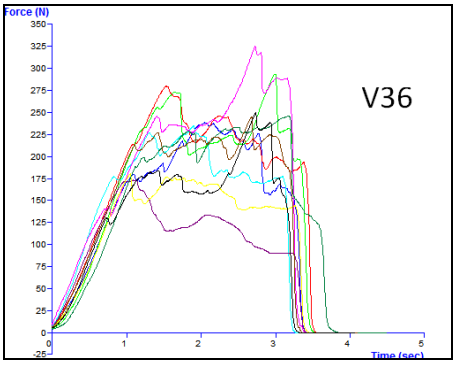

4kg Salmon Vertebrate 36 (n=10)

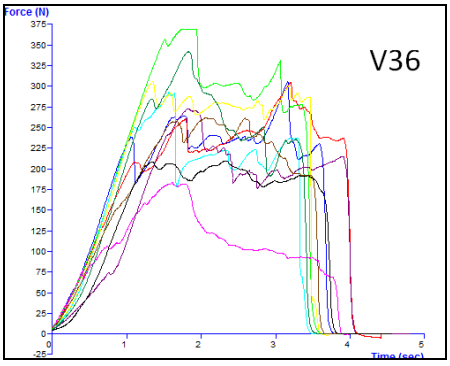

5kg Salmon Vertebrate 36 (n=10)

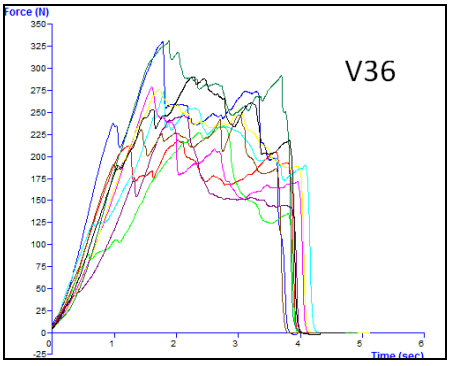

6kg Salmon Vertebrate 36 (n=10)

Fig 2. Force-time graphs for the eighth, twelfth, thirty-second and thirty-sixth vertebrae (V8, V12, V32, V36) of different Salmon weight classes

Appendix 3: Total average force-time graphs for the eighth, twelfth, thirty-second and thirty-sixth vertebra (V8, V12, V32, V36) of different Salmon weight classes

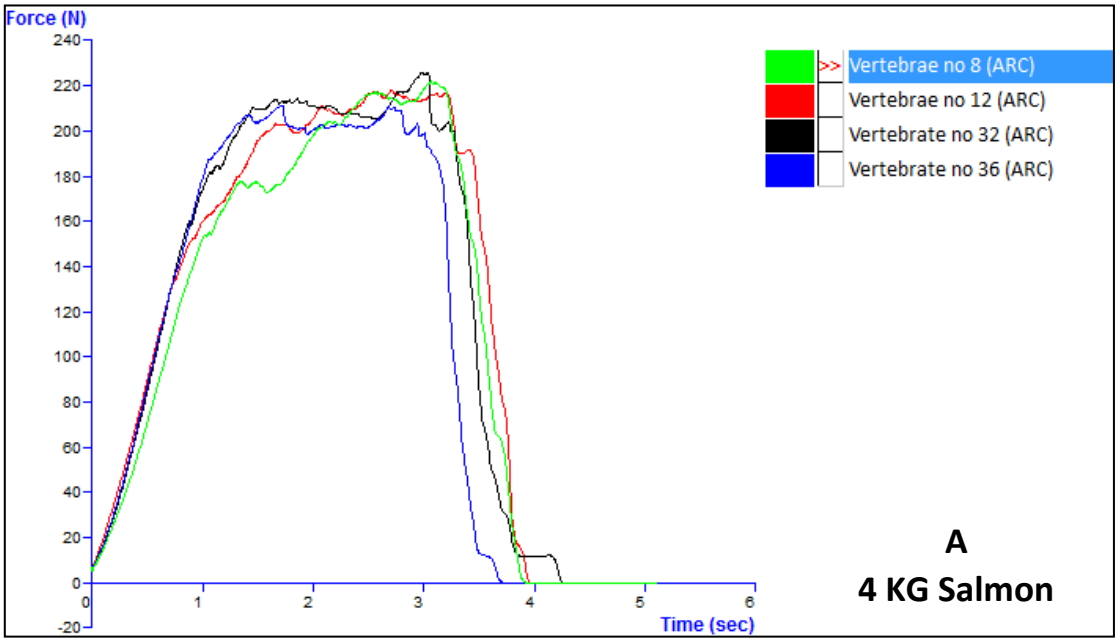

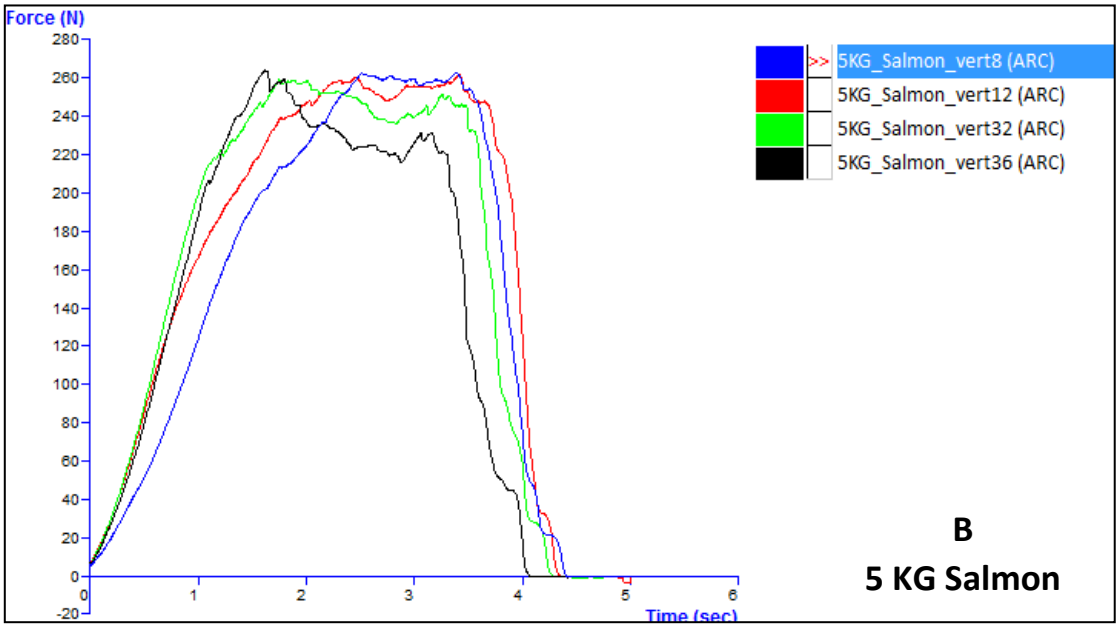

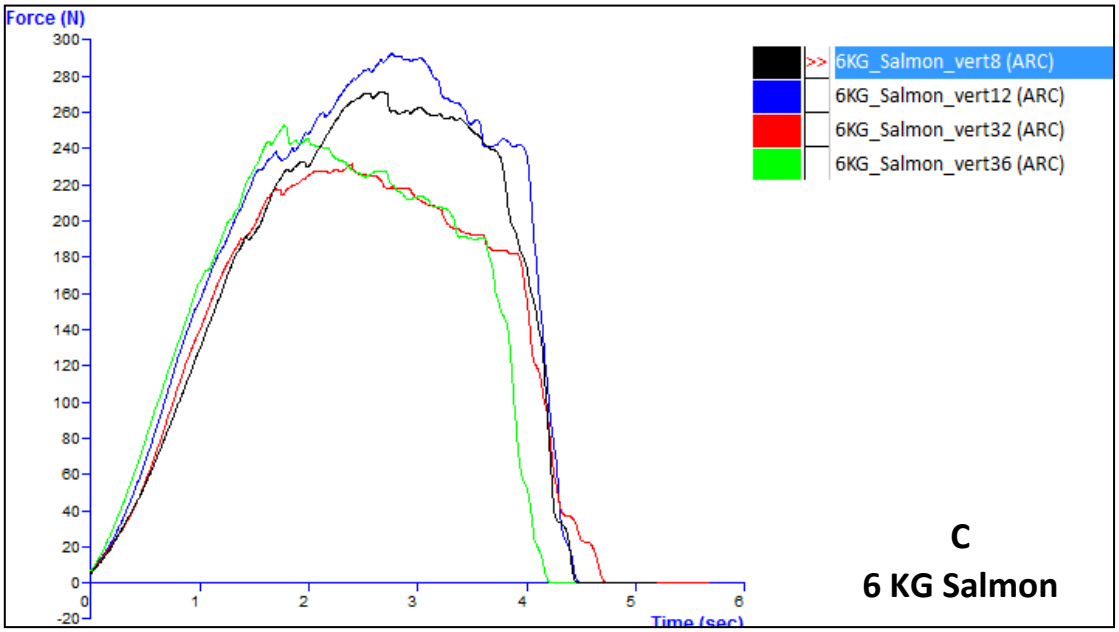

Fig 3. Total average force-time graphs for the eighth, twelfth, thirty-second and thirty-sixth vertebra (V8, V12, V32, V36) of different Salmon weight classes

Appendix 4: Force-time graphs for the eighth, twelfth, thirty-second and thirty-sixth vertebrae (V8, V12, V32, V36) of different fish species

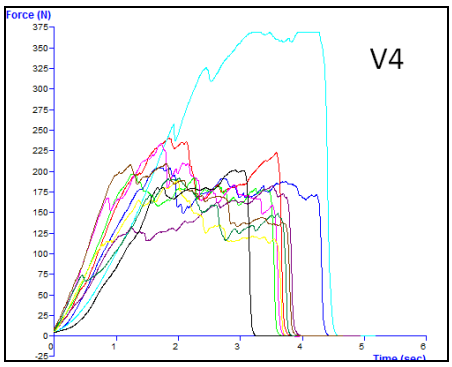

Salmon Vertebrate 4 (n=10)

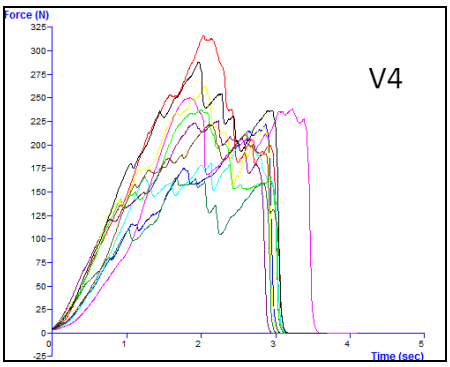

Trout Vertebrate 4 (n=10)

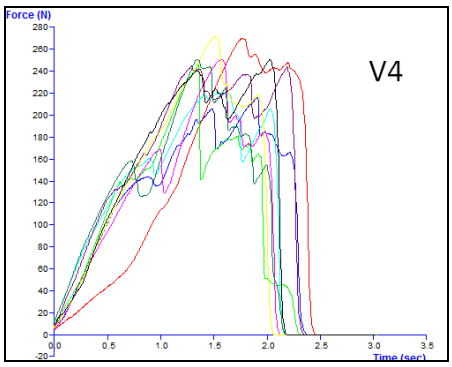

Carp Vertebrate 4 (n=9)

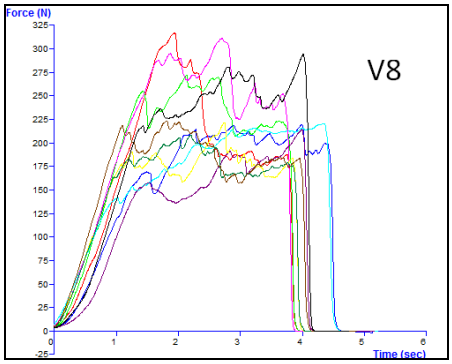

Salmon Vertebrate 8 (n=10)

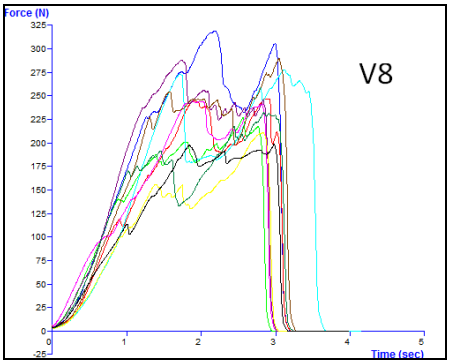

Trout Vertebrate 8 (n=10)

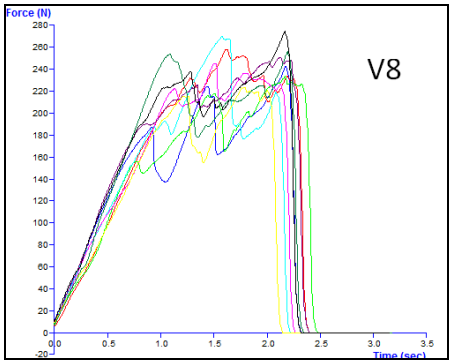

Carp Vertebrate 8 (n=9)

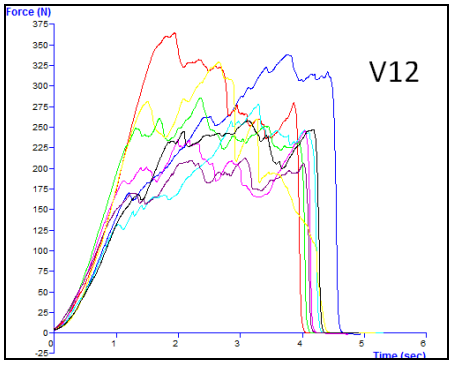

Salmon Vertebrate 12 (n=8)

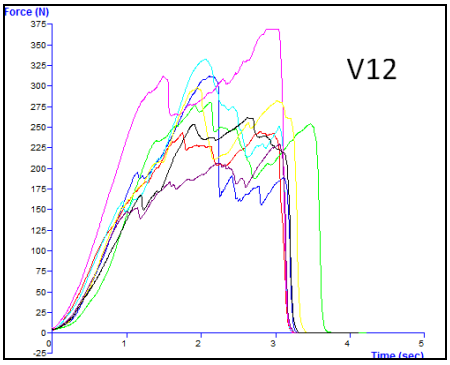

Trout Vertebrate 12 (n=8)

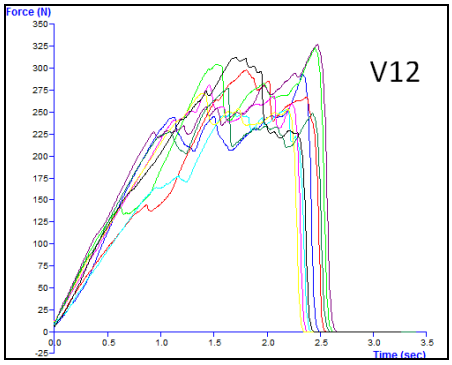

Carp Vertebrate 12 (n=9)

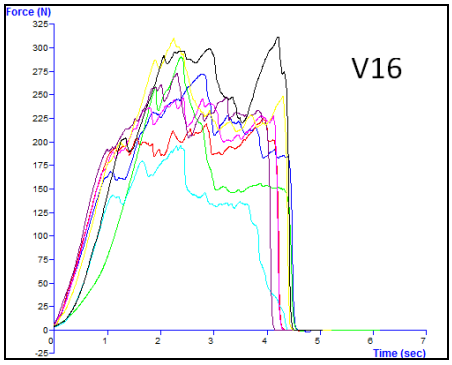

Salmon Vertebrate 16 (n=8)

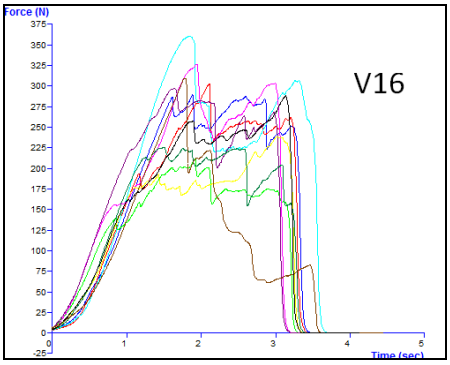

Trout Vertebrate 16 (n=10)

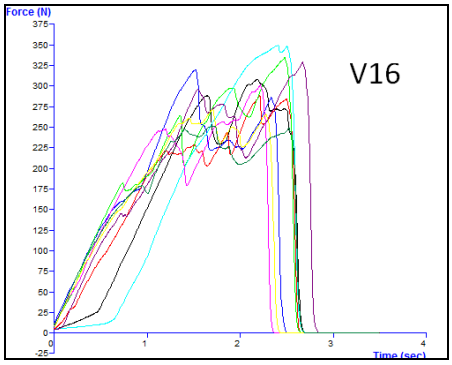

Carp Vertebrate 16 (n=9)

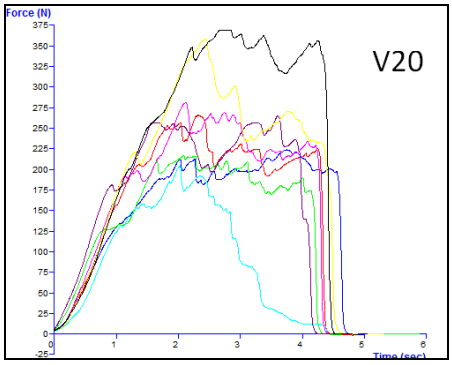

Salmon Vertebrate 20 (n=8)

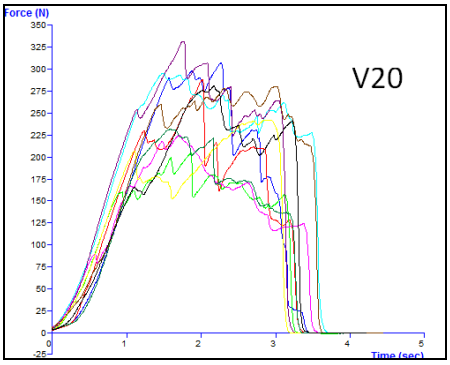

Trout Vertebrate 20 (n=10)

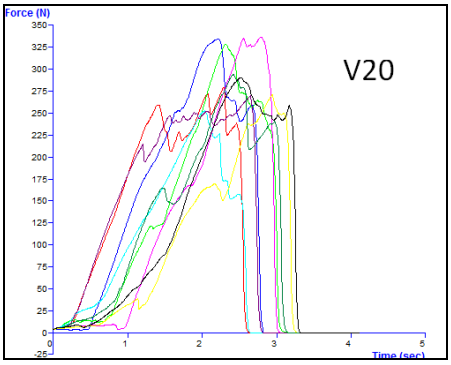

Carp Vertebrate 20 (n=9)

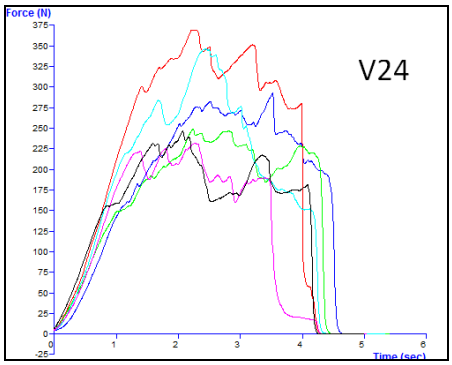

Salmon Vertebrate 24 (n=6)

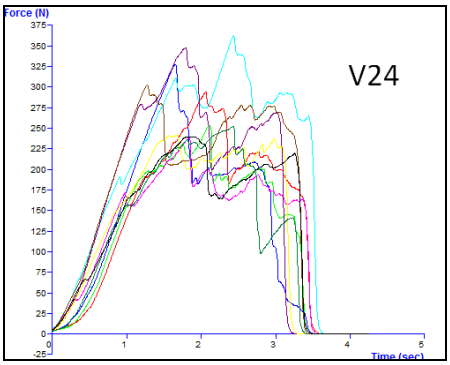

Trout Vertebrate 24 (n=10)

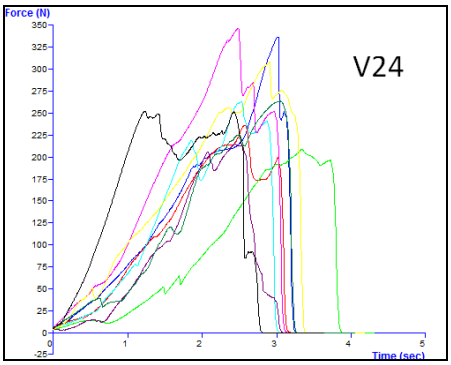

Carp Vertebrate 24 (n=9)

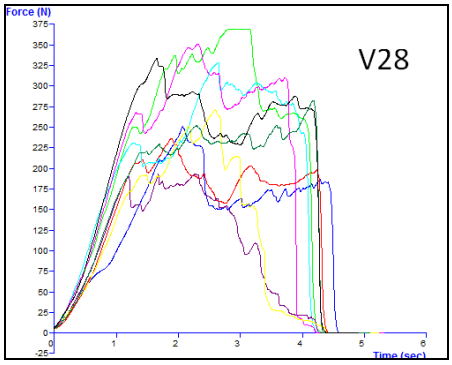

Salmon Vertebrate 28 (n=9)

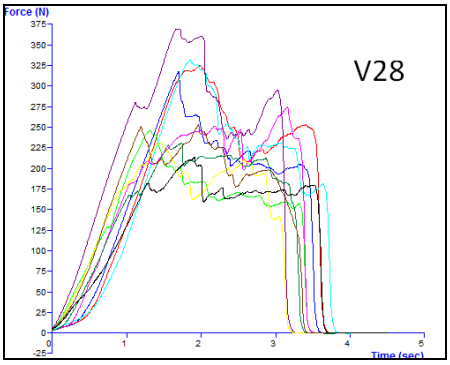

Trout Vertebrate 28 (n=10)

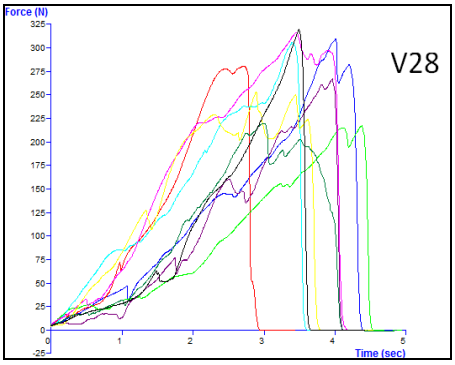

Carp Vertebrate 28 (n=9)

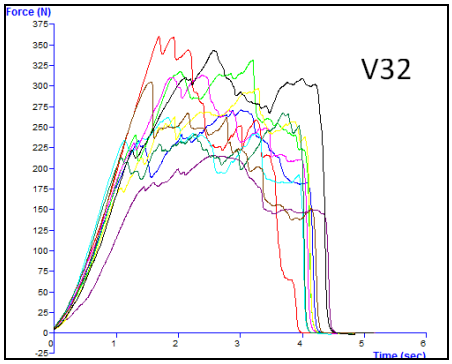

Salmon Vertebrate 32 (n=10)

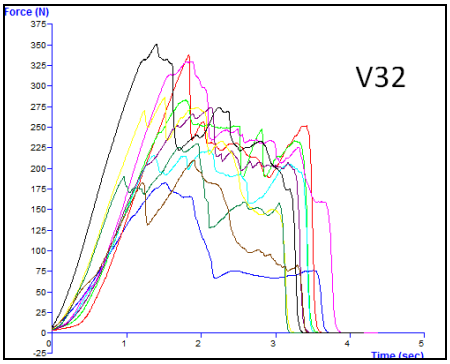

Trout Vertebrate 32 (n=10)

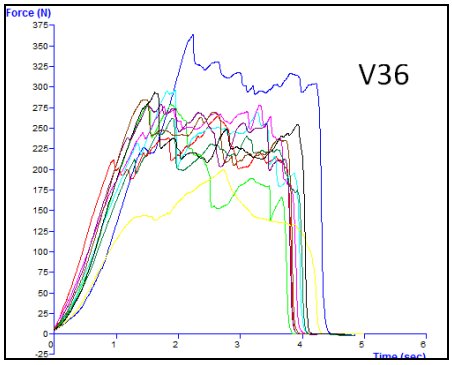

Salmon Vertebrate 36 (n=10)

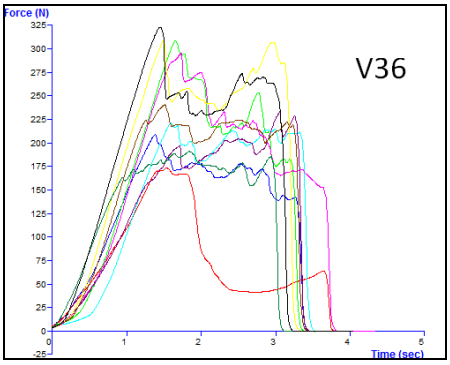

Trout Vertebrate 36 (n=10)

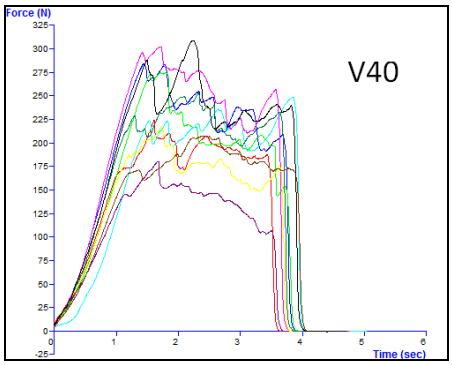

Salmon Vertebrate 40 (n=10)

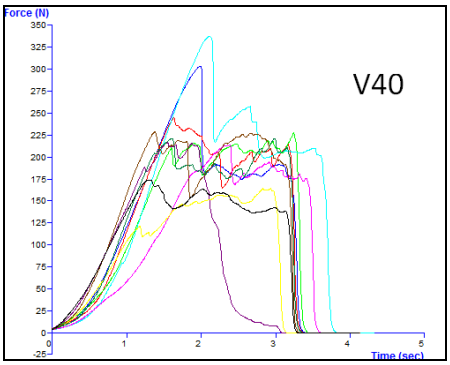

Trout Vertebrate 40 (n=10)

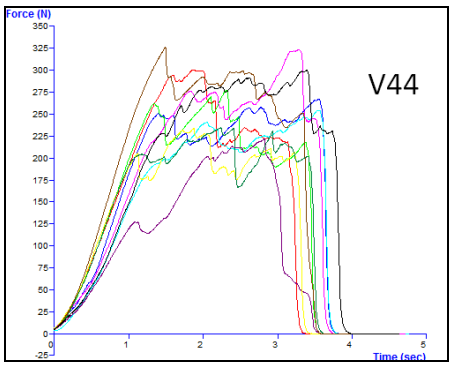

Salmon Vertebrate 44 (n=10)

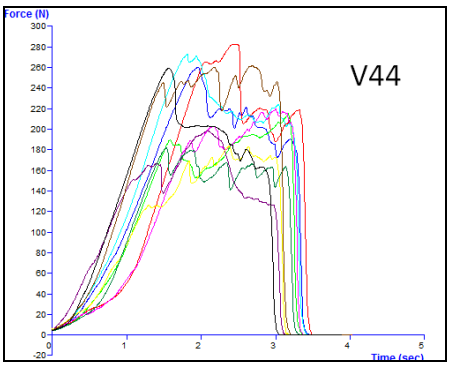

Trout Vertebrate 44 (n=10)

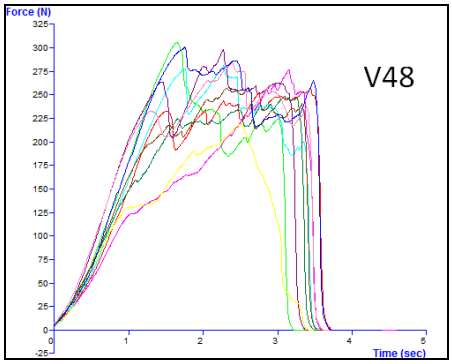

Salmon Vertebrate 48 (n=10)

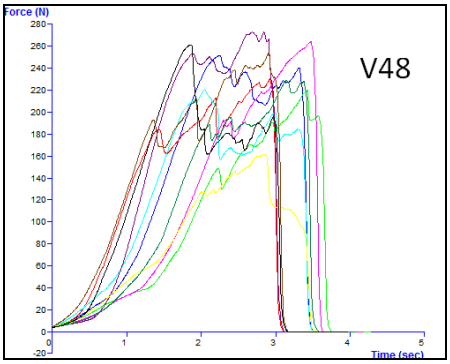

Trout Vertebrate 48 (n=10)

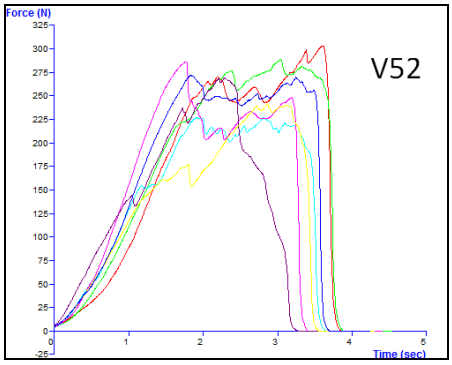

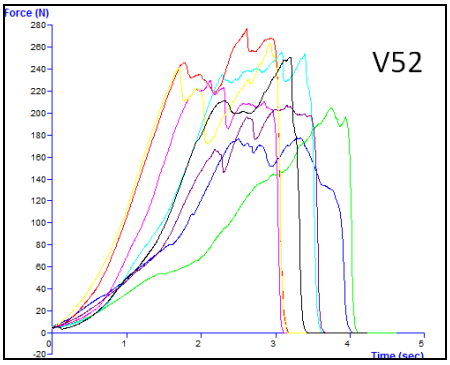

Salmon Vertebrate 52 (n=7) Trout Vertebrate 52 (n=8)

Fig 4. Force-time graphs for the eighth, twelfth, thirty-second and thirty-sixth vertebrae (V8, V12, V32, V36) of different fish species

Appendix 5: Force-time graph for the eighth, twelfth, thirty-second and thirty-sixth vertebra (V8, V12, V32, V36) of fresh and frozen Salmon

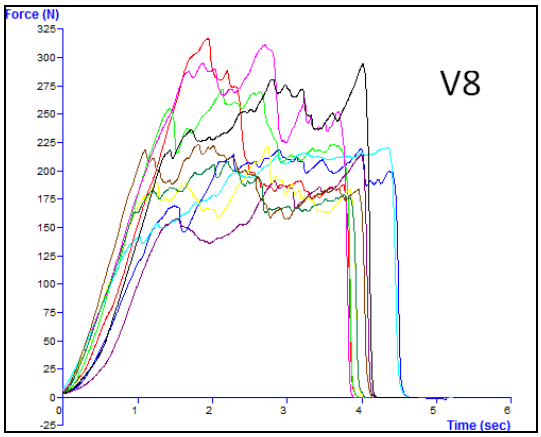

Fresh Salmon Vertebrate 8 (n=10)

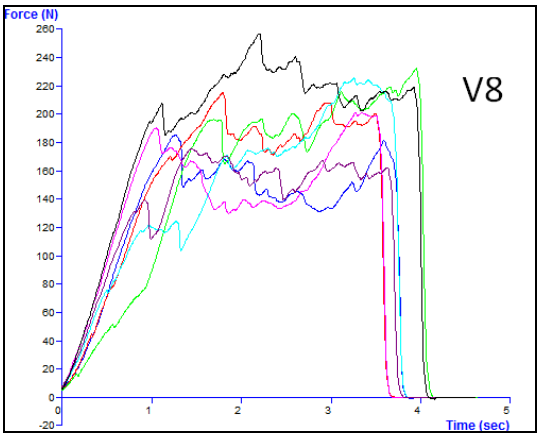

Frozen Salmon Vertebrate 8 (n=7)

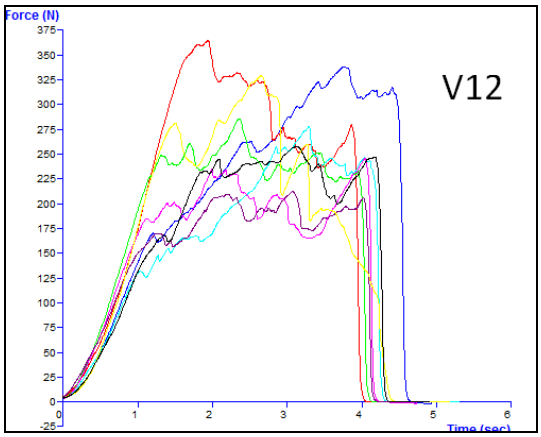

Fresh Salmon Vertebrate 12 (n=8)

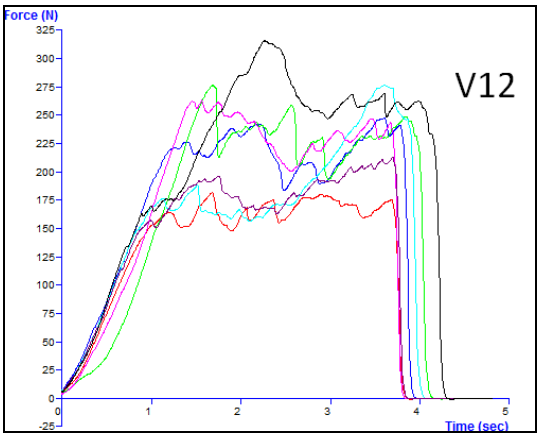

Frozen Salmon Vertebrate 12 (n=7)

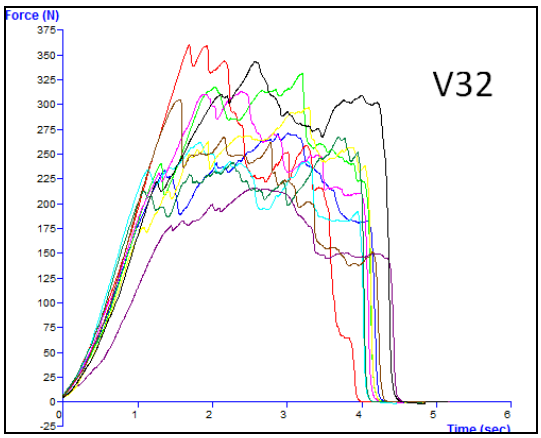

Fresh Salmon Vertebrate 32 (n=10)

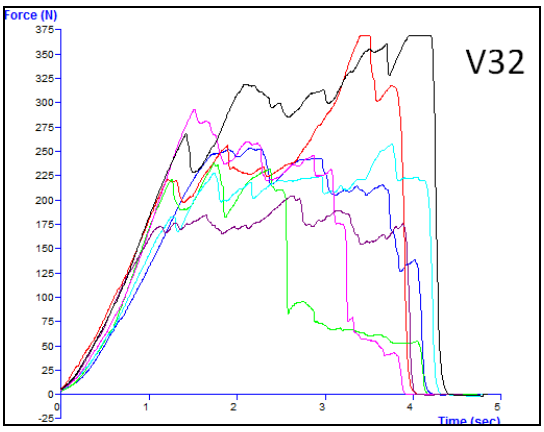

Frozen Salmon Vertebrate 32 (n=7)

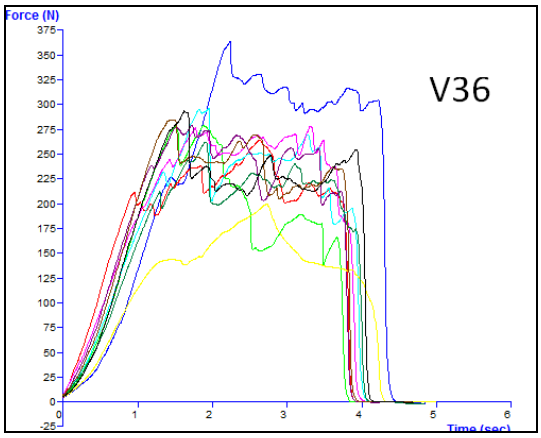

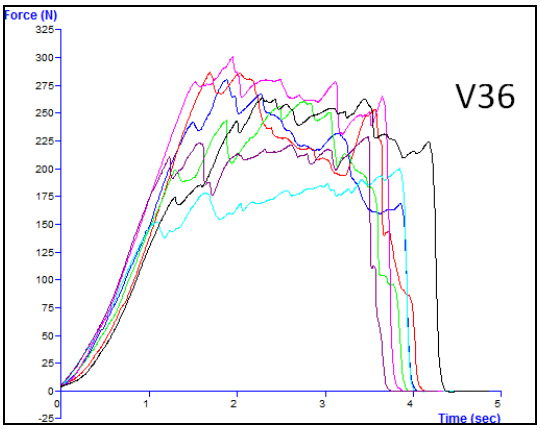

Fresh Salmon Vertebrate 36 (n=10) Frozen Salmon Vertebrate 36 (n=7)

Fig 5. Force-time graph for the eighth, twelfth, thirty-second and thirty-sixth vertebra (V8, V12, V32, V36) of fresh and frozen Salmon.

Appendix 6: Force-time graph for the eighth, twelfth, thirty-second and thirty-sixth vertebra (V8, V12, V32, V36) of fresh and frozen Trout

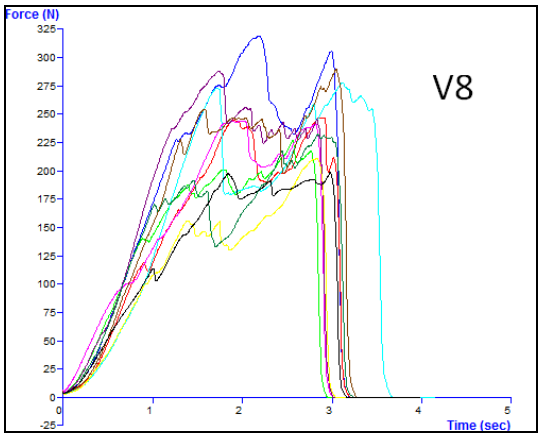

Fresh Trout Vertebrate 8 (n=10)

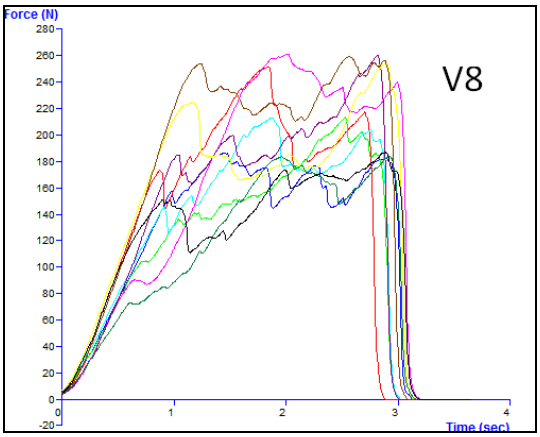

Frozen Trout Vertebrate 8 (n=10)

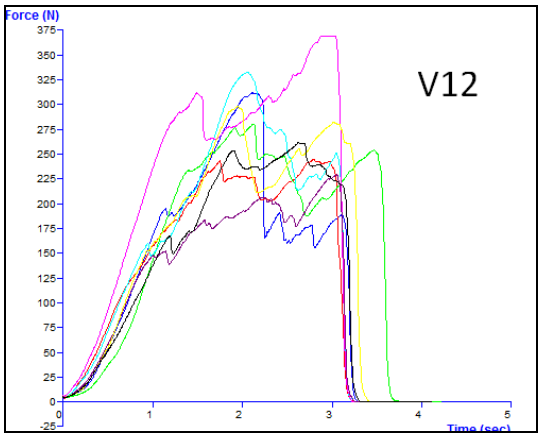

Fresh Trout Vertebrate 12 (n=8)

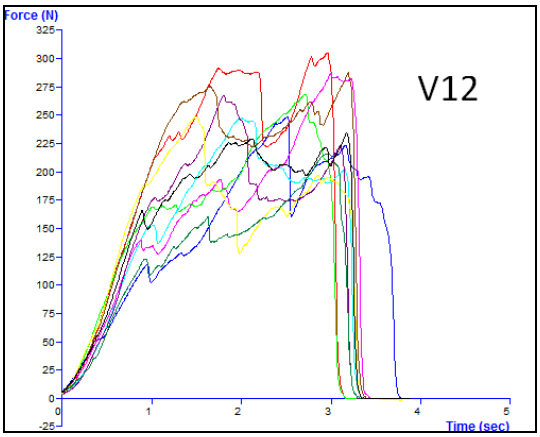

Frozen Trout Vertebrate 12 (n=10)

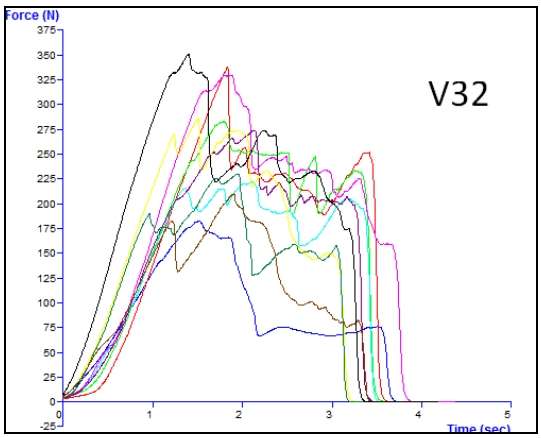

Fresh Trout Vertebrate 32 (n=10)

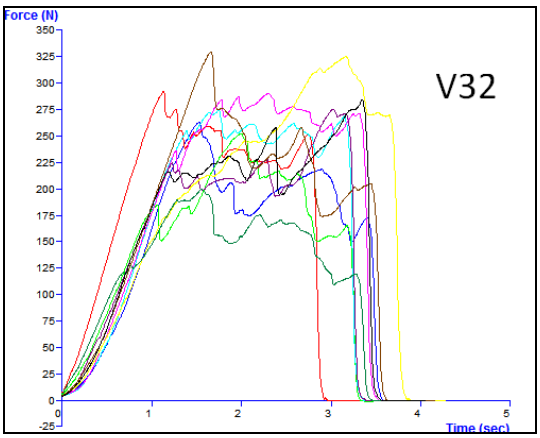

Frozen Trout Vertebrate 32 (n=10)

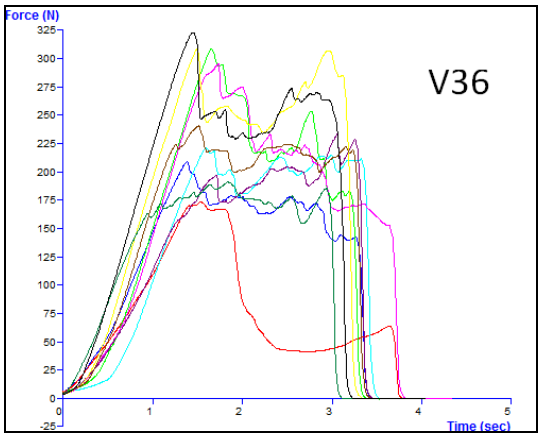

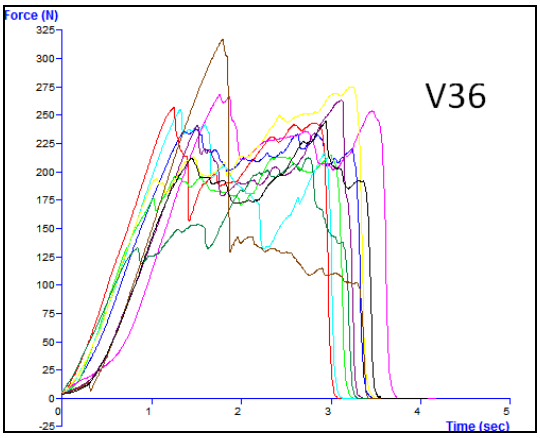

Fresh Trout Vertebrate 36 (n=10) Frozen Trout Vertebrate 36 (n=10)

Fig 6. Force-time graph for the eighth, twelfth, thirty-second and thirty-sixth vertebra (V8, V12, V32, V36) of fresh and frozen Trout

Norges miljø- og biovitenskapelig universitet
Noregs miljø- og biovitskapelege universitet
Norwegian University of Life Sciences

Postboks 5003
NO-1432 Ås
Norway